Thesis

Upscaling architected metamaterials for applications in civil infrastructure: auxetic lattices for confining concrete

Brian Dylan Schagen

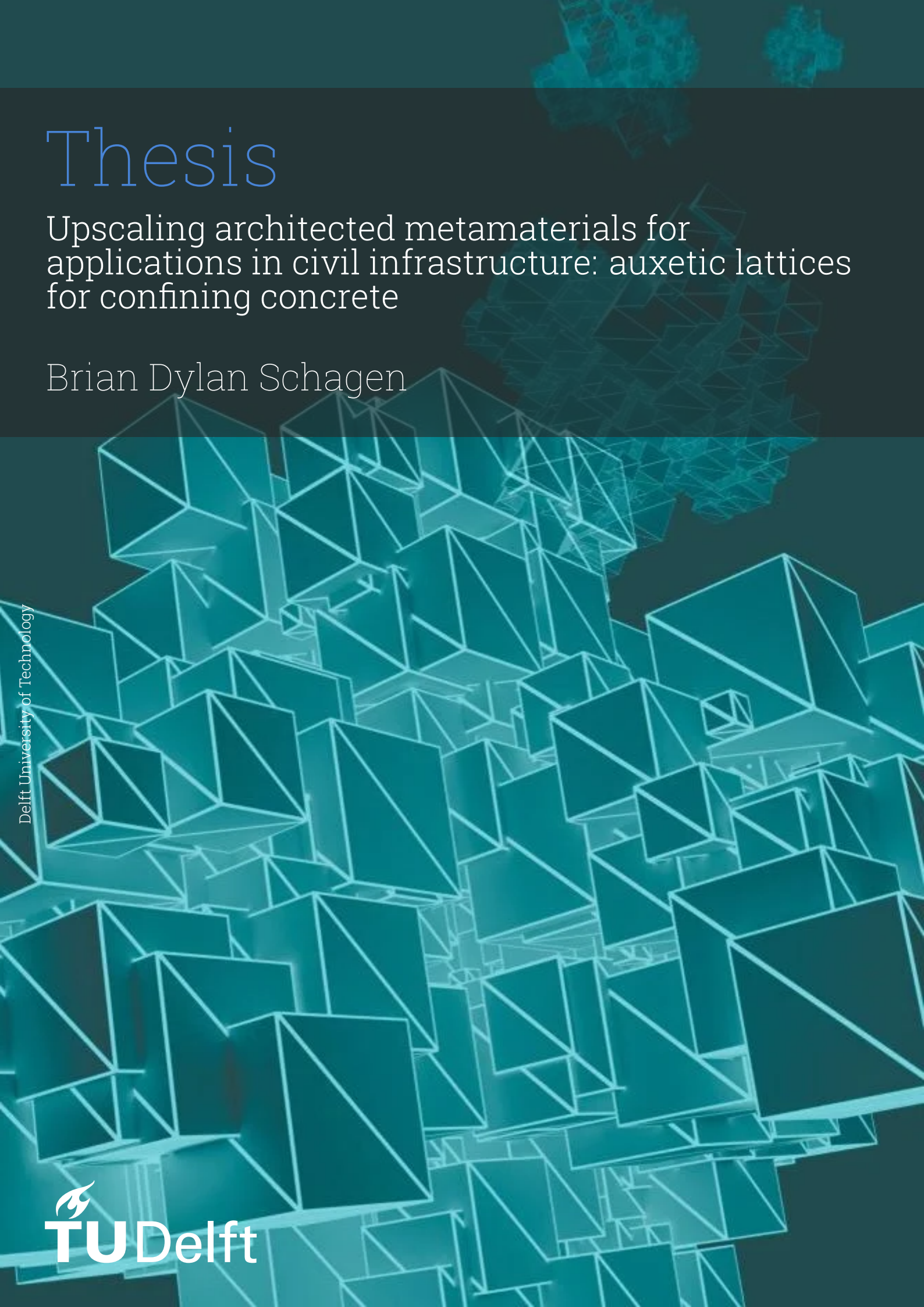

Delft University of Technology

TU Delft

Thesis

Upscaling architected metamaterials for applications in civil infrastructure: auxetic lattices for confining concrete

by

Brian Dylan Schagen

Student Name	Student Number
Brian Dylan Schagen	5183081

To obtain the degree of Master of Science in Structural Engineering
with a specialization in Steel, timber and composite structures
at the Delft University of Technology,
to be defended publicly on Tuesday December 12, 2023 at 15:45 PM.

Chair, TU Delft:	Prof.dr. M. Veljkovic
Supervisor, UMass Amherst*:	Dr. S. Gerasimidis
Daily Supervisor, TU Delft:	Dr. F. Kavoura
Supervisor, TU Delft:	H. Alkisaei
Daily Supervisor, UMass Amherst*:	T. Vitalis
Project Duration:	March, 2023 - December, 2023
Faculty:	Faculty of Civil Engineering and Geosciences, Delft
Faculty*:	College of Engineering, Amherst MA

TU Delft

Preface

During my bachelor thesis regarding the use fibre reinforced plastics (FRP) in bridges at Inholland University of Applied Sciences I became very interested in FRP. Therefore, when starting the master I was sure I wanted to go for the steel, timber and composite structures specialization. Throughout my master, I really liked the steel and composite courses and therefore wanted to do my MSc. thesis in that field. Besides that, one other reason I had for coming to TU Delft was having an abroad experience.

Going abroad became a reality when I got introduced to research about the use of auxetic metamaterials in civil engineering applications at UMass Amherst. For a period of three months I expanded my knowledge and became very interested in the topic. With that, I finished my additional research project successfully. As a result of my big interest in the research, I decided to go for a thesis in agreement with my committee and further dove into the potential of auxetic metamaterials.

Choosing this path has been one of my best decisions in my career and I am ready as ever to further pursue a Phd position after at UMass Amherst. Part of that, will be the upscaling of auxetic metamaterials in collaboration with Toggle robotics, where I am extremely excited for. Hopefully, this work and future research in this field can help us automate and further improve the sustainable construction sector, by using less material on the structural design without compromising the structure's safety. With that, I am slowly starting to say my goodbyes and really look forward giving my final presentation in Delft.

Brian Dylan Schagen
Amherst, December 2023

Acknowledgements

It is my pleasure to thank each and one of the following people that have contributed in many ways to this work:

My graduation committee: First of all, I would like to thank Florentia Kavoura. I am extremely grateful for your help in making my abroad dream a reality. We have had countless meetings to create an additional research project opportunity abroad in the first place. Besides, your continues support throughout the extension towards my thesis, the many letters of support, your enthusiasm and your expertise in the field. Simos Gerasimidis, for giving me the chance to work in your group at UMass Amherst and introducing me to this very interesting field of work. Besides, your guidance throughout my thesis and the numerous explanations about the key aspects in this research. Thomas Vitalis, for the fun and interesting discussions we had at the dinning hall, meetings and while working together. You have been very inspiring to me by your hard work and the challenges you overcome in your work. Milan Veljkovic, thank you for the critical way of thinking and important input during the committee meetings. You have helped me staying on track and choosing the right path throughout the thesis. Finally, Hoessein Alkisaei for your enthousiasm about the work, feedback in giving a good presentation and input during the meetings when it was needed.

The Structural Engineering and Mechanics group at UMass: Thank you Aidan Provost, for your enthusiasm and interest in my work. Also, introducing me to many things in Amherst and the fun we had together at EMI in Atlanta, Georgia. Shahrukh Islam and Joshua Govina, for the laughs, pizza and lunch lectures we had together.

My family and friends from home: My mom, dad and brother, for all the weekly calls we have had. I have learned to appreciate and value the things I have so much more since I started living in the USA. You have been a great motivation for me to keep up and a listening ear when I most needed it. Dad, you helped me share my biggest challenges and overcome them together. My aunt, for sharing her experience and supporting me with my biggest decisions. My dear friends from home, to keep me happy, supporting me and going throughout the thesis. Sharing my setbacks helped me overcome them easier and help me focus on my goals. The laughs I had during the calls and the fun sharing our experiences. And of course, my dear roommates in Delft for our great time together.

My U-BASE friends: My time at TU Delft wouldn't have been the same without them. I remember the countless "study trips", activities, drinks, coffee breaks, exam weeks and lunch times together. Also, the hard work we did together as board 7 of U-BASE and the committees I worked with. You have made my time in Delft unforgettable.

My UMass Amherst friends: Starting from scratch in a different country can be difficult, but with my friends and housemates it was very easy to get along and settle. Thank you for being there and making my time so far unforgettable. I will remember the numerous trips and the activities together forever.

Summary

Currently, there is lack of understanding in the use of auxetic metamaterials in structural engineering applications. The definition of an auxetic material is that it laterally contracts under compressive loads, in other words having a negative Poisson's ratio. As a result, a concept is expanded where auxetically boosted confinement is actively confining reinforced concrete members. However, There are many structural elements that are subjected to different types of loading, like compression, bending, tension and shear. So, how do auxetics behave under these types of loading?

The aim of the research is set in terms of goals to contribute to the current academic knowledge and close the research gap when it comes to the use of auxetics for steel reinforcement of structural concrete elements. The research aims to contribute to a sustainable construction sector, by using less material on the structural design without compromising the structure's safety. Moreover, literature shows that an increase of 140% of the compressive strength and ductile post-peak behavior is obtained when compared with conventional rebar, which is desirable for structural applications. In this work, the following goals are set to achieve a better understanding on the structural behavior of auxetics:

1. Describe the state of the art regarding auxetic materials and its contribution as confinement to concrete structural elements.
2. Discuss how auxetics perform under different loading conditions such as compression, tension, shear in the principal directions and pure bending.
3. Develop a geometrical design of auxetics that can be used as steel reinforcement for a structural element, such as a beam.
4. Perform a numerical analysis on the proposed beams by putting the beams under several loading conditions, such as compression, tension and bending. Furthermore, make comparisons on the Young's modulus and Poisson's ratio.
5. Describe the state of the art solutions for the upscaling of architected metamaterials.

From there, the report is following a step-by-step approach to obtain the main findings of this work. First of all, a literature study is performed to understand the use of different auxetics and their structural behavior when used as steel reinforcement for concrete structural members. Furthermore, one architecture must be chosen that is feasible for use in civil engineering applications. Moreover, it can be subjected to different loading conditions such as: compression, bending and tension while maintaining the benefit of active confinement. Besides, the architecture must be manufacturable using Laser Powder Bed Fusion (LBPF) and allow flow of mortar.

Secondly, a geometrical study is then performed with the chosen architecture. The goal of the geometrical study is to find an architecture that can accommodate several loading conditions such as: compression, tension and bending. A cantilever beam is chosen as structural element, which is subjected to rotation at the edge. With that, pure bending should be ensured in the beam using linear geometry, where a constant moment curve and zero shear along the length of the beam is expected. Moreover, the neutral axis of the beam is located in the middle and a gradual change from compression to tension is subjected to the beam. The architecture that is chosen for the 3D unit cells, must be feasible for stacking towards larger tessellations. Moreover, compatibility of the nodes must be ensured to have a continuous lattice.

Several unit cells need to be designed to achieve desired behavior of the lattice regarding the loading conditions it is subjected to. Moreover, the architecture must have the ability to be easily modified in to auxetic, cubic, non-auxetic for gradual change of behavior. From there, several beams need to be designed that can be used as steel reinforcement for concrete members. With that, issues regarding compatibility of the nodes and change in relative density of the unit cells can be found and compared. From there changes can be made in the design of the unit cells to have continuous structural behavior

in the lattices, which are studied for the numerical study.

Thirdly, the designed unit cells and beams in the geometrical study are used for the numerical study using the FEM software ABAQUS. In the numerical study the effective uni-axial Young's modulus of the unit cells and beams are needed to validate the models in accordance with literature. From there, a situation of pure bending can be created of the beam. With that, according to Euler-Bernoulli beam theory the following things can be concluded: the moment along the length of the beam should be constant, the shear should be zero, what effective modulus can be used, what moment of inertia is leading and finally if the Kappa remains constant. Furthermore, a study in Poisson's ratio is needed to validate if the active confinement is actually achieved with the proposed designs in the geometrical study. Values over the height of the beams will explain the behavior of the bare steel lattice under pure bending. Also, the influence of the boundary conditions is studied to understand how a clamped edge influences the results on the effective modulus as the tessellation increases.

Finally, literature is studied for possible technologies for the upscaling of auxetic lattices. Auxetics are currently only manufactured using LBPF technologies, where lattices on a small scaled are made. The goal here is to understand what is needed to manufacture a lattice on full scale using conventional rebar for concrete elements.

Based on the research in this report, the following approach is followed:

1. In this research, a bow-tie architecture is selected. Bow-tie lattices have the advantage that they can be easily modified into convex, cubic and auxetic lattices by changing the angle of the strut. This is directly related to the lattice having auxetic or non-auxetic behavior. Besides, the bow-tie architecture is manufacturable using Laser Powder Bed Fusion (LPBF) and has enough spacing for mortar to flow inwards.
2. Furthermore, a work approach is proposed, where the following ”single cells” are introduced: auxetic, cubic and non-auxetic based on the angle of the re-entrant strut. Where auxetic is <90 degrees, cubic is 90 degrees and non-auxetic >90 degrees. A column is an example where single angle cells can be used, which are mainly under compressive loading conditions. To accommodate a changing load within a beam, so called ”three angle” unit cells are introduced. Three angle cells include a gradual change of angle in steps of 2.5 degrees to accommodate the change of load in a beam. Finally, a range of unit cells between 80-100 degrees is chosen, given the fact these angles result in the most confining pressure.
3. A design expansion is then performed, where a 14x14x14 mm single unit cell is repeated in x-y-z direction towards a 3D lattice in the form of several beams given the dimensions of 4x4x20 unit cells, which resembles a bounding box dimension 56x56x280 mm. These dimensions are printable using Laser Powder Bed Fusion (LBPF) and take into account a relative density of 5% similar to the volume of steel in conventional steel reinforcement applications for structural concrete elements. A stacking sequence is developed, leading to an auxetic (85), cubic (90), non-auxetic (95), combined (85/95) and gradual (80to100) beam.
4. Given the complexity of the designed unit cells, linear geometry is used in the numerical models. It is concluded that constant moment curves are indeed obtained from the numerical models and zero shear is found, see Figure 4.7. Using analytical expressions of simple Euler-Bernoulli beam theory, it is concluded that the effective modulus of the beam becomes the dominating factor for the geometry of the lattice. Whereas, the moment of inertia remains constant over the length of the beam.
5. Based on the Poisson's ratios, a proof of concept is presented where the designed gradual changing beam from auxetic to non-auxetic has inwards behavior to accommodate the change in load from compression to tension over the height of the beam. This is favorable in civil engineering applications since the steel reinforcement will actively confine the concrete under loading.
6. Using multi-robotic fabrication, two or more robots work simultaneously together, where one robot places the bars and another robot performs the welds between the nodes. With that, the technology can fully automate the process of assembling an auxetic 3D lattice consisting out of conventional number #3 rebar. Different software, such as Rhinoceros 7 for Grasshopper and COMPAS

FAB are used to design the geometry and control the robots. Moreover, a layer-by-layer sequence is developed which enables the robot to successfully built the lattices without having collisions.

Finally, a summary of the findings of this report are presented below:

- The formula from Yang et al. for rectangular sections is modified towards circular sections, which is used for validation of the numerical models [34].
- From Euler-Bernoulli beam theory and the numerical results it is found that along the length of the designed beams using linear geometry:
  - Constant moment- and zero shear curves are obtained.
  - The moment of inertia is constant and related to the bounding box dimensions.
  - Effective modulus is the leading factor for the geometry of the beam.
  - Kappa slightly changes since the planes don't remain plane as assumed in Euler-Bernoulli beam theory. Due to the small applied rotation these results are however minimal.
- It is found that for beams under pure bending created from single angle cells that a symmetric behavior of Poisson's is obtained over the height of the beam. The Poisson's ratio remains either negative (0 to -0.041) for the auxetic beam and positive for the cubic (0 to 0.05) and non-auxetic (0 to 0.13) beam. When combining cells a changing Poisson's ratio of -0.031 to 0.13 is created for the 85/95 beam and -0.1 to 0.22 for the gradual beam. From these results, it can be concluded that the 85/95 and gradual changing beam are fully actively confining as steel reinforcement for the concrete structural element.
- It is confirmed with a tessellation study that the boundary conditions are not significantly effected in a comparison between 10, 20 and 40 unit cells in length.
- A peak load of 403 kN and a negative Poisson's ratio is found for an upscaled lattice of 512.3 x 512.3 x 527.4 mm following the design approach presented in this report.

Terminology

Term	Definition
Auxetics	Auxetics are structures or materials that have a negative Poisson's ratio. When stretched, they become thicker perpendicular to the applied force. This occurs due to their particular internal structure and the way this deforms when the sample is uniaxially loaded.
Architecture	The architecture of the lattice structures plays an essential role in the overall performance of the component, rendering a superior combination of mechanical and physical properties rather than their constituent materials.
Convex	Convex refers to the positive angle or "directed outwards" taken from the horizontal plane.
Cubic	Cubic refers to a zero degree angle taken from the horizontal plane. With that bounding box dimensions of a unit cell are identical in x-,y- and z-direction.
Laser Powder Bed Fusion	Powder bed fusion (PBF) methods use either a laser or electron beam to melt and fuse material powder together. The Powder Bed Fusion process includes the following commonly used printing techniques: Direct metal laser sintering (DMLS), Electron beam melting (EBM), Selective heat sintering (SHS), Selective laser melting (SLM) and Selective laser sintering (SLS).
Lattice	A lattice is a structure from a 3D tessellation of unit cells in x-, y-, and z-direction.
Metamaterial	The concept of metamaterials (meta means 'beyond' in Greek) was originally defined as novel artificial materials with unusual electromagnetic properties that are not found in naturally occurring materials. Recently, the concept of metamaterials has been extended to a class of materials whose effective properties are generated not only from the bulk behavior of the materials which produce it, but also from their internal structuring.
Non-auxetics	Non-auxetics are structures or materials that have a positive Poisson's ratio. When stretched, they become thinner perpendicular to the applied force. This occurs due to their particular internal structure and the way this deforms when the sample is uniaxially loaded.
Hexagonal honeycomb (bow-tie)	The widely studied hexagonal honeycomb (i.e., non-auxetic) and its auxetic counterpart, the re-entrant hexagonal honeycomb structure.
Re-entrant	Re-entrant refers to the negative angle or "directed inward" taken from the horizontal plane.
Selective Laser Melting (SLM)	SLM is a printing technique from the LPBF method used to manufacture higher metallic products, such as metallic and ceramic components.
Unit cell	A unit cell is a repeating unit formed by the vectors spanning the points in the form of a certain architecture.

Contents

List of Figures

List of Tables

1

Introduction

1.1. Context

In recent work, a feasibility study is performed on the upscaling of metamaterials using auxetics as confinement [26]. A first take on the upscaling of auxetics using conventional rebar is performed. The research is showing potentially new ways of using steel reinforcement in concrete. Besides, it describes procedures and protocols for using robotics to manufacture auxetic lattices. In recent research at UMass (University of Massachusetts) Amherst, different auxetic architectures such as the re-entrant bow-tie and double pyramid are created. A technique, called Laser Powder Bed Fusion (LPBF) is being used to manufacture the steel lattices, which are tested under compressive loading. In research by Tzortzinis et al. (2022) it is proven that an increase of 140% of the compressive strength was reached and ductile post-peak behavior when compared with conventional rebar, which is desirable for structural applications, see Figure 1.1 [29].

Besides structural elements, such as columns, which are mainly under compression, several other structural elements are often used in civil engineering. Beams for example are subjected to several types of loading, such as: compression, tension, shear in multiple directions and bending. Besides auxetic architectures, non-auxetic architectures become interesting or even a combination of the architected material which may benefit the concrete element. So far, to the best knowledge of the author no combination of an architected material is used, which benefit as steel reinforcement for concrete structural elements. Combining different types of architected materials leads to issues regarding compatibility. Therefore, adjustments must be made in the geometry in order to ensure compatibility and with that a continuous structure. Besides, change in load is expected when elements are subjected to bending. A gradual transition is therefore needed of an architected material that can accommodate the change of loading on the structural element. The concept of active confinement becomes important to ensure confining pressure of the steel reinforcement throughout the concrete structural element. By obtaining the Poisson's ratio of a strut of the lattice a conclusion can be drawn on the pressure of the steel strut on the concrete. Active confinement is ensured when inward behavior is found throughout the whole lattice.

Furthermore, compared to several sectors such as: agriculture, manufacturing and wholesale and retail, productivity in the construction sector is currently limited [7]. We therefore need state-of-the-art solutions in order to increase our productivity and be more efficient. The combination of multiple robots in construction offers significant advancements and possibilities. By having one robot holding an item while another robot performs tasks on the product, construction speed and precision can be greatly increased, showcasing substantial potential for further research [23]. The research has demonstrated that robotics can effectively create spatial structures with desirable structural behavior, flexibility, and efficient fabrication using manual welding. Combining the concept of steel reinforcement lattices and state-of-the-art solution would be of great benefit to our society. With that, there is enormous potential in auxetics for civil engineering applications.

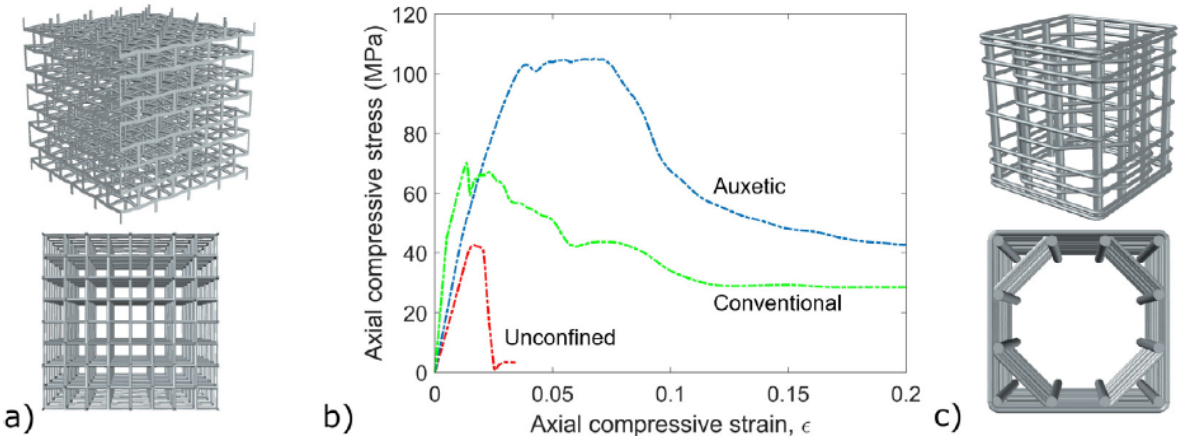

Figure 1.1: (a) New proposal for a steel reinforcement lattice of the auxetically confined model, (b) An comparison between computationally derived stress–strain curves of unconfined (red), conventionally confined (green) and auxetically confined (blue) members under compression demonstrating the significant increase in strength and ductility when the auxetic lattice is used for confining the member, (c) Conventional passive confinement configuration [29]

1.2. Problem

Currently, there is a lack of understanding in the use of auxetic metamaterials in structural engineering applications. The definition of an auxetic material is that it laterally contracts under compressive loads, in other words having a negative Poisson's ratio. However, there are many structural elements that are subjected to different types of loading, like compression, bending, tension and shear. So, how do auxetics behave under these types of loading? And wouldn't combining auxetic and non-auxetic architectures be beneficial when elements are subjected to different types of loading. Besides, auxetics are now mostly manufactured on small scale using techniques such as LPBF. But how do auxetics behave in full scale applications versus using conventional rebar? And with that, what state-of-the-art solution could help essemble upscaled structures Figure 1.2 is providing a possible application for the use of auxetics as steel reinforcement for concrete elements.

Figure 1.2: Composite behavior of an auxetic lattice as steel reinforcement for a concrete element [29]

1.3. Goal

The aim of the research is set in terms of goals to contribute to the current academic knowledge and close the research gap when it comes to the use of auxetics for steel reinforcement of structural concrete elements. The research aims to contribute to a sustainable construction sector, by using less material on the structural design without compromising the structure's safety. The following goals are set for this research:

1. Describe the state of the art regarding auxetic materials and its contribution as confinement to concrete structural elements.
2. From literature discuss how auxetics perform under different loading conditions such as compression, tension, shear in the principal directions and bending.
3. Develop a geometrical design of auxetics that can be used as steel reinforcement for a structural element following the concept of active confinement, such as a beam.
4. Perform a numerical analysis on the proposed beams by imposing the beams under several loading conditions, such as compression, tension and bending. Furthermore, make comparisons on the Young's modulus and Poisson's ratio.
5. Describe the state-of-the-art solutions for the upscaling of architected metamaterials. From there a state-of-the-art solution needs to be selected that is suitable for the upscaling of architected metamaterials using conventional rebar.

1.4. Research questions

In order to reach the goal of this study, the research questions are reported below. The MSc thesis is divided in parts, including: literature review, modelling, an outlook and the research outcome.

Part 1 - Literature Review
The first part of the thesis is discussing the state of the art of auxetics and their architectures, following by discussing the use of the LPBF technology and finally the current practice for using steel reinforcement in concrete. The following questions are used to reach the first goal:

1. Auxetics
    (a) What is an auxetic and how can it contribute as confinement for concrete structural elements?
    (b) What type of auxetic architectures could be used as confinement for different types of structural elements, like columns, walls and slabs?
    (c) What is laser powder bed fusion (LPBF) and how can auxetics be manufactured with LBPF?
    (d) What structural behavior is found when applying different types of loading conditions on auxetics?

Part 2 - Modelling
In part two, an expansion will be made towards the geometrical design of several beams, followed by a numerical study of the chosen designs.

1. Geometrical study
    (a) What is the influence on the structural behavior of unit cells when a change in angle is performed?
    (b) What design for a beam is favorable when it consists out of different types of unit cells as steel confinement for concrete?
2. Numerical study
    (a) What is the structural behavior of an auxetic material when different loading conditions such as: compression, tension and bending are applied?
    (b) What is the structural behavior of auxetics using different geometries?

Part 3 - Outlook
Potential technologies for the upscaling of architected metamaterials for applications in civil infrastructure are discussed in part 3.

- What state of the art technologies could be used for the upscaling of auxetic lattices and how can they be implemented?

Part 4 - Research outcome
The final part concludes the study with the findings of the research, which enables to give conclusions and future recommendations, the following main research question is set:

Main research question:

- To what extend can architected metamaterials as steel reinforcement be used in concrete structural elements under different types of loading, such as: compression, tension and pure bending.

1.5. Methodology

Following from the previous chapter a methodology is set on the goals mentioned in section 1.3. In which, the given structure in section 1.6 is followed. Furthermore, In order to have a feasible thesis project within the given time a scope is prescribed.

1.5.1. Modelling

To reach the end goal of the MSc. thesis a methodology is given, which is described step-by-step. The conclusions found will be combined in the last chapter and discussed. Finally, recommendations will be given for future research.

1. Choose an auxetic architecture that is suitable for concrete structural elements. The architecture must allow modifications from auxetic to cubic to non-auxetic behavior and maintain it's compatibility. Furthermore, space for flow of mortar needs to be guaranteed and finally the architecture must be suitable to manufacture using LBPF.
2. A geometrical study needs to be performed to expand single unit cells towards tessellations of beams that are subjected to compression, tension and pure bending. Modifications in design of the unit cells need to guarantee compatibility and similar relative densities. Furthermore, a combination of unit cells is needed to ensure active confinement of the steel reinforcement in the beam. The Poisson's ratio for a linear elastic material shows the deformation of the reinforcement. The Poisson's ratio will therefore conclude the performance of the steel reinforcement inside the beam. Besides that, a gradual changing load is expected in a beam under pure bending. For that reason, a unit cell must be designed that can be subjected to a changing load from compression to tension.
3. Firstly, the designed unit cells need to be deformed in the elastic region to obtain the effective modulus of the unit cells under compression and tension. From literature, an analytical expression is needed to validate the numerical results. Furthermore, by applying pure bending boundary conditions and using Euler-Bernoulli beam theory, conclusions can be drawn on the influence of parameters such as: the effective modulus, the moment of inertia and kappa. Besides, it should be confirmed that the moment curves are constant and zero shear along the length of the beam.
4. To validate the concept of active confinement the Poisson's ratio should be obtained over the height of the beam for all numerical models. A negative Poisson's ratio under compressive loads and positive Poisson's ratio under tensile loads will prove lateral inward behavior of the steel reinforcement and ensure active confinement.
5. Finally, a state-of-the-art technology is needed from literature to show that upscaling of architected materials is feasible. From there, with Grasshopper for Rhinoceros 7 a parametric model can be made that follows a building sequence of the struts that will allow full assembly of an upscaled lattice. Lastly, a numerical study will discuss what test set-up is required for the peak load of an upscaled auxetic lattice.

1.5.2. Scope

In order to make the research feasible for a MSc. thesis a certain scope is set, which is listed below:

1. Research is performed on bare steel unit cells and beams.
2. Create numerical models using beam elements consisting of auxetic, cubic, non-auxetic and combined geometries. in which, different types of loading, such as: compression, tension and bending are acting on the model.
3. Elastic behavior for steel is considered in the numerical models, plastic behavior would be a next step for future research.
4. Linear geometry is used in the numerical models.
5. The research is investigating current state of the art solutions for upscaled steel auxetic lattices in civil engineering applications.

1.6. Structure

An overview of the research approach is listed in Figure 1.3 below.

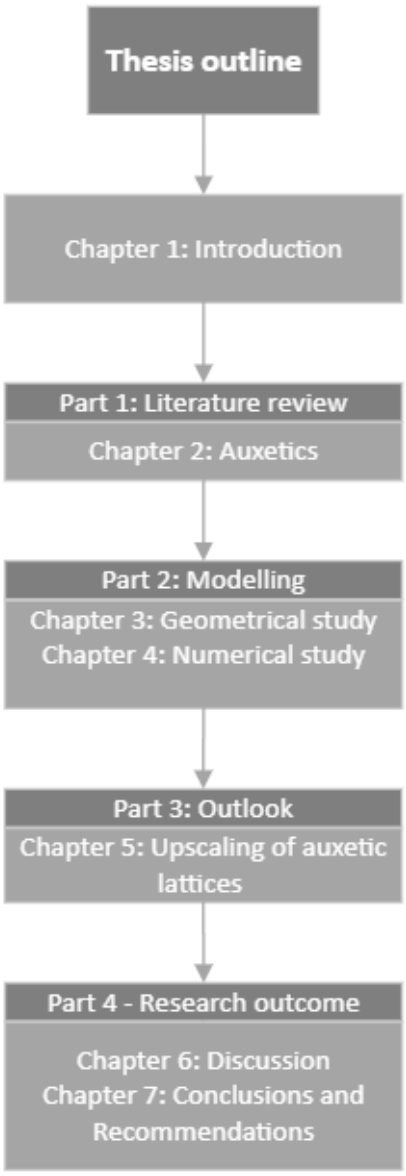

Figure 1.3: Outline thesis [2]

2

Litature review - Auxetics

In this chapter, literature is discussed to explore research gaps regarding the use of auxetics. The focus of the literature study is on the following:

- **Definition:** States the definition of an auxetic and how it can positively contribute as confinement to concrete.
- **Architecture:** To explore what types of auxetic architectures are studied in literature and what their structural behavior is.
- **Laser powder bed fusion:** Discusses the new emerging technology Laser Powder Bed Fusion (LPBF) and it's possible contribution to this research field.
- **Auxetics under different types of loading:** To study the behavior of auxetics under different types of loading conditions such as: compression, tension, shear in all principal directions and bending.

Finally, a conclusion is presented on the findings of the topics listed above.

2.1. Definition

Additive manufacturing, commonly referred to as 3D printing, has experienced significant growth in recent years due to its superior manufacturing efficiencies and increasing economic attractiveness. However, this technology also introduces unwanted defects such as surface roughness, imperfections, stress concentrations, deformations, and porosity, resulting from processing parameters such as laser speed and energy, powder thickness, and anisotropic mechanical properties [9].

Auxetic materials, which exhibit a negative Poisson's ratio and laterally contract under compressive loading, have emerged as a new generation of materials in the market. The architecture of a re-entrant lattice is a key factor in defining its auxetic behavior [3], where re-entrant refers to the negative angle or "directed inward" [15]. However, manufacturing of auxetic materials is challenging due to their complex architecture. LPBF is a new manufacturing technique, in which Selective Laser Melting (SLM) is used for higher melting products such as metallic and ceramic components, but it is more expensive than Selective Laser Sintering (SLS). Where, SLS is a suitable alternative for lower melting products such as nylon [12]. Besides, lattices with overhanging geometries and horizontal struts are difficult to manufacture using SLM due to heat conditions and laser limitations [24]. The choice between both technologies is therefore based on the desired end result.

Hao et al. used the Multi Jet Fusion (MJF) technique to manufacture specimens and investigate the compressive properties of different architectures [14]. They found that all lattice reinforced specimens demonstrated an increase in compressive strength. SLS is a similar technique with a slightly lower quality surface finisher, fine feature resolution, and less consistent mechanical properties [22]. It is commonly used to fabricate parts such as plastics, polymers, and resins with a low melting point.

2.2. Architecture

The architecture of truss-lattice materials is critical to the performance of concrete confinement. Gross et al. investigated four different truss-lattice architectures and found that truss-lattice materials are more sensitive to defects when they are less connected than their more connected counterparts [11]. Therefore, it is crucial to consider an architecture with the least number of defects and the best mechanical properties.

In the field of research, various lattice architectures, such as hexagonal honeycomb and re-entrant hexagonal honeycomb, have been explored using LPBF to investigate their auxetic properties [16]. However, the primary objective of this research was not to find an optimized architecture, but rather to separate the surface area and mechanical properties. Additionally, Geng et al. investigated other truss lattice architectures, including Gurtner-Durand, octet, octahedron, and tetrakaidecahedron, using two-photon lithography, with the focus on damage characterization of the architectures. The results showed a significant geometric error between the CAD model and the actual product, with unexpected failures such as bending of the struts and higher stress concentrations [9]. Moreover, a study using SLS was conducted, exploring more regular architectures such as circular, octagonal, strengthened octagonal, RO (rhombicubactahedron), cubic, and Kelvin, and it demonstrated that thermoplastic lattices also contribute to the mechanical properties of confined concrete. All lattices also contributed to higher strength, with the octagonal architecture performing the best with a 71.36% higher strength compared to the plain concrete specimen.

As discussed above, there are numerous of architectures that all result in different mechanical properties. In Figure 2.1 an overview of positive- and negative Poisson's ratio (NPR) architectures is given. The most common auxetic architectures are discussed below.

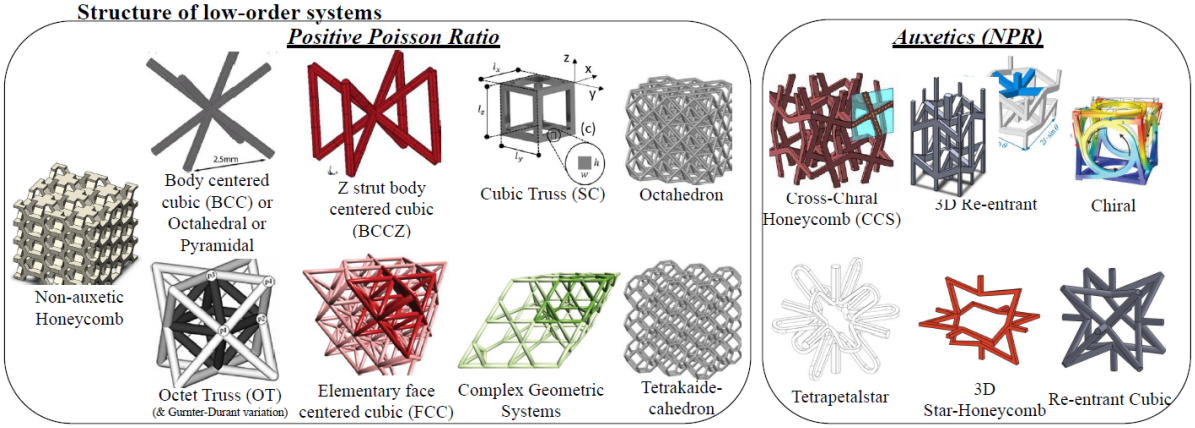

Figure 2.1: Geometric systems of 3D truss lattices [30]

2.2.1. Auxetic architectures

There are several architectures which are classified as auxetic, such as: a re-entrant bow-tie, re-entrant double pyramid and chiral architectures. In this part, the auxetic architectures are discussed, including the expansion into a three-dimensional architecture.

Re-entrant bow-tie

The first architecture which is discussed, is the re-entrant bow-tie. According to research by Master & Evans, deformation can occur due to three mechanisms, which are: hinging, flexure and stretching. Besides, It is found that by comparing regular isotropic bow-tie and re-entrant cells, that re-entrant cells are truly anisotropic [20]. Furthermore, a re-entrant bow-tie does have an increased transverse Young's and shear modulus compared to a regular bow-tie under the same relative density [27]. where the transverse shear modulus is also depending on the strut slenderness ratio (w/l) [25]. Another aspect, is the strut thickness, when reducing the strut thickness for the diagonal struts and maintaining a constant thickness for the vertical struts, a decrease in E_x and E_y is observed, but an increase for

the Poisson's ratio in ν_{yx} and ν_{xy}. However, while keeping the thickness of the vertical strut constant and decreasing the diagonal thickness both E_y and ν_{yx} decrease [31]. This is because the vertical ribs do not deform when loaded in x-direction and are therefore redundant. Moreover, the main cause of deformation is concluded to be flexing of the diagonal struts when the difference in thickness is similar or lower than the vertical struts. But, when load is applied in y-direction, stretching will be the dominant failure mode, when the vertical strut thickness is significantly lower than the diagonal rib [31].

Furthermore, an expansion into three dimensional re-entrant structures is discussed, which enables the auxetic being applicable for structural engineering applications as steel reinforcement. to ensure repeatability many researchers chose to use additive manufacturing to study the behavior of 3D re-entrant structures. In research by Yang et al. it is shown that at similar relative densities a 300% higher strength can be obtained when comparing a metallic and foam structure [33]. Besides, a smaller re-entrant angle also leads to an increase of 400% in strength. in research by Geng et al. the geometry of an 3D re-entrant bow-tie is shown [9]. In Figure 2.2 the architecture is shown of a 3D re-entrant bow-tie. Since the angle of bow-tie is smaller than 90 degrees the auxetic behavior is obtained.

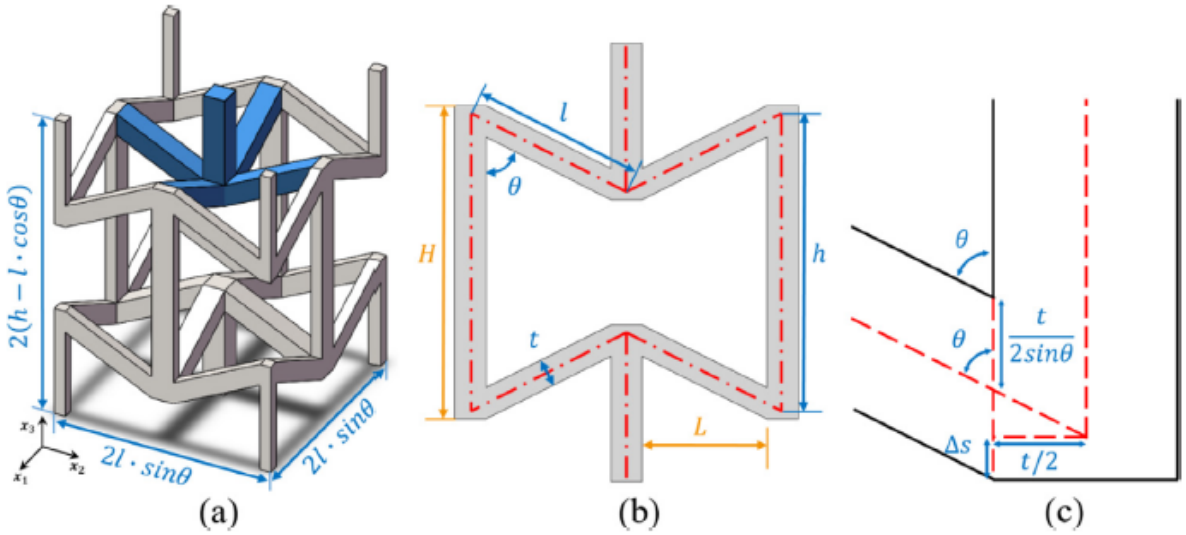

Figure 2.2: architecture 3D re-entrant bow-tie: a) Unit cell, b) geometry parameters and c) the geometric relation of the node [9]

In research by Georgios et al. a 3D re-entrant architecture is proposed, specifically the bow-tie, as confinement, and demonstrated that an increase of compressive strength up to a 140% and post-peak ductile behavior can be obtained [29]. This is explained by the reinforced material being resilient and besides maintaining a high load carrying capacity even after local failure of the steel struts in the lattice. As a result, the study of lattice architectures is being expanded into different re-entrant angles, namely 75, 80, and 85 degrees, with a focus on studying and comparing their mechanical properties and contribution to the composite action with concrete. A next step would be to upscale this architecture to a conventional rebar size used in practice.

Double pyramid

Besides, the re-entrant bow-tie, a double pyramid architecture was first proposed in research by Larsen et al. [17]. It is confirmed that intersecting double pyramid architectures, changing length ratios and angles have a direct influence on the Poisson's ratio. Moreover, an anisotropic material behavior is found [18]. Furthermore, the geometrical characteristics of a double pyramid unit cell is presented in Figure 2.3a. In which, a double pyramid cell is defined by three parameters, the length a0 and angles α0 and β0. Furthermore, Figure 2.3b is showing how auxetic behavior can be obtained from choosing several angles of β0 [5]. In research by Brighenti et al. the non-linear deformability of 2D double pyramid plates is investigated theoretically, experimentally and numerically. To do this a rigid link option is introduced to in order to take into account the finite size of the nodes of the analysed specimens. This

correction has enabled good agreement with the experimental results.

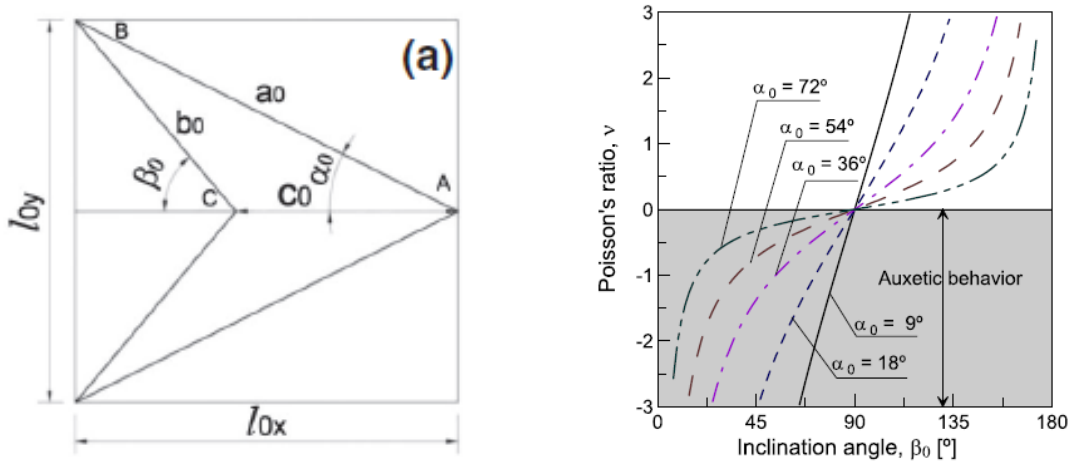

(a) Double pyramid geometry

(b) Poisson's ratio by using several angles

Figure 2.3: Double pyramid unit cell [5]

Chiral

First of all, in research by Kolken et al. chiral structures are discussed. A characteristic of a chiral structure is the central cylinder attaching the ligaments tangentially. Furthermore, under mechanical loading the ligaments will flex due to rotation. Depending on the type of loading, the ligaments will either fold or unfold [15]. In research by Novak et al. an auxetic chiral architecture is used for a sandwich panel, which is fabricated using Selective Electron Beam Belting (SEBM). The composite sandwich panel is then subjected to compressive loading conditions and the ballistic performance is tested, showing a proof of concept [21]. Apart from the re-entrant and double pyramid architecture, the Poisson's ratio for the chiral cells are independent of their angle. An example of a chiral structure is shown in Figure 2.4.

Besides, for 3D chiral lattices it is found that the Young's modulus and effective shear modulus strongly depend on the number of unit cells per side, which tends to converge to a constant value in the end [13]. Furthermore, an increase in cells tends to decrease the stiffness, while the opposite is observed with the rib-to-slenderness ratio. Finally, a negative Poisson's ratio is reached by a sufficient number of cells.

To conclude, several two-dimensional, three-dimensional and re-entrant architectures are compared with their in-plane Poisson's ratio vs. normalized Young's modulus E/E_p based on several studies. In Figure 2.10 an overview of positive- and negative Poisson's ratio (NPR) architectures is given. In A, it is concluded that re-entrant structures generally outperform rotating rigid and chiral structures. Rotating rigid structures have a high Young's modulus by the amount of bulk material included, but in turn decreases the Poisson's ratio. And, chiral structures have an extra degree of freedom which explains the relatively low stiffness. From there an expansion towards 3D is performed in B, this again concludes better properties for re-entrant structures. Finally, a comparison is made between re-entrant structures in Figure 2.10C, where it is shown that re-entrant hexagonal unit cells can cover a range of mechanical properties. It is therefore stated, that a stiff NPR structure is best obtained by adjustments of parameter for the re-entrant hexagonal unit cell.

Finally, bow-tie lattices have the advantage that they can be easily modified into re-entrant, cubic and convex lattices by changing the angle. This is directly related to the lattice having auxetic, cubic or non-auxetic behavior. Because of this smooth transition the architectures can be manufactured using LBPF and on larger scales using robotics and welds. Moreover, the architecture is enabling sufficient space for mortar to be poured through. This is a critical condition when being used as steel confinement

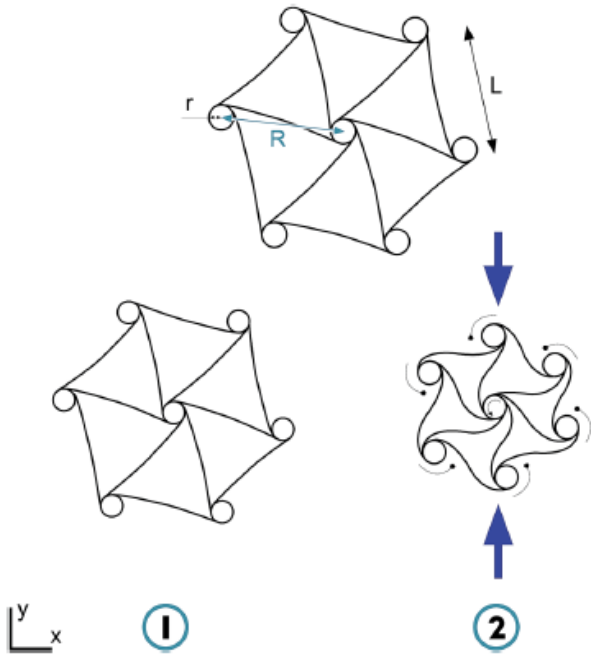

Figure 2.4: Chiral geometry [16]

for concrete elements in civil engineering applications.

2.2.2. Non-auxetic

In Figure 2.2 an auxetic architecture is created by having an angle below 90 degrees. on the contrary, by having an angle larger than 90 degrees the architecture becomes non-auxetic. Therefore, it would expand laterally under compressive loading, meaning a positive Poisson's ratio. In research by Kolken et al. both auxetic and non-auxetic are successfully designed and discussed [15]. Following from the stress-strain curved presented in Figure 2.9 a typical fluctuation is observed after reaching the plateau region. The reason for this, is the collapse of layers within the lattice. Besides, the auxetic lattices are taking a considerable amount of energy because of their behavior.

Furthermore, it is found that both auxetic and non-auxetic show elastic anisoptropic behavior. However, it is confirmed that the normalized effective stiffness values were lower for auxetic designs in upright position than non-auxetic designs. Besides, a Poisson's ratio of 0.747(+/-0.04) is found for the non-auxetic and -0.335 (+/-0.03) for the auxetic lattices. From the Solid TI-6Al-4V compression tests it is shown that an estimated bulk material elastic modulus E_s is obtained of 30.2 GPa. By using the simulated effective stiffness values, a normalized effective stiffness is obtained per lattice.

2.2.3. Combining auxetic and non-auxetic architectures

To the best of the authors knowledge, the performed research on designs consisting out of auxetic- and non-auxetic architectures is limited. It is therefore still an important field to explore for future research.

2.2.4. Active confinement

In research by Georgios et al. a comparison is made between conventional passive confinement of reinforced concrete members based and a new idea is proposed on how to actively confine reinforced concrete members by auxetically boosted confinement [29]. A network made out of an auxetic truss-lattice generates confining pressure even without lateral expansion of the surrounding matrix, see Figure 2.5. Besides, the periodicity in 3D is a main advantage compared to conventional reinforcement, where it is able avoid the weakest link in contrary to the weakest hoop of conventional rebar.

Furthermore, the confining pressure of several bow-tie architectures is shown. Confining pressure

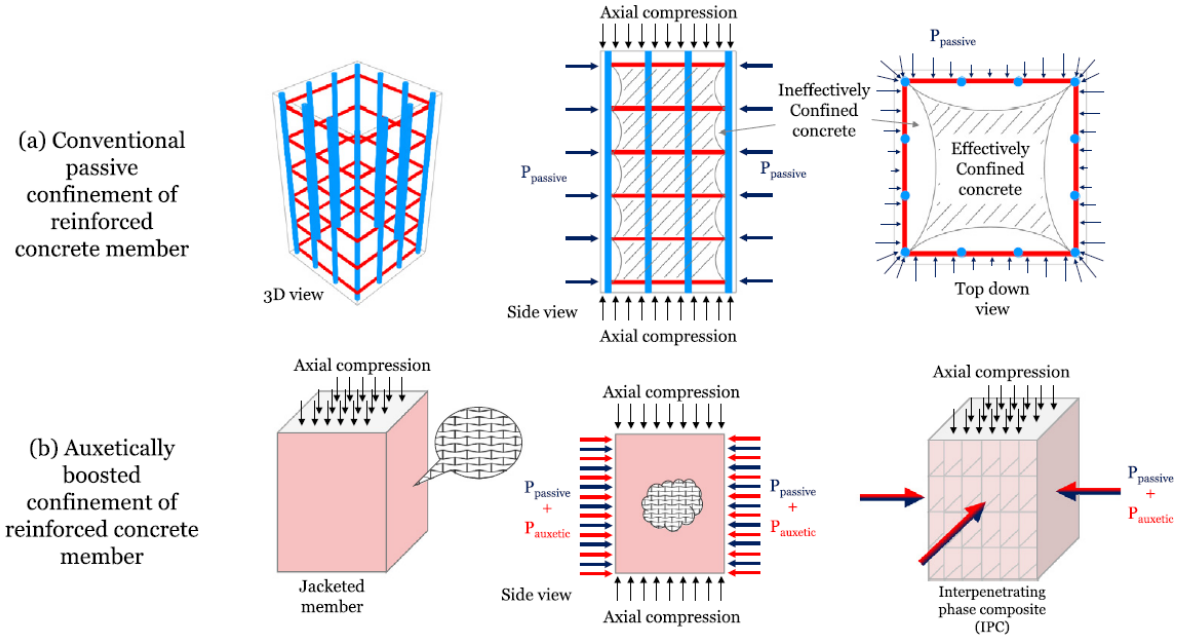

Figure 2.5: Schematic concept of the auxetically confined composite: (a) A reinforced concrete (RC) column passively confined using conventional steel transverse reinforcement bars (in red), (b) a concrete column confined using an auxetic jacket or an interpenetrating phase composite of concrete and an open-cell auxetic network. The confinement pressure is a combination of passive confinement and auxetically-induced confinement [29]

is where active confinement is applying external pressure on a concrete element before loading. It is the auxetic network that generates this confining pressure. From Figure 2.6 it is becoming clear that larger re-entrant angles result in a higher confining pressure up to 140%. However, the transverse modulus tends to drop from 90 degrees and downwards. It is therefore observed that where the lowest Poisson's ratio is observed, the highest confining pressure is acting. A so called analytical Voigt model is then used to validate the finite element (FE) results.

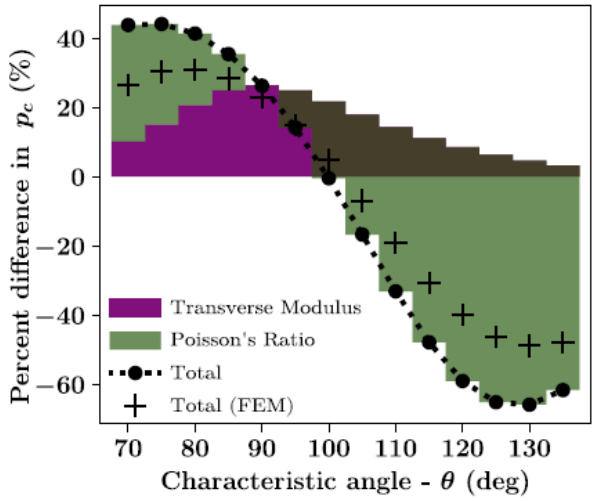

Figure 2.6: Effect on confining pressure relative to pure mortar [29]

2.3. Laser bed powder fusion

As mentioned before a technique called LPBF is the general name for processes such as Selective Laser Melting (SLM) used to manufacture higher metallic products, such as metallic and ceramic components using the EOS M 290. The EOS M 290 has a construction volume of 250 x 250 x 325 mm, which enables it to 3D print steel under strict environmental conditions [8].

Furthermore, LPBF technology can make complicated lattice structures, which has led to research on lightweight structures made up of repeated three-dimensional cells. These structures allow engineers to easily change how strong and dense the final product will be [37]. Since the 3D printed lattices are relatively small, the quality of the prints are greatly influenced by several parameters, such as the slice height, exposure time, points distance and laser power. Therefore a trial and error approach is often used to find the correct printing parameters [16]. But, 3D printing remains a challenge with these complex types of architectures and therefore the geometries have to be printed under an angle, with respect to the base plate. Moreover, the quality of a 3D printed lattice is severely worse with horizontal printed struts due to local heat concentrations in the powder bed. Besides, the mechanical properties generally decrease when printed under an angle. Also, it is concluded that severe errors in the prints can occur by comparing the CAD model and the sample. As a result, significant impact is observed in the mechanical properties in a study by Geng et al. [9].

Next to that, a study with induced fabricated geometric imperfections using LPBF, shows that defects have close relation to the mechanical properties, damage initiation and failure mechanisms of metallic lattices [19]. The imposed defects in this study are strut thickness variation, strut waviness and strut oversizing/undersizing. However, it is mainly the strut waviness and strut thickness variation that can decrease the elastic modulus and compressive strength drastically. By upscaling these geometric defects by 250%, a decrease of 50% is observed for the Young's modulus and 40% for the strength. Whereas, the oversizing/undersizing can control the type of failure. In the linear elastic regime it is found that the Young's modulus is most attached in the building direction as a result of overmelting. 84% and 87% of the young's modulus is reached for X- and Y-direction, whereas 70% for the Z-direction for a regular octet [19].

2.3.1. Parameters

In LPBF, laser power, scanning speed, hatch spacing, and layer thickness are the common process parameters adjusted to optimize the process. Furthermore, Figure 2.7 is giving a clear image of each parameter. Mostly, a trial and error approach is needed to find the correct print parameters. With a gradient size of the printer being 40 microns, the smallest diameter of strut able to be manufactured is 1 mm. The risk of damage and imperfections is becoming to larger when lower diameter are used. To make a valid comparison between conventional rebar applications, a relative density of 5% is used, which is directly influencing the geometry of the lattice that is designed.

2.3.2. Validation

For validation, the most common visual validation parameters are the relative density, strength, microhardness, porosity and surface roughness [37]. Besides, there are several geometric defects that can affect the quality of the print during the process as described before. In terms of bonding to concrete, a certain surface roughness is desirable, which enhances the composite behavior.

2.4. Auxetics under different types of loading

In this part, the behavior of the auxetic and non-auxetic lattices under several types of loading are discussed according to literature. Since the benefit of auxetics are that it laterally contract under compressive loading, where as the non-auxetic material would expand. The behavior of auxetics is therefore worth considering under different types of loading. Furthermore, in research by Vigliotti et al. an extensive procedure is prescribed to perform an analysis on three-dimensional open and closed cell lattices. As a result, stiffness and strength can be determined of three dimensional periodic lattices [1].

Furthermore, in Figure 2.8 the components are given for the nodal DOFs. These can be constrained to obtain the correct boundary conditions for the models. Besides, the normal force, the bending moments

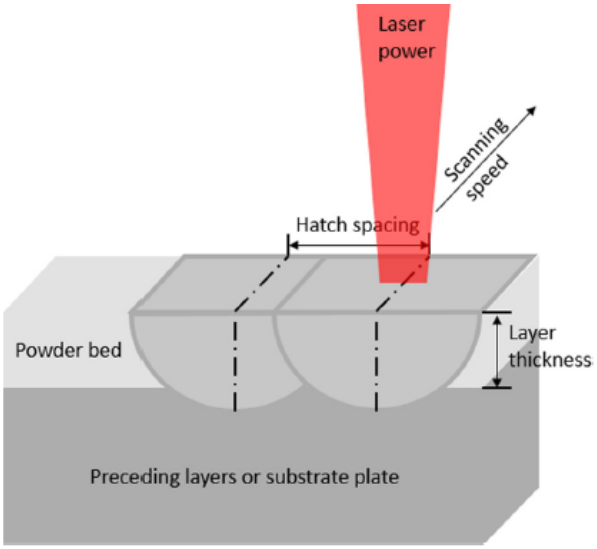

Figure 2.7: LPBF print parameters [37]

and the torsion moments are given by the following equations:

$$N = E_s * A * s \tag{2.1}$$

$$M_y = E_s * I_{zz} * \kappa y \tag{2.2}$$

$$M_z = E_s * I_{yy} * \kappa y \tag{2.3}$$

$$T = \frac{G_s * J_p}{L} * \phi \tag{2.4}$$

Compression

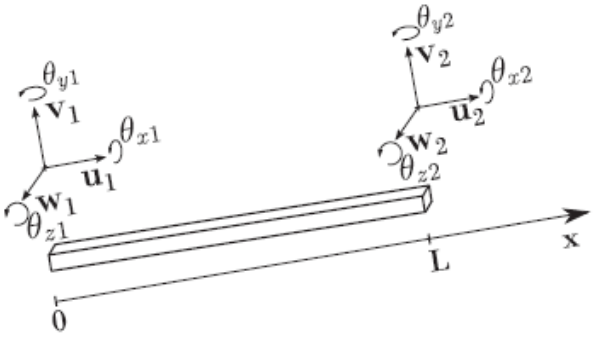

Figure 2.8: Edge and nodal DOFs [1]

In research by Kolken et al., both an auxetic and non-auxetic 3D re-entrant bow-tie are tested under axial compression till up to 5 mm [16]. Furthermore, the experiments were performed in two directions, standing upright and tilting the lattices under a 90 degrees angle. It is observed from Figure 2.9 that ductile behavior occurs in the auxetic lattice, whereas the non-auxetic lattice loses most of the strength directly after reaching the peak load of 50 MPa. Since the material is made out of a porous bio-material, an elastic modulus of about 5000 MPa is achieved.

Besides this, Yang et al. proposes an analytical equation for the effective modulus of an 3D re-entrant lattice structure [34]. This formula comes from a study based on four design parameters:

- Length of the vertical struts (H)
- Length of the re-entrant struts (L)

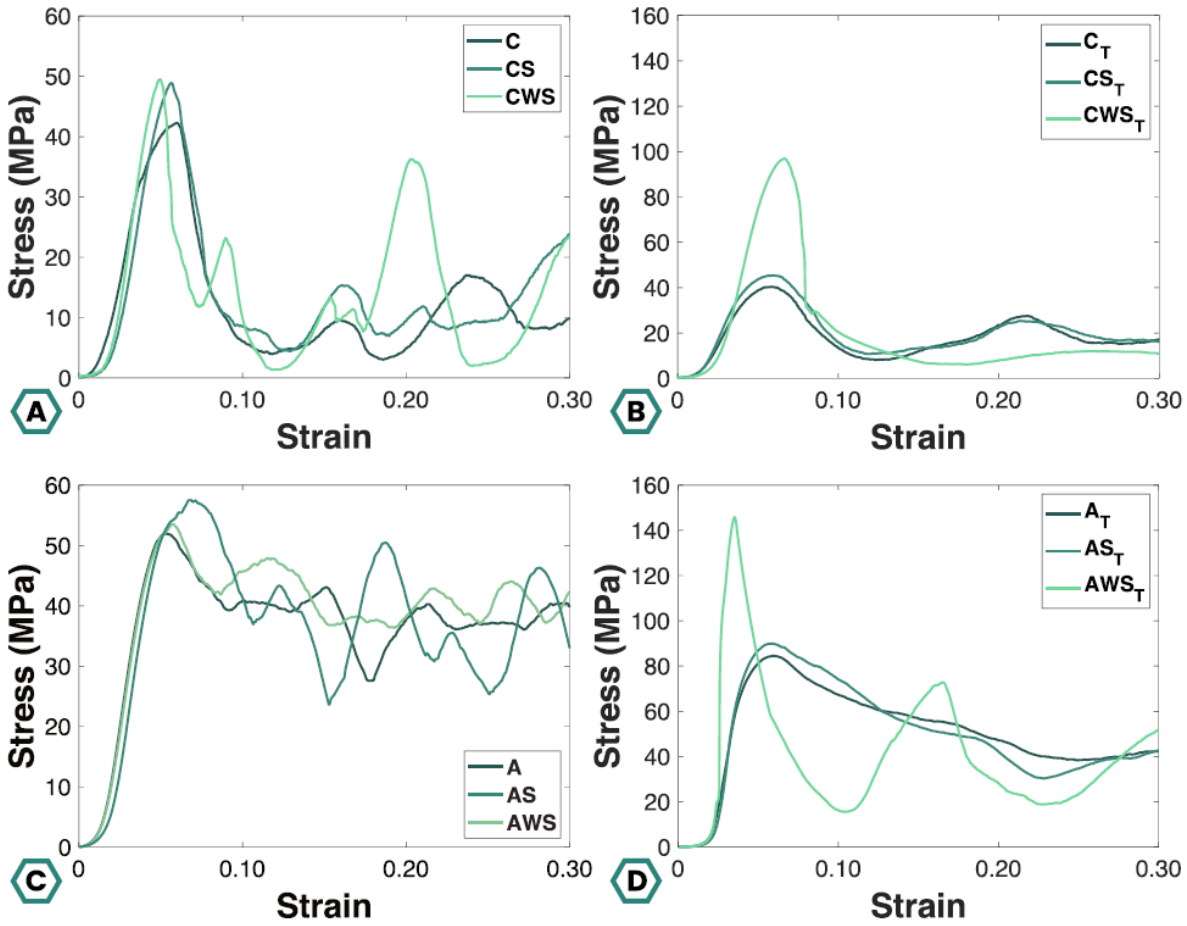

Figure 2.9: Stress-strain curves [16]

- re-entrant angle (θ)
- the square cross-section thickness (t)

Furthermore, a couple of assumptions are used in the study, regarding: the unit cell being part of an infinitely big structure, where boundary effects are being eliminated and maximum structural symmetry retained, the joints in the structure are considered rigid and deformation is primarily caused by bending of the re-entrant struts and axial compression of the vertical struts and finally no torsional effects are considered.

Firstly, the deformation is determined of the vertical struts based on linear superposition. This includes three components, the compressive deformation of the vertical struts, bending induced deflection from the re-entrant strut and the shear-induced deflection from the re-entrant strut.

$$\Delta_{y1} = \frac{2 * \sigma * H * L^2 * sin^2\theta}{E * t^2} \tag{2.5}$$

Furthermore, Timoshenko beam theory is used, for the angle deflection of the re-entrant strut.

$$\theta' = \frac{d\omega}{dx} + \gamma \tag{2.6}$$

Where ω is the deflection of the strut and γ is the shear strain. Which result in the following equations.

$$\frac{d\omega}{dx} = \frac{ML}{EI} \tag{2.7}$$

$$\gamma = \frac{P}{\kappa * GA} \tag{2.8}$$

With the following factors:

- κ is the geometrical factor, where κ= 5/6 for a solid rectangular cross-section [28].
- G is the shear modulus of the material.
- A is the cross sectional area of the strut.

Finally, the deflection angle is determined by combining the previous equations into:

$$\theta_1 = \theta_2 = \frac{ML}{6EI} + \frac{6P}{5GA} \tag{2.9}$$

Where I is the moment of inertia of the cross section. With the assumption of the joints being rigid the angle should remain unchanged following deformation. However, the deflection of the re-entrant strut causing the size change of the structure is expressed as:

$$\Delta x = Lsin(\theta + \theta_1) - Lsin(\theta) \approx L\theta_1 * cos(\theta) \tag{2.10}$$

$$\Delta_{y2} = Lcos(\theta - Lsin(\theta + \theta_1) \approx L\theta_1 * sin(\theta) \tag{2.11}$$

As a result, the effective modulus of a 3D re-entrant lattice structure is obtained as:

$$E_y = \frac{\sigma}{\epsilon_y} = \frac{\sigma(H - Lcos\theta)}{\Delta_{y1} + \Delta_{y2}} = \frac{(\alpha - cos\theta)}{\frac{2\alpha * L^2 sin^2\theta}{Et^2} + (\frac{L^4}{2Et^4} + \frac{3L^2}{5Gt^2})sin^4\theta} \tag{2.12}$$

Where E_y is the effective modulus and E the modulus of the solid material. In Appendix D the calculation is presented to determine the effective modulus of a 3D re-entrant lattice structure.

Tension
It is common practice that elastic properties, such as the effective modulus and Poisson's ratio remain constant, no matter which loading direction. It can therefore before verified if the results of the loading conditions under tension match the compression loading conditions. In research by Yang et al. it is confirmed that the same results were obtained [32]. It is therefore concluded that these type of boundary effects don't play a role.

Shear
Besides tensile and compressive mechanical properties of auxetics, also shear properties such as the shear modulus and shear strength are a main interest. There are three principal directions (xy, xz and yz), which have close relation to the geometrical design of an auxetic. In research by Yang et al. it is concluded that the design of structures are feasible since high shear modulus and shear strength were observed [36]. Besides, a re-entrant auxetic structure faces severe size effect under shear loading.

Bending
Another loading condition is bending, where the flexural properties of the material play a role. In research by yang et al., a re-entrant bow-tie using 45- and 70 degrees is tested [35]. The stiffness of design variation 1 (DV1) is 11.25 (+/-0.43) and design variation 2 (DV2) is 1.88 (+/-0.08) GPa. It is worth mentioning, that the unit cells are stacked down in z-direction. The principal Von Mises stress can be determined following the equation from [34]. In work by Schwahofer et al. several 3D beams using auxetics are proposed using an algorithm. It is stated that the lattice structures have good potential for energy absorption.

2.5. Conclusions

Finally, in this section the conclusions are drawn from the literature study that is performed in this chapter. The following conclusions are drawn:

- In literature it is proven that a 140% increase of mechanical properties and post-peak behavior is observed when using an auxetic re-entrant bow-tie lattice as steel reinforcement for concrete [29].
- There are several auxetic architectures, such as: The re-entrant bow-tie, re-entrant double pyramid and chiral architecture [15].

- Deformation of honeycombs can occur due to three mechanisms, which are: hinging, flexure and stretching [20].
- It is found that by comparing re-entrant and regular isotropic bow-tie cells, re-entrant cells are truly anisotropic [15].
- A re-entrant bow-tie has an increased transverse Young's and shear modulus compared to a regular bow-tie under the same relative density [27].
- for 3D chiral lattices it is found that the Young's modulus and effective shear modulus strongly depends on the number of unit cells per side, which tends to converge to a constant value in the end. An increase in cells tends to decrease the stiffness, while the opposite is observed with the rib-to-slenderness ratio. Finally, a negative Poisson's ratio is reached by a sufficient number of cells [15].
- It is reported that a re-entrant bow-tie architecture in general outperform chiral architectures in terms of their stiffness and Poisson's ratio. This can be explained by the extra degree of freedom that is introduced by the rotation of the cylinders [15].
- Bow-tie lattices have the advantage that they can be easily modified into re-entrant, cubic and convex unit cells by changing the angle. This is directly related to the lattice having auxetic, cubic or non-auxetic behavior. Besides, it enables smooth manufacturing possibilities using SLM. Moreover, a lattice can be produced on a larger scale using conventional rebar and welds. Besides, concrete can be poured through, where it serves as steel reinforcement for concrete elements in civil engineering applications [29].
- Followed from results in stress- and strain curves, typical fluctuations are observed after reaching the peak load of the auxetic and non-auxetic lattices under compressive loading conditions. This can be explained by the collapse of layers within the lattice [16].
- in research by Yang et al. an analytical expression is found for the uniaxial effective modulus of a rectangular 3D re-entrant bow-tie lattice. To make it applicable in this research, a modification towards a circular section needs to be performed. Moment of inertia, effective area and kappa must therefore be replaced [34].
- Manufacturing of auxetic materials is challenging due to their complex architecture. Laser powder bed fusion (LPBF) is a new manufacturing technique in which SLM is suitable for higher melting products such as metallic and ceramic components [1].

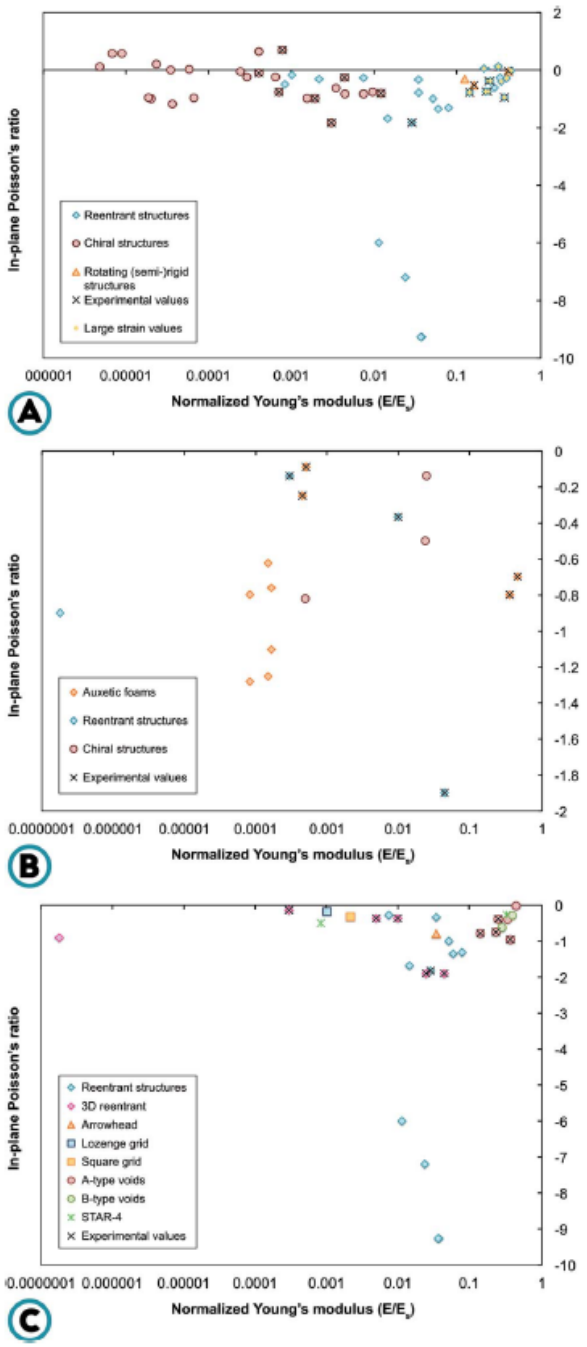

Figure 2.10: Comparison of several articles where Poisson's ratio vs. normalized Young's modulus for (A) 2D and (B) 3D auxetic metamaterials is compared and (C) re-entrant structures [15]

3

Geometrical study

In this chapter a geometrical study is performed on the behavior of different beams using different types of unit cells, such as re-entrant, cubic, convex and combined in AutoCAD. To accommodate different types of loading it is beneficial to combine different geometries of unit cells. This is because an inward behavior is desired for steel reinforcement in concrete elements to ensure active confinement. The use of auxetic and non-auxetic architectures is discussed in chapter 2. It is concluded that re-entrant bow-tie architectures in general outperform chiral architectures. Besides that, a bow-tie can be easily modified from convex to re-entrant, which is in close relation to the architecture being non-auxetic and auxetic. As a result, a bow-tie architecture is applicable as confinement in beams since it will be acting under different types of loading such as compression and tension over the height of the beam when a moment is applied. In this chapter, a design protocol is discussed to create a beam which consists out of auxetic and non-auxetic unit cells to adapt such behavior. At first, the most basic beams are discussed consisting purely out of cubic, convex and re-entrant unit cells. Furthermore, to cope with tension and compressive loading conditions in the beam, an idea is presented where convex and re-entrant cells are combined. Finally, a work approach for a gradual changing beam is presented to accommodate the gradual change of loading over the height of the beam. In short the following parts are discussed:

- **Basic cases:** As a staring point of this chapter, the idea of using re-entrant, convex and cubic bow-tie unit cells for a beam is further explored. In this case, the beams are geometrically modelled and discussed.
- **Auxetic and non-auxetic beam:** To understand the behavior when different unit cells are combined. Furthermore, compatibility issues are disccused.
- **Gradual increase of auxetic to non-auxetic beam:** Several types of geometrical models are discussed to accomodate a changing load with in a structural elements, such as a beam. Special modifications are made and discussed to ensure compatibility between so called three angle cells. The three angle cells geometrically take into account the changing load of the beam.

3.1. Basic cases

As previously mentioned, there are convex, cubic and re-entrant bow-tie unit cells. Moreover, a bow-tie unit cell becomes convex with angles larger than 90 degrees and re-entrant below 90 degrees taken from the vertical plane. Besides, the cell is cubic with exact 90 degrees angles. As a result, same dimensions of a so called ”bounding box” in x-y-z-direction is observed. Whereas, different dimensions are observed with convex and re-entrant cells. This causes compatibility problems when for example convex and re-entrant cells are combined. However, to start simple, some basic cases are described where only the strut length and height is modified to create cubic bounding box dimensions. Firstly, the strut length is modified to create a matching width by using the cosine of the angle. This adjustment is presented in Figure 3.1, in which the cubic cell is used as reference for the length of the re-entrant cell in red. Secondly, the height of the middle struts is decreased for convex unit cells and increased for re-entrant cells, which is presented in blue.

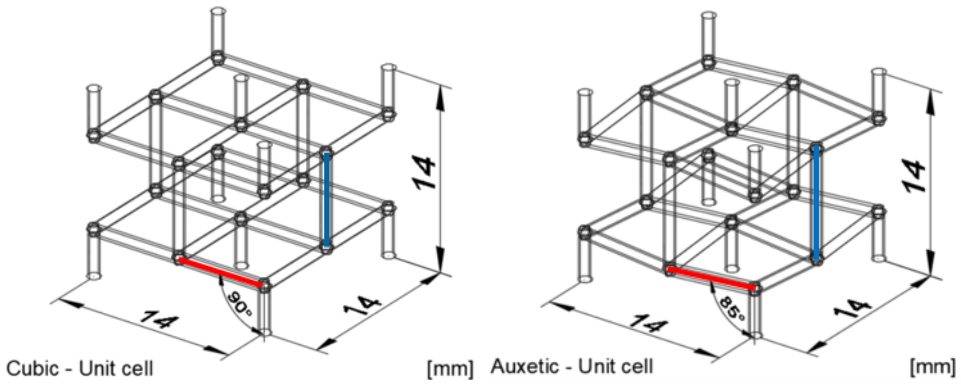

(a) Reference strut length **(b)** Modified strut length

Figure 3.1: Modification strut length

3.1.1. Cubic beam

First of all, a beam consisting out of cubic unit cells is designed based on 3D 90 degrees bow-tie unit cells. A unit cell is cubic when the bounding box dimensions are equal, in this case 14x14x14 mm. A strut length of 7 mm is chosen in combination with a strut thickness of 1.2 mm, to obtain a relative density close to 5%. Currently, 5% is used as conventional steel confinement in concrete elements. Besides, the design for the selective laser melting machine should be as small as possible to reduce costs for printing. From experience, a strut thickness of 1 mm is the lowest value to maintain a good quality print. Furthermore, this unit cell, consists of pure vertical and horizontal struts, which is the simplest case for this type of bow-tie. In Figure 3.2 the unit cell is shown. From there, the unit cells are stacked into a 4x4x20 beam configuration, based on their outer nodes.

In this case, we see from figure 4.3 that the beam has a continuous straight shape without sudden deviations. Besides, the center-to-center distances between the strut are all equal.

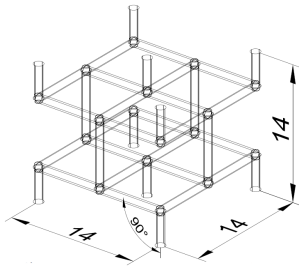

Figure 3.2: 90 degrees unit cell

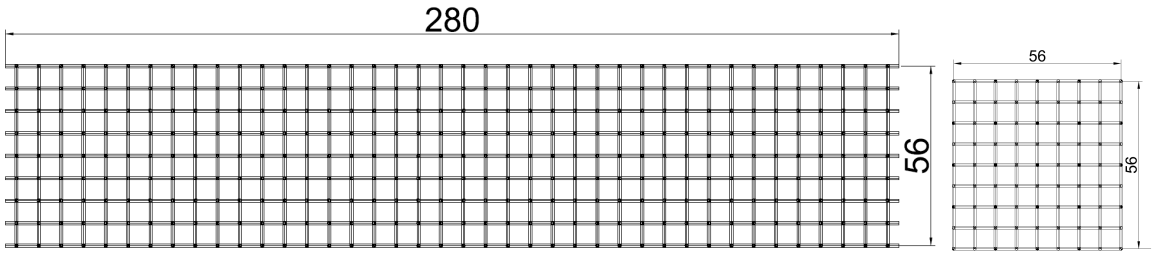

(a) Side view **(b)** Front view

Figure 3.3: Cubic - 90 degrees beam

3.1.2. Non-auxetic beam

Furthermore, a non-auxetic beam is designed from 3D degree bow-tie unit cells. To create a cubic unit cell, the width and height must be modified. For the correct width, a cosine of the angle is taken with reference to the 90 degrees design. Moreover, a 7 mm strut length must be achieved in order to be compatible. Besides, the height of a unit cell increases when a convex bow-tie is chosen, the height of the middle strut must be therefore be decreased. As a result, the box dimensions of 14x14x14 mm are obtained to have equal dimensions of the beam.

In contrast to the cubic beam, variations are observed in the center-to-center distance of the struts. This can be explained by the need to decrease the height of the middle strut to have matching bounding box dimensions. Furthermore, from the side view an overlapping behavior of the struts is observed. In reality this is not overlapping, but since the unit cell is diagonal inwards for the outer struts and outwards for the center struts a difference is observed.

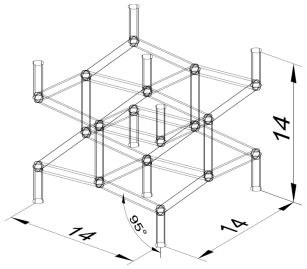

Figure 3.4: 95 degrees unit cell

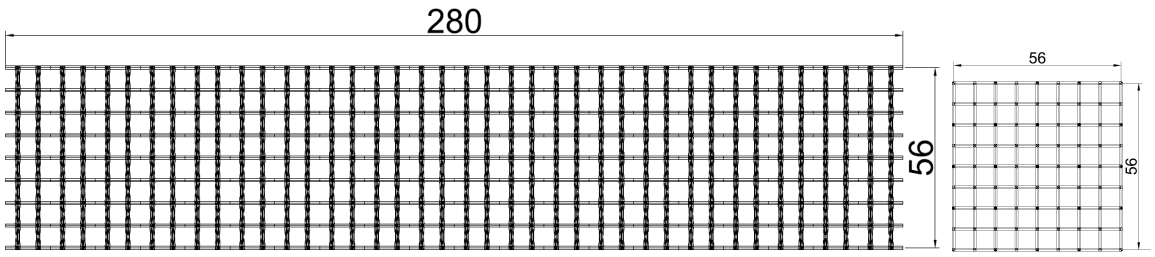

(a) Side view **(b)** Front view

Figure 3.5: Non-auxetic - 95 degrees beam

3.1.3. Auxetic beam

Similar to subsection 3.1.2 adjustments have been made to the geometry of the unit cell. In this case, a 85 degree auxetic unit cell is designed. On the contrary, the height of the middle strut for unit cell must be increased, since the struts are modelled diagonally inwards to compensate the height. Also the cosine is used again to obtain the 14 mm width.

Besides the non-auxetic beam, variations are observed in the center-to-center distance of the struts. This can be explained by the need to increase the height of the middle strut to have matching bounding box dimensions. It is actually the opposite of what is happening to the non-auxetic beam. Next to that, from the side view an overlapping behavior of the struts is observed. In reality this is not overlapping, but since the unit cell is diagonal outwards for the outer struts and inwards for the center struts a difference is observed.

3.2. Auxetic and non-auxetic beam

Furthermore, a geometrical study consisting of auxetic and non-auxetic bow-tie unit cells is chosen and designed in the form of a beam. The goal of the unit cells are to ensure active confinement over

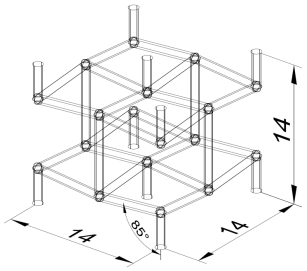

Figure 3.6: 85 degrees unit cell

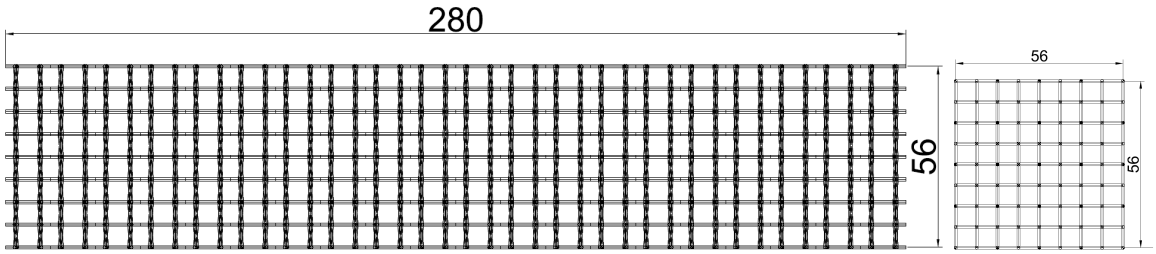

(a) Side view **(b)** Front view

Figure 3.7: Auxetic - 85 degrees beam

the height of the beam. Since different loads occur in a beam, different types of unit cells need to be used. Moreover, when bending is applied on the beam, forces such as tension on the bottom side and compression on the top side of the beam are acting. As a result, having difference in auxetic and non-auxetic architectures start playing a role. Moreover, an auxetic architecture performs desirable under a compressive load when it compresses laterally, but under a tensile load it does the exact undesirable opposite effect. Therefore, 4x2 85 degree unit cells are placed on the upper part and 4x2 95 degree unit cells on the lower part. As a result, the desired behavior is better ensured under a bending load.

However, we learn from Figure 3.8 that a shift of center-to-center distance of the struts is observed, which leads to stress concentrations. As mentioned before, this is caused by the change in length of the middle struts that is made to create equal bounding box dimensions. A closer look of this compatibility issue is presented in Figure 3.9. On the other hand, the pattern of the front-view remains constant for all different designed beams, which is desired.

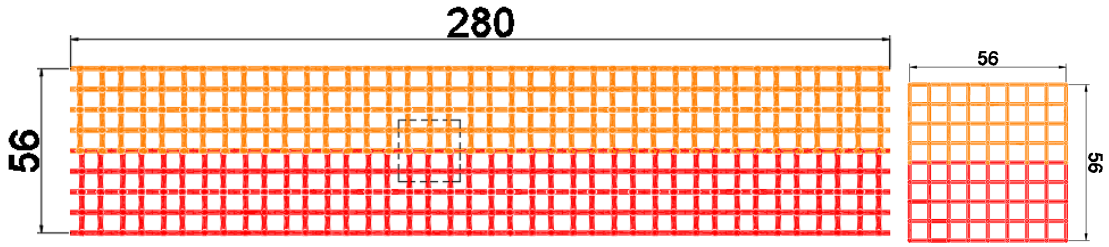

(a) Side view **(b)** Front view

Figure 3.8: Auxetic and non-auxetic - 85/95 degrees beam

3.3. Gradual beam

In this section, a next step for the model is implemented where a gradual increase from auxetic to non-auxetic is applied in the model. Moreover, the bow-tie architecture is changing from 80 degrees to 100 degrees. This is needed, since a beam under pure bending gradually changes from compression to tension over the height of the beam. It is therefore desired too, to make use of unit cells that follow

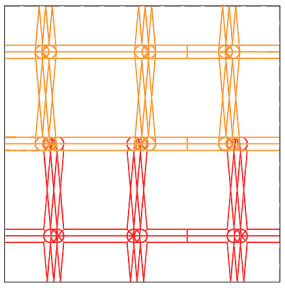

Figure 3.9: Compatibility 85/95 degrees beam

this loading behavior.

Geometry unit cell

In this case, the unit cell itself is gradually increasing. In Figure 3.10 the idea is presented on how the unit cell changes. It is a given criteria that the nodes when stacking unit cells, must be compatible. To achieve this, the following adjustments are performed to the geometry of the unit cell:

1. A bounding box is designed of 14x14x14 mm to achieve compatibility at the other nodes. The 90 degrees bow-tie is cubic and therefore decisive for the dimensions of the other unit cells. The 7 mm strut lengths can then be modified using the cosine for the other angles. This modification is necessary to create an equal width between the unit cells.
2. The height of the unit cell must either be increased for the auxetic and decreased for the non-auxetic unit cell by changing the height of the middle vertical struts.
3. As presented in Figure 3.10 a 80/85 degrees unit cell consists out of a 80, 82.5 and 85 degrees unit cells. This 2.5 degrees change ensures a smooth transition between the angles.
4. Finally, the stacked unit cells must exactly match. For example, the right side of a 80/85 degrees and left side of the 85/90 degrees must be used to ensure compatibility.

The same approach is also chosen to create the 80/85, 85/90, 90/95 and 95/100 degree unit cells. The relative density is determined for all different unit cells having a 1 mm diameter strut thickness, which were respectively 4.2%, 4.1%, 4.1% and 4.0%. The aim however is to be as close to 5% as possible to have a valid comparison between the amount of reinforcement in conventional concrete elements. To achieve this, the strut thickness is increased to 1.2 mm resulting in a closer value to 5%. A next

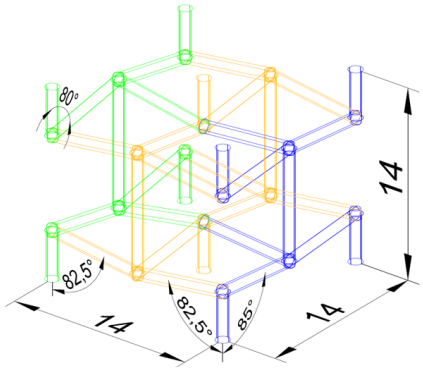

Figure 3.10: Unit cell gradually increasing from 80 to 85 degrees

step is stacking the several unit cells and create a beam. In the design presented in Figure 3.11 the gradual increase is shown from 80 degrees to 100 degrees over the height of the beam. Since a beam is experiencing tensile loads in the bottom side and compressive loading in the top side, a gradual increase is preferred for active confining pressure over the height of the beam. Moreover, this loading is also gradually changing over the height of the beam. The gradual change in geometry is presented in Figure 3.12. This close-up shows the gradual change of angle over the height of the beam, whereas the front view remains the same as the other beams.

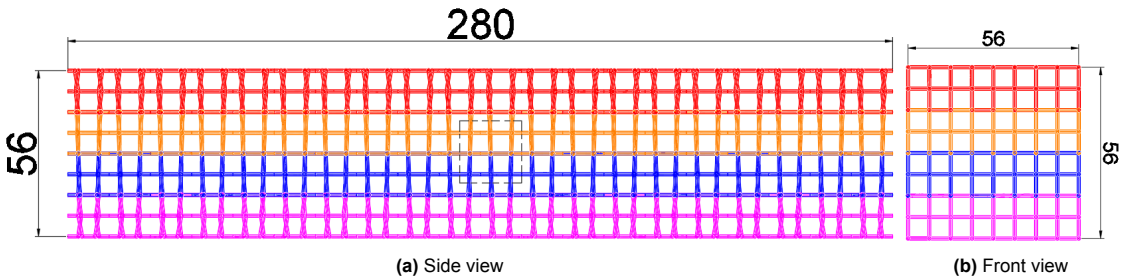

(a) Side view **(b)** Front view

Figure 3.11: Beam geometry from 80 to 100 degrees

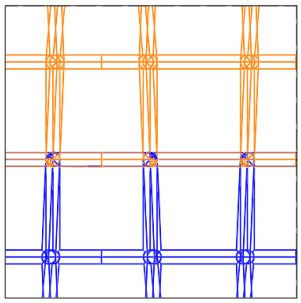

Figure 3.12: Compatibility gradual beam

3.4. Conclusions

In this section the conclusions of the geometrical study are discussed. The following conclusions are drawn:

- A work approach is developed to design cubic, auxetic and non-auxetic bow-tie cells, which all have the same bounding box dimensions of 14x14x14 mm. As discussed in Figure 3.1, an adjustment in the re-entrant strut length and vertical strut length is performed to create the dimensions of the reference cubic cell. 14x14x14 mm with a strut diameter of 1.2 mm is chosen to have a relative density close to 5% and maintain small dimensions to ensure manufacturability using LBPF.
- Several geometries are successfully modelled using cubic, auxetic, non-auxetic and combined unit cells. Depending on the type of structural element, different cells are favorable. Moreover, auxetic cells are favorable to use for columns, since columns are mainly under compression. Whereas, concrete elements such as beams are subjected to compression, tension, shear and bending. non-auxetic cells would then be needed for the tensile part and auxetic cells for the compression part of the beam.
- Variations in center-to-center distances between struts are observed due to modified middle strut lengths to maintain equal bounding box dimensions. This will cause undesired stress concentrations in the beam, which is unfavorable for design of reinforcement concrete elements.
- A work approach is developed to design a gradual changing unit cell in steps of 2.5 degrees angles. This unit cell consists out of three components, as shown in Figure 3.10. This design is beneficial since it excludes stress concentrations and has a gradual transition, which takes in to account the change of loading which a structural element like a beam is subjected to.
- A work approach is developed for designing a gradual increasing beam from auxetic to non-auxetic while maintaining the nodes compatible. This gradual design for a beam will take into account the change of load over the height of the beam from tension to compression.
- A diagonal inward and outward behavior of the vertical struts is observed over the height of the beam. This can be explained by the change of height of the middle strut.
- It is concluded that the pattern for the front view remains the same for all designed beams. This is desirable when used as steel confinement for concrete.

4

Numerical study

In this chapter a numerical study is performed on the behavior of the selected beams from chapter 3 using ABAQUS. The structural behavior of the geometries are determined under different types of loading conditions such as compression, tension and bending. The following parts are discussed:

- **Unit cells:** The structural behavior is discussed for several unit cells experiencing different types of loading, such as compression and tension.
- **Beams:** The overall structural behavior of several beams is discussed, which consists out of the designed unit cells in chapter 3. The beams are subjected to compression, tension and bending.
- **Validation:** A validation of the elastic properties in terms of the effective modulus for several 3D unit cells is performed.

Finally, some conclusions are presented of the overall work.

4.1. Unit cells

The geometry of the unit cells from chapter 3 are used to perform a numerical study using the FEM software ABAQUS. The unit cells are divided in two main categories: the ”single angle” and ”three angle” unit cells. The single angle unit cell, consist out of pure 80, 85, 90, 95 and 100 degrees angles, which can be used for structural elements such as columns or foundation piles since they are mainly under compression or tension. Whereas, the three angle unit cells are increasing gradually from 80 - 85, 85 - 90, 90 - 95 and 95 - 100, with steps of 2.5 degree angles. A gradual increase is needed to ensure smooth geometrical transition between the angles, which is favorable for beams which are subjected to a changing load from compression to tension.

4.1.1. Single angle unit cells

All unit cells have comparable boxing dimensions of 14x14x14 mm. The reason for this is to ensure compatibility between the nodes, when the unit cells are expanded towards beams. The struts of the unit cells are modelled using B31 elements, since the unit cells are bending dominated architectures. The boundary conditions are presented in Figure 4.1 and Figure 4.2. Based on these boundary conditions, the effective modulus of the unit cells are determined in the three principle directions.

An overview is given of the moduli for the unit cells Table 4.1 and visually in Figure 4.3. In this table the stiffness is determined for a displacement of 0.1 mm for compression and tension to remain in the elastic region. Besides, linear geometry is used. First of all, the lateral moduli E11 and E22, show a symmetric behavior with the cubic cell having the highest lateral moduli. Since the load is effecting the struts directly from both sides, the highest moduli is logically obtained there. As the struts are inclining, the stiffness drops symmetrically either being re-entrant or convex. Furthermore, In terms of the unixial moduli E33, the results show that the auxetic cells have a lower stiffness compared to cubic and non-auxetic cells. This can be explained by the re-entrant strut being loaded in tension, where as the strut is loaded in compression for cubic and non-auxetic cells. In this case, the struts are not directly connected and therefore show different behavior than E11 and E22. Because of linear geometry,

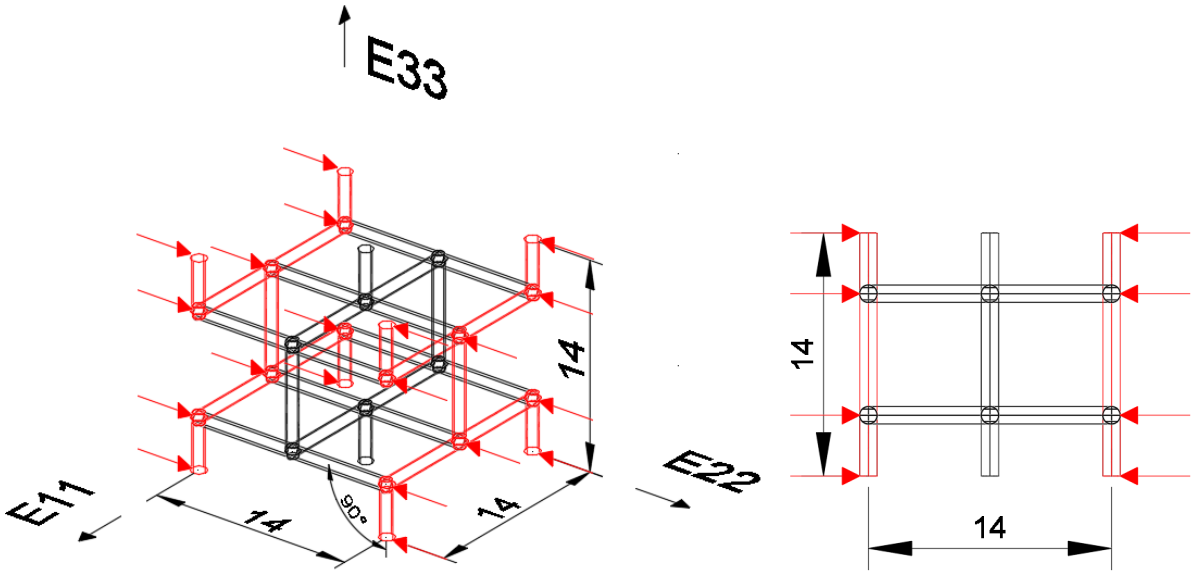

(a) E11, E22 - 3D view

(b) E11, E22 - Front view - Boundary conditions

Figure 4.1: E11, E22 - Boundary conditions - Unit cells

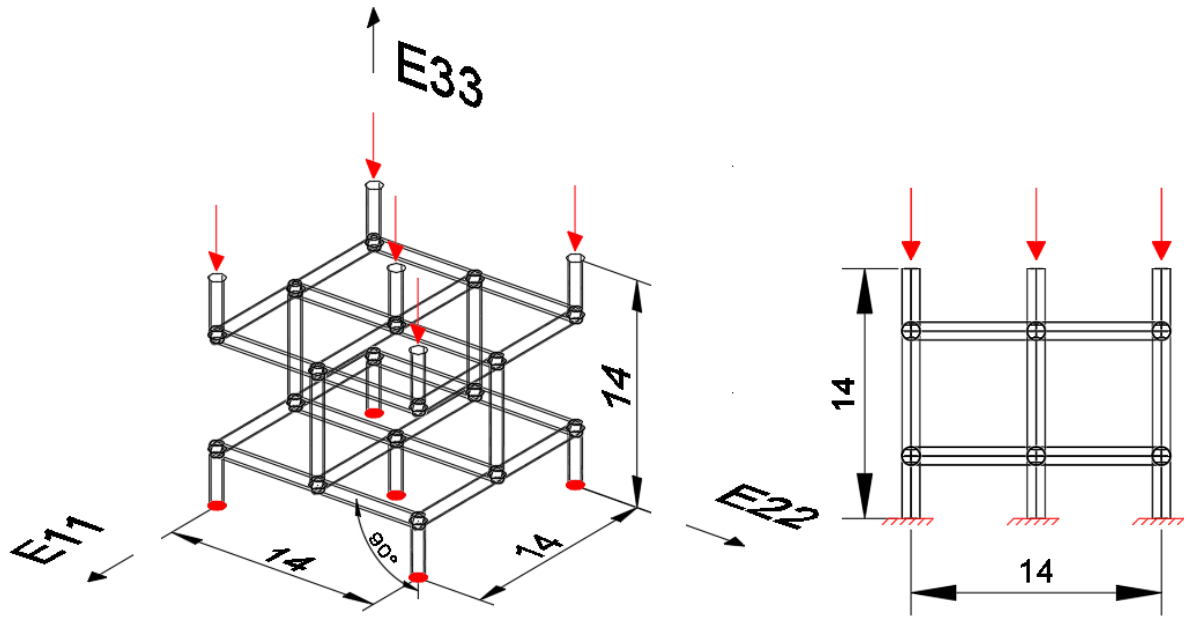

(a) E33 - 3D view

(b) E33 - Front view - boundary conditions

Figure 4.2: E33 - Boundary conditions - Unit cells

results in compression and tension are similar for the effective modulus. The obtained stiffness of the unit cells are used to validate the overall stiffness of the beams made out of these unit cells.

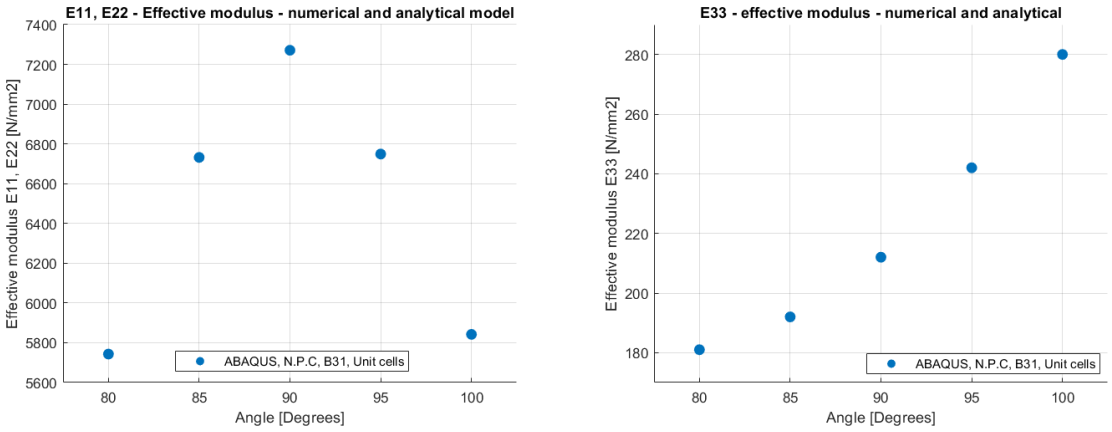

(a) E11, E22 - Effective modulus - single angle cell

(b) E33 - Effective modulus - single angle cell

Figure 4.3: Effective moduli - Single angle cells - numerical models

Table 4.1: Elastic material properties - single angle unit cells

Unit cell	**E11**	**E22**	**E33**	**Drawing**
[°]	$[N/mm^2]$	$[N/mm^2]$	$[N/mm^2]$	[-]
80	5743	5743	181	Figure A.1
85	6732	6732	192	Figure A.2
90	7271	7271	212	Figure A.3
95	6749	6749	242	Figure A.4
100	5842	5842	280	Figure A.5

4.1.2. Three angle unit cells

Following the same work flow as the single angle unit cells, the effective modulus of the three angle unit cells are determined. These are presented in Table 4.2 and visually in Figure 4.4, which are in accordance with Table 4.2 the same order of magnitude for the stiffness E_y obtained for the single angle unit cells. Again, an increase in stiffness is observed when the angle of the bow-tie is being increased. It is worth noting, that an average of the single angle cells is found for the moduli of three angle cells. Which is explained by the fact that it also partly consists out of both single angle cells.

Besides, a study is performed in the magnitude of displacement that is applied. It is concluded that the material will pass the elastic region and therefore a reduction in displacement should be applied. In this case, also 0.1 mm satisfies the condition of being within the elastic region. Also linear geometry, greatly influences this effect. It is found that the displacement can be increased while staying in the elastic region. But, an approximate 1% displacement is used compared to the bounding box dimensions to ensure a small deformation of the unit cells

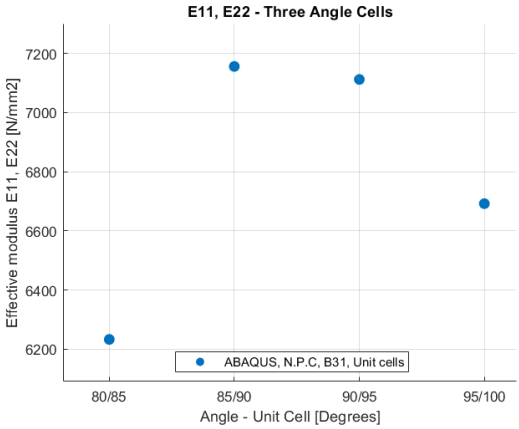

(a) E11, E22 - Effective modulus - Three angle cell

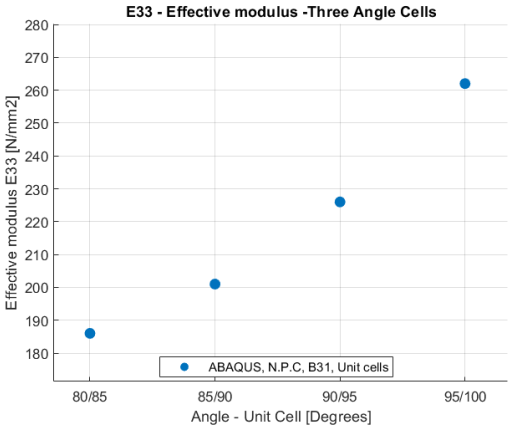

(b) E33 - Effective modulus - Three angle cell

Figure 4.4: Effective moduli - Three angle cells - numerical models

Table 4.2: Elastic material properties - three angle unit cells

Unit cell	**E11**	**E22**	**E33**	**Drawing**
[Degrees]	$[N/mm^2]$	$[N/mm^2]$	$[N/mm^2]$	[-]
80/85	6233	6233	186	Figure A.6
85/90	7156	7156	201	Figure A.7
90/95	7112	7112	226	Figure A.8
95/100	6692	6692	262	Figure A.9

4.2. Beams

A numerical study is performed using the FEM software ABAQUS. A geometry consisting of cubic, auxetic, non-auxetic and combined bow-tie unit cells are chosen and modelled in the form of a beam. it is worth mentioning, that the models contain the same overall dimensions, boundary conditions and material behavior. Therefore, valid comparisons can be made between the models.

In this section, several loading conditions are discussed, such as: compression, tension and bending. The following beams are subjected to these loading conditions and compared:

1. 4x4x20 - Auxetic beam - 85 degrees
2. 4x4x20 - Cubic beam - 90 degrees
3. 4x4x20 - Non-auxetic beam - 95 degrees
4. 4x4x20 - Auxetic- and non-auxetic beam - 85 and 95 degrees
5. 4x4x20 - Gradual beam - 80 to 100 degrees

Each beam is consisting out of the unit cells that have been discussed in section 4.1. So for example, the auxetic beam is consists out of purely 85 degrees unit cells. All beams have the same global dimensions, strut diameter, material, loading conditions, boundary conditions. The comparison that is made between the models are purely based on on the given geometry. It is desired to have difference in geometry since structural elements, such as beams are subjected to several loading conditions. For example, a beam under pure bending is subjected to a gradual change from compression to tension over the height of the beam. It is therefore favorable to design with both auxetic- and non-auxetic unit cell geometries. Moreover, a gradual design as presented in section 3.3 is needed.

An introduction is given for the general input of the models after which several loading conditions are discussed that are applied on the beams. The axial modulus is then determined of all beams, which is validated using the results of the previous section. Furthermore, since beams are often experiencing bending, a more in depth study is performed on this loading condition.

Input
The geometry concluded in the section 3.3 is used to built the numerical models. B31 elements are used to do research into the behavior. The reason for this is that this allows modelling of bending dominated architectures. For now, research is done into the behavior of bare steel lattices. Therefore, the use of solid elements is not needed. This could be interesting for modelling bonding between steel and concrete, which is a next goal. The goal of this study is to understand the expected behavior of the bare lattice in terms of compression, tension, bending and Poisson's ratio using linear geometry.

The model is compared with several models, including a fully auxetic, cubic and non-auxetic beam, representing 85, 90 and 95 degrees bow-tie architectures. All models have the same unit cell box dimension of 14x14x14 mm. The unit cells are then repeated and stacked upon each other to create a 4x4x20 unit cell beam of 56x56x280 mm. In accordance with the gradually numerical mode, the same boundary conditions and loading are applied to have a valid a comparison.

Material behavior
The material behavior stated in research by Tzortzinis et al. is used [29]. The steel auxetic lattice contains the following properties; a density of 7800 kg/m^3, a modulus of 210 GPa and a Poisson's ratio of 0.3. A total of 53280 beam elements is used to accurately capture the behavior, which slightly changes per model depending on the geometry. For the symmetric beams it remains 53280 beam elements and for the gradual beam it slightly increases to 53700 beam elements. The expected difference in outcome is expected to be small, since the same approximate global size spacing is used and therefore neglected.

4.2.1. Compression

Displacement control is used to create boundary conditions for compressive loading conditions. A displacement of 1 mm is given to remain in the elastic region of the model before non-linear behavior of the model starts. For validation reasons of the model, a solid steel beam is modelled given the same

Table 4.3: Young's modulus beams

Model	Compression (N/mm^2)	Tension (N/mm^2)	Drawing
Solid beam	210000	210000	Figure B.1
4x4x20 - Auxetic beam (85)	192	192	Figure B.2
4x4x20 - Cubic beam (90)	194	194	Figure B.3
4x4x20 - Non-auxetic beam (95)	196	196	Figure B.4
4x4x20 - Auxetic- and non-auxetic beam (85/95)	209	209	Figure B.5
4x4x20 - Gradual beam (80 to 100)	198	198	Figure B.6

56x56x280 mm dimensions. The value of 210 GPa is found, which is also used as modulus in the models. Furthermore, due to linear geometry the results in compression and tension are similar.

in Table 4.3 and visually in Figure 4.4b the results of the moduli for the beams are presented. From there we find that there is a significant decrease in axial modulus. This can be explained by the reason that the modelled beams are not solid steel beams anymore, the geometry becomes the leading factor for the effective modulus. Furthermore, the results in moduli become close to each other, this can be explained by the modifications made for all cells to be cubic and therefore compatible. For auxetic cells, the middle struts are shortened and for the non-auxetic cells the middle struts were increased. When increasing the tessellation in x-, y- and z-direction the difference in effective modulus for the beams becomes closer. There is one outlier in the data, being the 85/95 degrees beam, this is caused by the extra struts that are located between the 85 and 95 layer. This is because the struts in the middle don't perfectly overlap and an extra layer of struts is created, which is another reason why an extension towards a gradual beam is needed. Another option would be removing the struts of either the 85 or 95 degrees unit cells in that layer.

4.2.2. Tension

Following from the same reasoning as subsection 4.2.1 a 1 mm displacement in positive x-direction is applied to obtain tensile loading conditions and remain in elastic state.

An overview of the Young's modulus for the beams in tension are given in Table 4.3. Similar results are found for the Young's modulus of the beams when applying tension because of linear geometry. Also, an increase is presented from auxetic to gradual beam. An exception is the auxetic- and non-auxetic beam, which shows a sudden increase. This is explained by the stiffness that is created in the transition from 85 to the 95 degrees unit cells as previously mentioned.

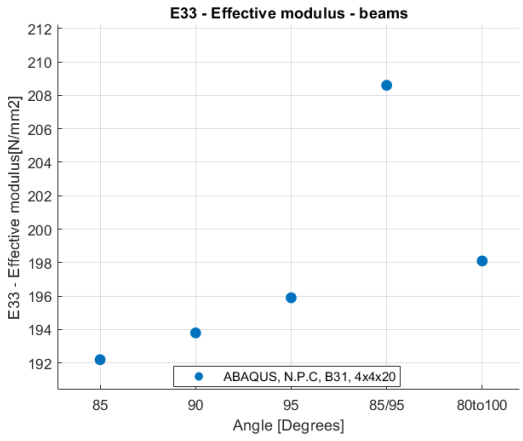

Figure 4.5: E33 - effective modulus - beams - numerical model

4.2.3. Bending

To achieve pure bending in the beam, the following boundary conditions are applied: a rigid body is applied on both sides of the beam centering to a reference point. On the left side, the beam is clamped and on the right side a rotation of 1 degree is applied to have equal behavior over the length of the beam. In Figure 4.6, the boundary conditions are presented to ensure bending loading conditions. Besides this, the neutral axis is now in the middle of the beam. As a result, a pure bending loading condition is created for the beam.

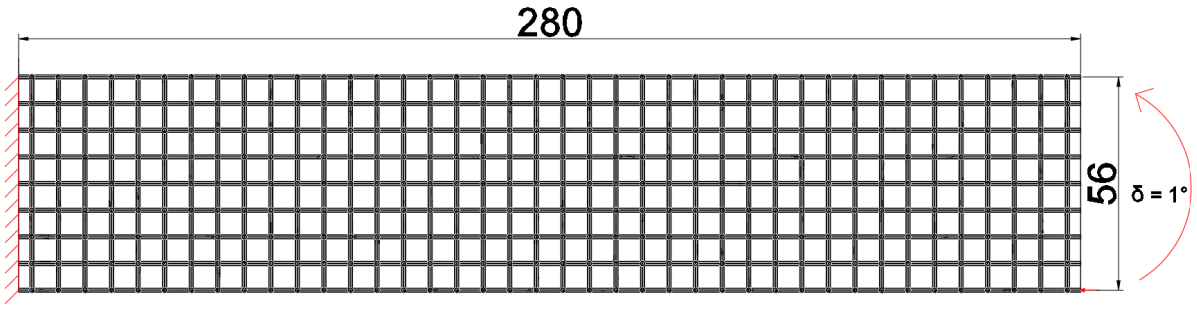

Figure 4.6: Boundary conditions - Beam models

Moment

For each model the acting moment is obtained over the length of the beam. The cross-section at the start of the unit cell is chosen to obtain the moment every 14 mm, given the length of a unit cell. However, it is concluded that with linear geometry the moment of inertia remains constant and the moment of inertia of the bounding box is leading. Besides, ABAQUS can differ between an deformed and undeformed shape. In order grab the moment consistently, with the correct moment of inertia, the undeformed shape is used to obtain the moment over several points on the beam. In Table C.1 an overview of data is given from the numerical model of the auxetic beam. At several points over the length of the beam at the beginning of each unit cell, the data for the Moment and Shear is listed at these points.

The moment of inertia is determined using a hand calculation and verified using AutoCAD. Following from the calculation, a moment of inertia of $819541.3\ mm^4$ is obtained. Using beam theory and Equation 2.2 a moment of $1.04 * 10^4\ Nmm$ is obtained. This does match the $1.04 * 10^4\ Nmm$ obtained from the numerical model, but the Kappa slightly changes. This is because, the planes don't remain plane as is assumed in the Euler-Bernoulli beam theory. With that, the young's modulus obtained for the beam in Table 4.3 is used to take into account the geometry that is used instead of conventional homogeneous beam.

In Table 4.4 data is presented which leads to all the moment and shear diagrams obtained from the numerical models of the beam. Besides this, in Figure 4.7 an overview of all moment diagrams of the beams are presented. It is concluded that the moment graphs remain constant due to the pure bending situation that is created given the applied boundary conditions. It is therefore also expected that the moment curves should be constant. Furthermore, the modulus of the beams is the dominating factor for obtaining the moment graph, whereas the moment of inertia and Kappa remain mostly constant. A slight difference in Kappa is observed, because of the difference in stiffness. The moment of inertia is depending of the cross section of the bounding box, being 56x56 mm. The difference in moment is also directly explained by the use of use accommodating cells compared to the load that is acting in the beam, resulting in the gradual beam having the best moment curve. However, in practice the bare steel trusses are use as reinforcement in concrete beams. It is therefore recommended to understand how the steel beams would perform as a composite with the concrete. It is however crucial to create a geometry which remains ensures active confinement over the height of the beam, which is explained later with the Poisson's ratio.

Shear

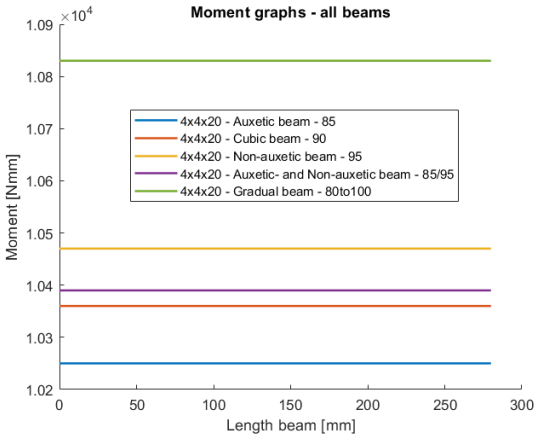

Figure 4.7: Moment curves - beams - numerical models

Table 4.4: Moment and Shear diagrams obtained from ABAQUS

Model	Moment Diagram	Shear Diagram
4x4x20 - Auxetic beam (85)	Figure C.1	Figure C.2
4x4x20 - Cubic beam (90)	Figure C.3	Figure C.4
4x4x20 - Non-auxetic beam (95)	Figure C.5	Figure C.6
4x4x20 - Auxetic- and non-auxetic beam (85/95)	Figure C.7	Figure C.8
4x4x20 - Gradual beam (80 to 100)	Figure C.9	Figure C.10

The goal of these boundary conditions is to create a pure bending loading condition. As a result, the shear in the beam is expected to be zero. From the shear diagrams presented in Table 4.4 we confirm that zero shear is found over the length of the beam since negligible small values are found. An overview of the shear diagrams is presented in Figure 4.8.

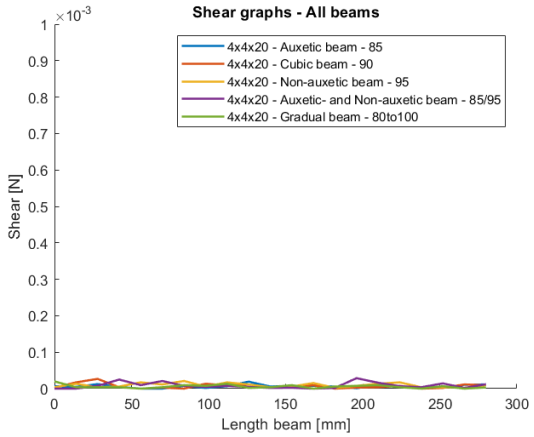

Figure 4.8: Shear curves - beams - numerical models

Poisson's ratio

Under bending loading conditions the change of Poisson's ratio becomes very interesting, since it is changing over the height of the beam. This can be explained by the change of load from compression to tension and the changing unit cells over the height of the beam. An overview is given in Table 4.5 of the Poisson's ratio per layer. The Poisson's ratios for the same type of beams from section 4.2 are used. The Poisson's ratio is determined using Equation 4.1, where the transverse and axial strain are

determined from the numerical model.

$$\nu = -\frac{d\epsilon_z}{d\epsilon_x} \tag{4.1}$$

Where:

- ν is the resulting Poisson's ratio
- ϵ_{trans} is transverse strain
- ϵ_{axial} is axial strain

In Figure 4.9 a visualization is given of what is meant with the layers in Table 4.5. Each layer, is representing a certain location over the height of the beam. This is important to consider, since the Poisson's ratio changes. The Poisson's ratio is obtained halfway the beam at the start of the unit cells. From the table we learn that there is a change in sign of the Poisson's ratio, which is explained by the change in load from tension to compression over the height of the beam. Besides this, a gradual change of the Poisson's ratio is also shown over the height of the beam.

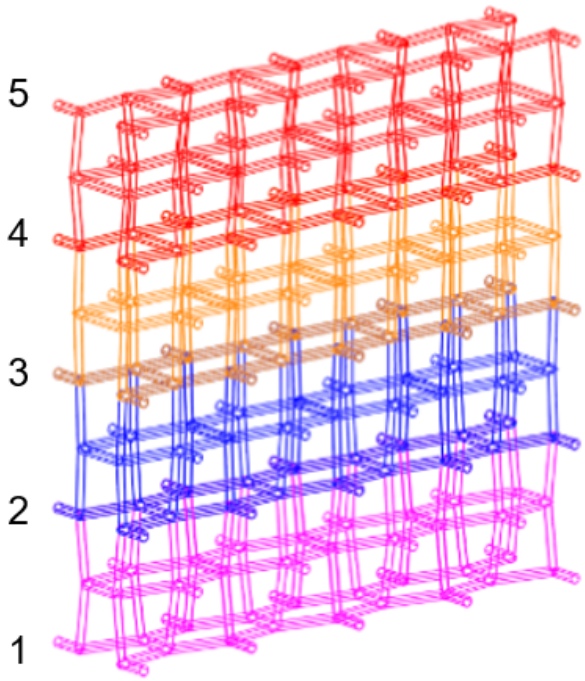

Figure 4.9: Layers Poisson's ratio

There are many observations to be made from Table 4.5 and Figure 4.10, the following are listed below:

1. Starting with the change of sign that has a direct relation with the type of unit cell being used. Besides that, the change of load from compression to tension is critical for the sign of the Poisson's ratio.
   (a) It is found that the Poisson's ratio of the auxetic beam generally stays negative.
   (b) The Poisson's ratio for the cubic and non-auxetic beam are generally positive over the height of the beam.
   (c) The auxetic- and non-auxetic beam and the gradual beam are showing a change of sign over the height. Since the upper layers are in compression and the unit cells either cause an inward or outward effect of the unit cell the sign is different. When the beam shows inward behavior under compression the sign is negative and positive when the beam is

going outwards. For the bottom layers, it works vice versa. These layers are under tension and can also be going inwards or outwards depending on the type of unit cell. When the sign is negative the beam is going outwards and positive when the layers are going inwards. This is beneficial as steel reinforcement in concrete, since you will have active confinement pushing inwards.

2. The geometry of the beam becomes the leading factor for the Poisson's ratio, instead of the Poisson's ratio of 0.3 that is given in the models for steel as material property.
3. By comparing the introduced geometries of the beam in chapter 3, it is concluded that the gradual beam has a positive influence on the Poisson's ratio of the beam. In which, the steel reinforcement in the beam will tend to move inwards over the height of the beam and auxetically boosted confinement is achieved. Besides a gradual increase of effect is observed when going to the outer layers, such as layer one and five. These layers contribute mostly to the active confinement active of the steel reinforcement.

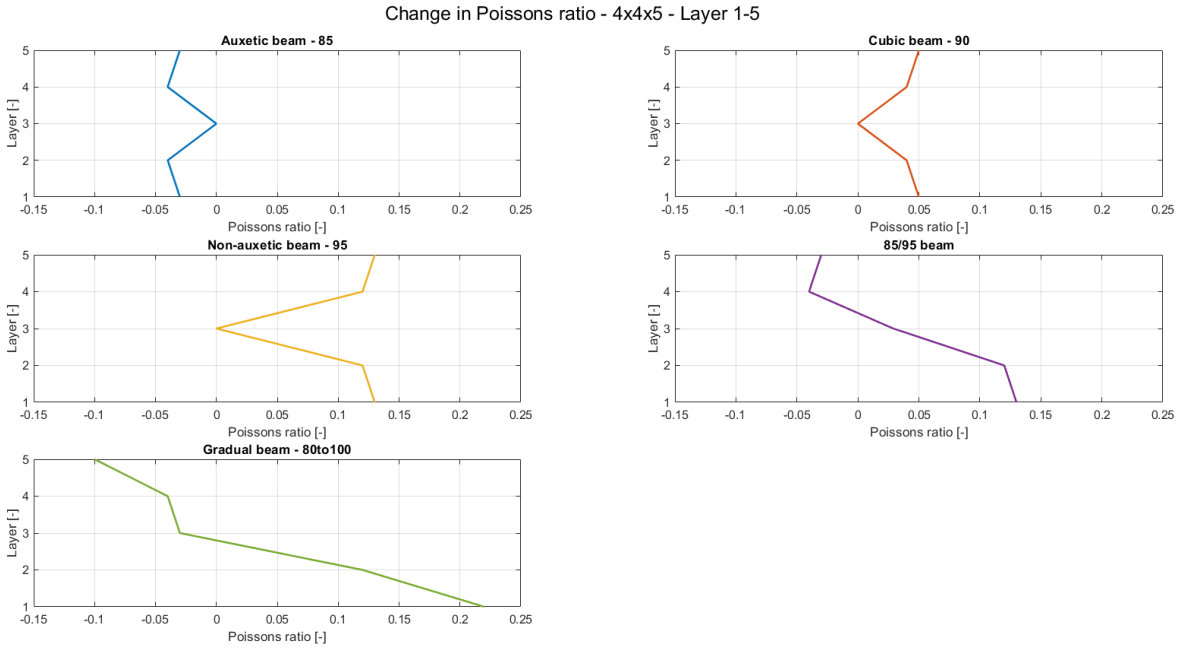

Figure 4.10: Poisson's ratios - All beams

Table 4.5: Poisson's ratio

	Auxetic beam	Cubic beam	Non-auxetic beam	Auxetic- and non-auxetic beam	Gradual beam
Layer	[-]	[-]	[-]	[-]	[-]
5	-0.031	0.05	0.13	-0.031	-0.1
4	-0.041	0.04	0.12	-0.041	-0.04
3	0	0	0	0.029	-0.03
2	-0.041	0.04	0.12	0.12	0.12
1	-0.031	0.05	0.13	0.13	0.22

4.3. Validation numerical study

In this section, a validation is performed on the numerical models by comparing the results on several loading conditions from literature. The following points are discussed:

- Discussion of the Yang et al. paper [34]

- Discussion of the Tzortizinis et al. paper [29]
- Validation of the numerical results
- Study on the tessellation effect in the numerical models

Yang et al. paper
A comparison is made between a rectangular and circular cross-section [34]. In this case the analytical formula for the effective modulus in axial direction of a periodic 3D re-entrant unit cell is used. However, this formula only applies for rectangular cross-section, which needs to be adjusted to circular sections for it to be valid in this research. Therefore, a couple of adjustments are made in the area, moment of inertia and kappa of the cross-section. All these parameters are dependent on the cross-section and therefore need to be adjusted.

The following adjustments are made in the formula:

- The area for a circular section is $\pi * r^2$
- The moment of inertia is changing from $\frac{\pi * D}{64}$
- The geometrical factor κ for circular sections is $\frac{6}{7}$ [28]

As a result the following equation can be found for the deflection angles of the re-entrant strut. A full workout of the problem leading to the effective modulus of a circular section is presented in Appendix D.

$$\theta_1 = \theta_2 = \frac{ML}{6EI} + \frac{7P}{6GA} \tag{4.2}$$

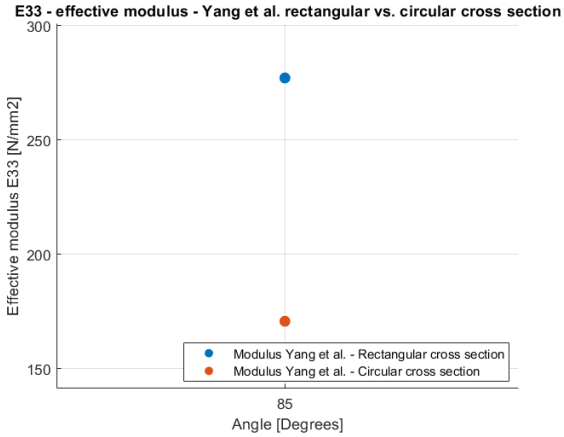

Figure 4.11: E33 - Rectangular vs. circular cross-section

Tzortizinis et al. paper
Besides Yang et al., a paper is published by Tzortizinis et al. (2022) in which the effective moduli of several 3D re-entrant lattice structures is discussed. In this research, the effective moduli is obtained from equation 5.3 below:

$$E^{'} = \frac{E^{'}}{p^{'} * E^{(t)}} \tag{4.3}$$

In which:

- $E^{'}$ Is the elastic modulus of the bare truss.
- $p^{'}$ the relative density of the bare truss, in the paper a relative density is used of 0.05, which is a typical volume fraction as steel reinforcement in reinforced concrete structural members.
- $E^{(t)}$ the Young's modulus of steel, which is 200 GPa.

Using Figure 4.12, the values are obtained for the elastic moduli of the bare truss lattices. These obtained values are used to make a valid comparison with the obtained moduli from the numerical models in this research.

Comparison - single angle cells

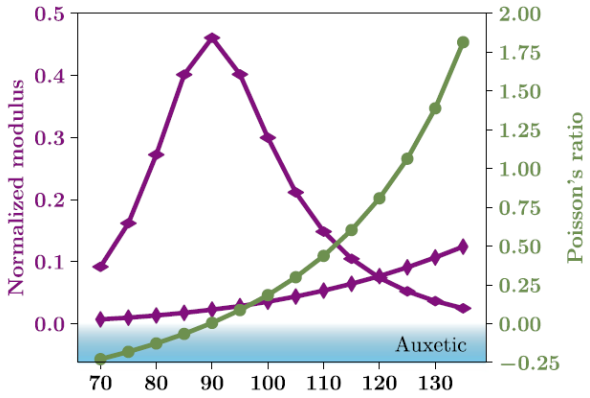

Figure 4.12: Poisson's ratio and normalized elastic moduli for bare truss lattice

in Figure 4.13 the results are presented of three independent approached for obtaining the effective modulus E33 for an auxetic 85 degrees unit cell. In the comparison the numerical result is compared to two results from papers by Yang et al. and Tzortizinis et al. 85 degrees is chosen since Yang et al. paper only applies for re-entrant 3D unit cells and is the closest geometry to being cubic. Because of the adjustments made to the single angle cells to obtain compatibility between the nodes, the numerical results easily deviate from literature. In this comparison, an overestimation is found for the effective modulus E33, in the numerical model. An explanation could be difference in elements used, being beam element for the numerical models in this research and solid in the Tzortizinis et al. paper. Another reason would be the increase in length of the middle strut that is given to make the unit cubic. Since the result is within an error of 10%, the results are sufficiently accurate to use for the other unit cells.

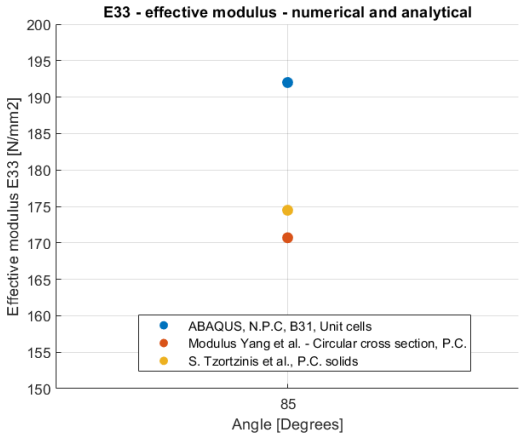

Figure 4.13: E33 - Single cells - 85 degrees

Tessellation effect

To have an understanding in the influence of the number of unit cells in the length compared to the applied boundary conditions, a study is performed on the tessellation effect of the unit cells. The goal is to understand if the clamped boundary condition of the cantilever beam has a substantial impact on the axial modulus of the beam. In this comparison, a 4x4x10, 4x4x20 and 4x4x40 beam is modelled and compared as displayed in Figure 4.14. For manufacturing reasons using LBPF the length of the

beam should be below 300 mm. Therefore, the longest logical distance possible is 4x4x20 unit cells, which resembles a bounding box dimension of 56x56x280 mm, which dimensions are also chosen. In Figure 4.15, the results are presented of the three beams. it becomes clear that a decrease in stiffness is observed when a longer length is chosen for the beam. However, this difference is not significant and therefore a 4x4x20 beam has a resembling axial modulus compared to the 4x4x10 and 4x4x40 unit cell beams.

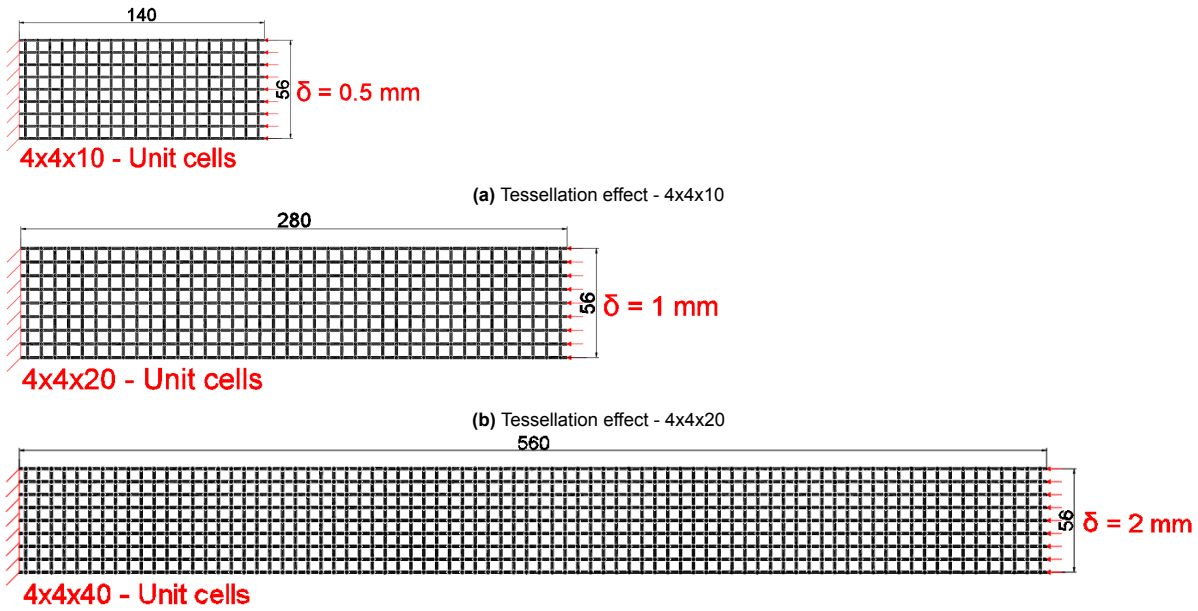

(a) Tessellation effect - 4x4x10

(b) Tessellation effect - 4x4x20

(c) Tessellation effect - 4x4x40

Figure 4.14: Tessellation effect - modelled beams

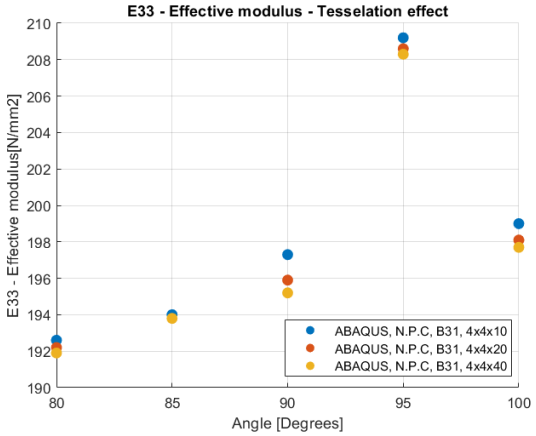

Figure 4.15: Tessellation effect of the cells

4.4. Conclusions

In this section the conclusions are presented of the numerical study. The following conclusions are drawn:

- The axial stiffness of several unit cells is determined and presented in Table 4.1 and Table 4.2. It is concluded that auxetic cells have an overall lower axial stiffness than cubic and non-auxetic

cells. This can be explained by the re-entrant struts being in tension, whereas for convex unit cells they are in compression and therefore add to the stiffness.

- The lower degrees unit cell becomes the leading stiffness of the three angle unit cells. Following from the weakest part being the critical stiffness in the end.
- The results of the axial stiffness of a beam is in accordance with the axial stiffness of individual unit cells. From this it is becoming clear that the increase in tessellation towards a beam doesn't have a considerable influence.
- An increase in axial stiffness is observed for the beams from 196 to 213 N/mm^2. Furthermore, the same axial stiffness is found for compression and tension. The results in axial stiffness are presented in Table 4.3. From here, it can be concluded that the young's modulus of the beam is greatly influenced by the geometry of the beam and becomes the leading stiffness.
- Moment diagrams of the several beams are presented in Figure 4.7. Constant moment diagrams are observed, which can be explained by the applied rotation on the end of the cantilever beam. Moreover, a situation of pure bending is created. From this, it is concluded that the effective modulus in uni-axial direction becomes the dominating factor. Whereas, the moment of inertia stays constant and the curvature of the beam slightly changes since the plane sections don't remain plane as assumed in Euler-Bernoulli beam theory. Besides that, shear diagrams are presented that show a shear force close to zero which is in accordance with the pure bending conditions that is created using rotation.
- An interesting phenomenon is observed in which the Poisson's ratio is changing over the height of the beam due to the change of geometry over the height of the beam. The results for the Poisson's ratio are presented in Table 4.5. Besides, a non-linear effect is observed where the Poisson's ratio is changing as the load of the applied rotation is increasing and reaches beyond the elastic stage of the material.
- it is concluded that the Young's modulus of the material is being influenced by the geometry of the beam. It severely drops from 2.1 GPa to a stiffness of around 200 MPa. This is a result of the struts being designed in angles instead of continuous longitudinal bars such as conventional steel reinforcement.
- The analytical equation presented in the literature review by Yang et al. is successfully modified for circular sections. With that, an equation for the effective modulus of a 3D re-entrant lattice structure is obtained. Modifications in terms of the moment of inertia, effective area and kappa are made. The analytical results show good agreement between the numerically obtained results of a 85 degrees re-entrant unit cells.

5

Upscaling of auxetic lattices

In this chapter a literature study is performed on the upscaling of auxetic lattices to discuss the possibilities and limitations in the current practice. Furthermore, the potential for upscaling auxetics in civil engineering applications using a state-of-the-art technology is discussed. The focus of the literature study is on the following:

- **Robotics:** Discusses how robotics can be used for development of upscaled lattices.
- **Upscaled lattices:** Explains the context behind the use of upscaled lattices based on literature. Besides, the potential is discussed for civil engineering applications and a numerical study is presented.

Finally, conclusions are presented on the findings of the topics listed above.

5.1. Robotics

Currently, traditional construction methods are reaching their limits in terms of performance, growth, and defect rates. To overcome these challenges, the integration of robotics in the construction industry is considered a state-of-the-art innovation. However, compared to several sectors such as: agriculture, manufacturing and wholesale and retail, robotics' involvement in construction is currently limited [7]. A clear indication of the construction industry's lagging productivity can be observed from Figure 5.1. While the manufacturing, agriculture, wholesale and retail has increased significantly, the construction industry has shown little progress in this area and even decline in productivity. Therefore, there is significant need in automation in construction industry to improve the productivity.

Looking ahead, there is significant potential in the field of digital fabrication, wherein the integration of design and construction processes in a tightly planned manner proves to be highly efficient [10]. This approach offers several benefits, including reduced accidents, minimized waste, and improved material efficiency. However, it is important to note that the final assembly stage in construction still heavily relies on manual labor. Furthermore, when comparing the stagnation and technical limitations within the construction industry to emerging developments, initiatives, and technologies, a clear relationship becomes apparent [4]. which include: 1) robotic design, 2) robotic industrialization, 3) construction robots, 4) site automation, and 5) ambient robotics. Additionally, the study by Bruun et al. outlines key aspects required to achieve a fully automated construction process [6]. Furthermore, according to Bruun et al., the initial utilization of robotics arms was observed in the construction of modular homes, marking a significant milestone in the application of robotics in this sector.

In collaboration with Toggle an upscaled design of the auxetic bow-tie lattice is proposed. To start fabrication a design for an 80 degrees auxetic bow-tie architecture is proposed to ensure it's auxetic behavior and repeatability. Besides, since the goal of this lattice is to be made on full scale, conventional American number #3 rebar is used for fabrication. In Appendix E, a drawing is presented of the auxetic lattice. The global dimensions of the lattice is approximately 0.5x0.5x0.53m (lxwxh). Furthermore, the 80 degrees bow-tie unit cell is repeated in x-y-z direction by 4x4x5.

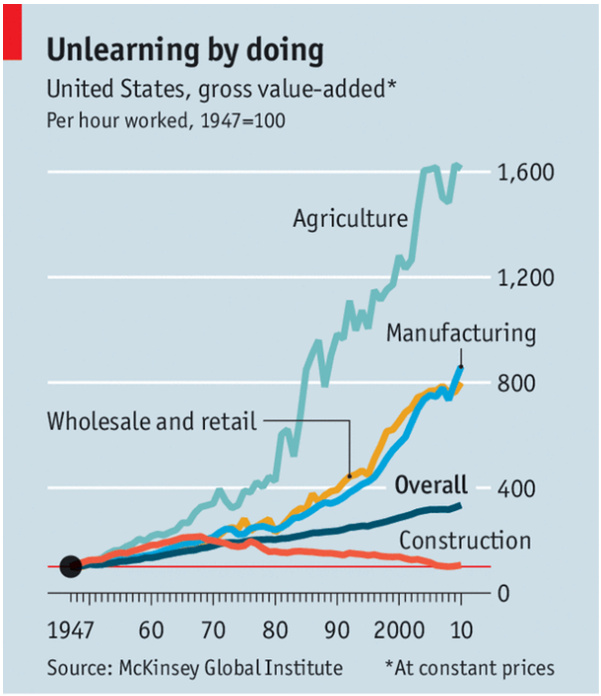

Figure 5.1: Productivity [7]

5.1.1. Multi-robotic fabrication

Figure 5.2: Confidential

5.1.2. Sequencing

Figure 5.3: Confidential

5.1.3. Plugin Robots

Figure 5.4: Confidential

5.1.4. Orientation of the gripper

Figure 5.5: Confidential

5.2. Upscaled lattices

Figure 5.6: Confidential

5.2.1. Conventional rebar

Figure 5.7: Confidential

5.2.2. Welds

Figure 5.8: Confidential

5.2.3. Numerical study

Figure 5.9: Confidential

5.3. Conclusions

In this section, the conclusions are drawn of this chapter. An introduction is given for the potential of robotics for civil engineering applications and the upscaling of auxetic lattices with it.

- The use of robotics is actively being studied currently in literature. It is found that productivity in the construction industry has been constant or even decreasing, where as other industries significantly increase their productivity by using robotics. With the use of multi-robotic fabrication, robotics can be actively implemented in the construction process for prefabricated steel reinforced cages.
- Production of upscaled lattices are very labour intensive. There are several reasons for that, including cutting of the reinforcement bars, assembling of the rebar, programming of the full production and assembling the product using the robots. However, it is therefore recommended to fully automate the whole process. Where the bars are cut and directly assembled by the robots. Having this process fully automated, enables a continuous production of prefabricated steel cages without the need of labour.
- A bi-linear plastic model is given to the lattice of typical A36 steel, which led to a peak load for the lattice of 403 kN. In future research a test set-up should be designed, which has a minimum capacity of 403 kN. Preferably, a higher capacity is needed to include unexpected increase of capacity and other uncertainties.

6

Discussion

Based on the work presented in this report a discussion is performed on several topic regarding:

- **Geometrical study:** Several design cases are discussed on their design choices and assumptions in taking in to account the compression, tension and bending loading conditions.
- **Numerical study:** The numerical study on the unit cells and beams for the use as steel reinforcement for concrete structural elements is discussed. Moreover, the modelling approach, the made assumptions and their consequences to the results.
- **Upscaling of auxetic lattices:** The potential for upscaling of auxetic lattices and manufacturing technologies is discussed.

6.1. Geometrical study

Basic cases

In this report, designs are presented for auxetic (<90), cubic (90) and non-auxetic unit cells (>90). There are several reasons why different unit cells are needed in conventional steel reinforced concrete elements. First of all, the beneficial characteristic of auxetic, where a negative Poisson's ratio is obtained. Meaning a lateral inward behavior is obtained under compressive loading conditions, but is undesirable under tensile loading conditions. The goal of having auxetic reinforcement, is to actively confine the concrete throughout the concrete member, Secondly, a transition in loading can only be accounted for when a change in geometry is implemented. An advantage of a bow-tie architecture, is that it can be easily modified from re-entrant to cubic to convex by increasing the angle. Therefore, design of beams implementing several unit cells are the only solution for structural members under different types of loading.

A bounding box dimension of 14x14x14 mm and a strut diameter of 1.2 mm for the unit cells. These dimensions, take into account the relative density of 5% used for conventional steel reinforced concrete members. With that, it is feasible to manufacture with the technology LBPF using an EOS M290. Given the small dimensions that are printable, scaling towards a beam in x-,y- and z-direction is possible and it takes into account the needed angle which ensure high confining pressure on the mortar. However, several relative densities, bounding box dimensions and scaling sizes are interesting to model. It is for the designer important to understand the application which it is being used for and which form of unit cell to apply.

Besides that, a range of bow-tie architecture cells is used between 80-100 degrees. This range of cells is chosen because of the confining pressure it can obtain as presented in Figure 2.6. Besides, the cells can be easily modified from re-entrant (<90) to cubic (90) to convex (>90) by changing the angle of the re-entrant strut relative to the vertical strut. Considering different loads in different structural elements, a change is needed in geometry.

Given the dimensions of the EOS M 290 a printing volume of 250x250x325 mm is available. A logical symmetric 4x4x20 cell tessellation is used, being 56x56x280 mm in total. Both a limit in costs and

a symmetric shape of cells are reasons for this tessellation.

Auxetic and non-auxetic beam
In this part, a concept is introduced where both auxetic (85) and non-auxetic (95) unit cells are used to accommodate tension and compression in the beam. These angles are chosen to enhance the needed Poisson's ratio over the height of the beam, besides both have a substantial confining pressure. However, a more optimal angle can be chosen to accommodate the loads and have a higher confining pressure. For simplification reasons and comparisons with literature these angles are favored in this research.

A 85/95 design of a beam leads to two interface problems. Firstly, the sudden switch in the interface layer between the 85 and 95 degrees single angle cells and secondly extra struts are created since they don't perfectly overlap. The sudden switch is not favorable for design as steel reinforcement in concrete elements due to the increase load concentrations on part of the reinforcement. Furthermore, the extra struts lead to an increase in the uni-axial modulus E33, which is explained more elaborate below.

Gradual beam
Furthermore, a design approach is introduced to design three angle cells. This design is created under the assumption that the beam is subjected to pure bending, resulting in a neutral axis in the middle of the beam and a smooth transition between compression and tension. In reality, this is hardly ever the case for beams and therefore a different distribution of unit cells would be needed. However, using this simplification, the concept in which inward behavior is found over the height of the beam is proven, which is one of the goals in this study.

In this research, the aim for the single and three angle unit cells is to have a relative density of 5%. However, since the unit cells have cubic bounding box dimensions and similar thickness of the struts obtaining an exact percentage of relative density is not feasible. For simplification reasons, a strut diameter of 1.2 mm is chosen, which is close to a relative density of 5%. However, different relative densities ranging from 4.8% to 5.2% are obtained. It is therefore, important to state that the designed beams have different relative densities, which increases complexity of the beams. Especially for the 85/95 beam and gradual beam, where it changes through the beam.

6.2. Numerical study

Unit cells
Modelling for the numerical study is performed in the FEM package ABAQUS, using linear geometry. It is found that there is a significant increase in complexity when non-linear geometry is used. This leads to changing Poisson's ratios due to non-linear deformation, decrease in moment curves over the length of the beam with pure bending loading conditions and change in modulus. Furthermore, beam elements (B31) are used to obtain axial deformation and include the bending dominated behavior of the struts. Whereas, truss elements would only include the axial behavior of the struts. However, since bare steel lattices are only considered, modelling with beam elements gives a sufficiently accurate outcome. But, the expansion towards modelling a composite including the concrete, only using beam elements would not work. Linear hexahedron solid elements (C3D8R) can be used to obtain the behavior of the full composite. Besides, the running time of the model will drastically increase with solid elements.

Given the complexity of the three angle cells, fully understanding the results analytically is beyond the aim this work. The numerical results are verified using the results of the single angle cells. As a result, difference between numerical results are more difficult to understand and explain. But, given the agreement of the single angle unit cells and the three angle cells being an average of the single angle cells, it is safe to say that the models are correctly defined given the made assumptions.

In terms of compatibility between the nodes of the unit cells, no stress concentrations are found in the models. Furthermore, the beams are showing continuous deformation along the geometry. Furthermore, the three angle cells also contain the same bounding box dimensions to ensure the compatibility.

Beams
As discussed above, the unit cells are expanded towards a 4x4x20 tessellation. For most beams this is completely feasible, however the interface layer for the auxetic- an non-auxetic beam is adding an extra strut, since they don't fully overlap. Therefore, the small peak in young's modulus can be explained. To prevent this effect, the double struts should be manually deleted from the models, which leads to a more complex model. A decision should be made in whether to remove the struts of the 85 or 95 degrees unit cells. To make readers aware of the local increase in Young's modulus and the interface that is created between the layers the struts have not been manually deleted. In Figure 6.1 a visualization of the detail is given, where the overlapping struts are shown. The unit cells in orange and red are presenting the 85 and 95 degrees cells of a part of the full 85/95 degrees beam.

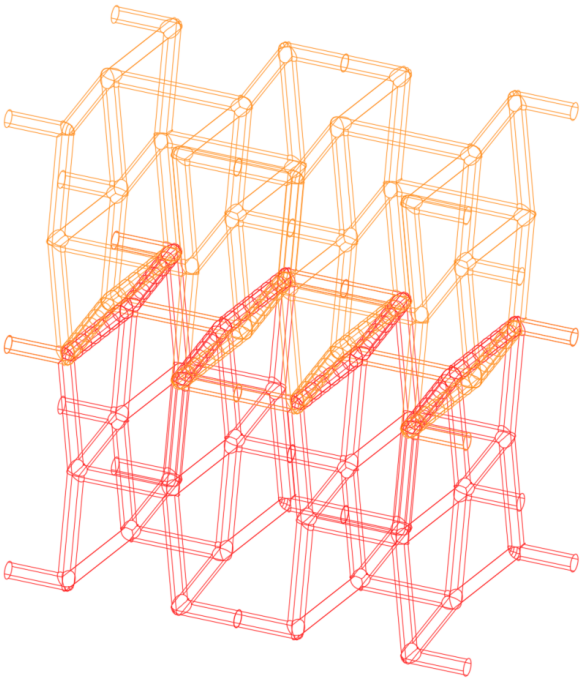

Figure 6.1: Overlap detail - Interface layer 85/95 degrees beam

A pure bending situation is created to ensure zero shear, constant moment and a neutral axis in the middle of the beam. This is used as a starting point to design a lattice that is capable of obtaining different loads while maintaining the property of active confinement in the beam. However, in reality beams are hardly subjected to pure bending and several different design conditions for the lattice need to be taken into account.

In this research, the Poisson's ratio is obtained for bare steel trusses. In practice, the lattice structure is used as steel reinforcement for concrete structural members. Therefore, the lattice will work as a composite and as a result the Poisson's will change. Since a relative density of 5% is chosen for the lattice, the steel is a fraction of the composite. Research is therefore needed on how drastically the Poisson's ratio will change as a composite.

Furthermore, from Table 4.3 moduli are found which are rather similar of different beams. Moreover, the moduli for single unit cells where found to be increasingly different from each other. Figure 6.2 visually helps explaining the reason for this. Moreover, as the tessellation of the number of unit cells in x-direction is increasing the modulus tends to converge. This can be explained by the relative density becoming the leading factor for the modulus as the boundary effects start to decrease. A difference, is still observed since the relative density of the three angle cells are slightly different compared to each.

As mentioned before, the relative densities are between a range of 4.8% to 5.2%. Meaning 4.8% for the 80/85 and 5.2% for the 95/100% three angle cells.

A comparison is made between analytical results of literature and the numerical models in Figure 4.13.

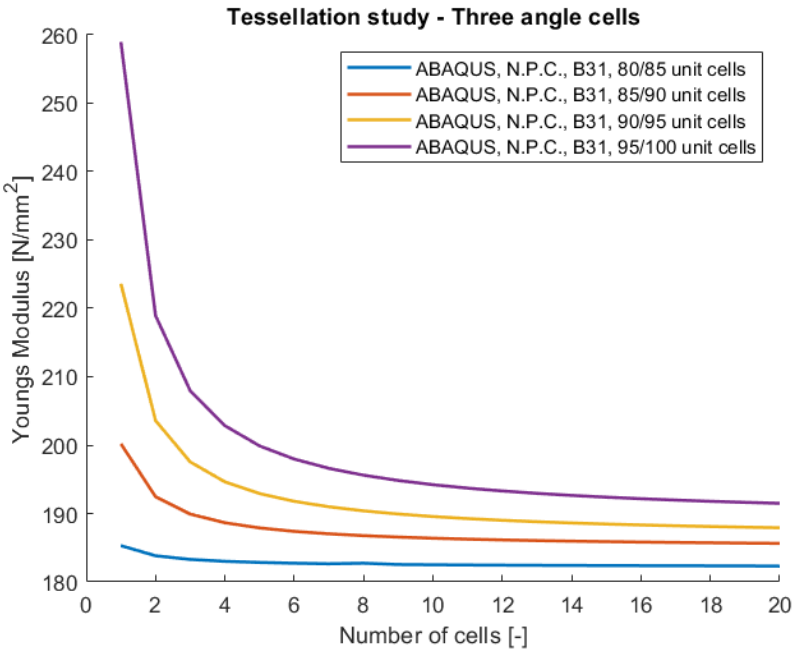

Figure 6.2: Tessellation study - Three angle cells

The reason why 85 degrees is only selected is because the analytical expression from Yang et al. only applies for symmetric 3D re-entrant cells (<90). However, the designed unit cells are compatible and therefore have the same bounding box dimensions. As a result, the further away from a 90 degrees unit cell, the more the unit cell will deviate from the made comparison. This also explains, why results of the different designed unit cells are not included in the comparison.

6.3. Upscaling of auxetic lattices

Robotics

In Figure 5.1 it is shown that there is a huge need for increase in productivity for the construction sector. In this study a state-of-the-art technology is proposed where robotics are being used in construction. In a feasibility study by Parascho et al. the technology is successfully used in several studies [23]. However, using robotics requires an extensive planning process, which is labor intensive and costly. But, repeatable products such as prefabricated steel reinforcement cages for concrete elements, such as columns would be a possible application. Moreover, large projects where for example hundreds of columns are implemented in the design are a suitable option for the use of robotics.

Upscaled lattices

One of the assumptions made in the numerical model for the upscaled lattice is that the nodes are continuous and of the same steel quality as the bars. However, in reality the bars are connected using welds and therefore made out of a different quality steel. Besides, imperfections are not taken in to account such as: misalignment of the bars, tolerances in length of the bars, different qualities of the welds and local failure of the welds that can drastically decrease the load capacity of the lattice.

7

Conclusions and recommendations

In this chapter, the conclusions and recommendations following from this work are presented. The goal of this chapter is to answer the main research questions that are presented in section 1.4. Besides, recommendations are given for future work.

7.1. Conclusions

The following conclusions are drawn based on the research in this report, the work is presented per part.

Geometrical study

- Auxetic and non-auxetic unit cells can be successfully modified towards cubic unit cell bounding box dimensions by adjusting the length of the re-entrant strut and middle vertical strut.
- It has been found that auxetic, cubic- and non-auxetic bow-tie architectures can be effectively combined. Compatibility of the structure is ensured for the designed 85/95 and gradual beam in this work. With that, a continuous steel reinforcement structure is created for concrete structural elements.

Numerical study

- The results show that for the elastic region under tension and compression on the single angle and three angle unit cells a significant drop of stiffness compared to the actual 210 GPa Young's modulus of steel is obtained. A lateral stiffness of 5743-7271 MPa and uni-axial stiffness of 181-280 MPa is found for the single angle cells and 6233-7156 MPa and 186-262 MPa for the three angle cells.
- A same observation is made for the uni-axial stiffness of beams. A range from 192-209 MPa is found, since the beams consist out of a tessellation of single angle or three angle cells.
- The formula from Yang et al. for rectangular sections is modified towards circular sections, which is used for validation of the numerical models [34]. Besides, it is concluded that rectangular sections have higher effective modulus than circular section, this can be explained by the increase in stiffness of the nodes. A comparison between the analytical results of Yang et al. and numerical results from S. Tzortzinis et al. and this report shows that an approximate difference of 10% in modulus is obtained. An explanation is the different types of elements (solid or beam) and boundary conditions (periodic and non-periodic) used.
- From Euler-Bernoulli beam theory and the numerical results it is found that along the length of the designed beams using linear geometry:
  - Constant moment- and zero shear curves are obtained.
  - The moment of inertia is constant and related to the bounding box dimensions.
  - Effective modulus is the leading factor for the geometry of the beam.
  - Kappa slightly changes since the planes don't remain plane as assumed in Euler-Bernoulli beam theory. Due to the small applied rotation these results are however minimal.

- It is found that for beams under pure bending created from single angle cells that a symmetric behavior of Poisson's is obtained over the height of the beam. The Poisson's ratio remains either negative (0 to -0.041) for the auxetic beam and positive for the cubic (0 to 0.05) and non-auxetic (0 to 0.13) beam. When combining cells a changing Poisson's ratio of -0.031 to 0.13 is created for the 85/95 beam and -0.1 to 0.22 for the gradual beam. From these results, it can be concluded that the 85/95 and gradual changing beam are fully actively confining as steel reinforcement for the concrete structural element.
- It is confirmed with a tessellation study that the boundary conditions are not significantly effected in a comparison between 10, 20 and 40 unit cells in length.

Upscaling of auxetic lattices

- It is found that multi-robotic fabrication is a state-of-the-art technology that can help the construction sector further increase its productivity. A successful feasibility study is performed using Grasshopper for Rhinoceros 7. With that, an upscaled lattice is fully assembled using a layer-to-layer sequence.
- A peak load of 403 kN and a negative Poisson's ratio is found under compressive loading conditions for an upscaled lattice of 512.3 x 512.3 x 527.4 mm following the design approach presented in this report.

7.2. Recommendations

Based on the work presented in this report, recommendations are formed for future work. The following recommendations are stated:

- Architected metamaterials
  - Besides, the bow-tie architecture there are several other auxetic and non-auxetic architectures that could be interesting to use as steel reinforcement. A possible idea could be to combine several architectures and use them where they are most desired. Moreover, a combination of bow-tie and double pyramid architectures for example. However, this does severely increase complexity in the model, so it is important to keep that in mind. Besides, upscaling becomes more difficult and costly.
  - To accommodate different types of structural elements, it would be beneficial to perform a parametric study on different relative densities ranging between 1-10 % to account for all conventional structural members in civil engineering applications. A better understanding in the change in mechanical properties would be obtained. By modifying, the length, angle and thickness of the struts a change in relative density is easily obtained.
  - It is worth exploring the idea of placing the lattices in the concrete member where they are most needed, instead of having a lattice running through the whole beam. Material can possibly be saved in this way. Another idea would be to decrease the thickness of the strut throughout the beam depending on where the steel is most needed. However in practice, this might be difficult considering the costs.
  - To test out ideas with combinations of architectures and different parameters it is recommended to use LPBF. Relatively cheap products using Selective Laser Sintering (SLS) can be manufactured from plastic. From there experimental tests can be performed to understand the behavior and modifications can be made when needed.
- Modelling
  - It is recommended to perform research in the non-linear effects of architected metamaterials as lattice. An effect where the moment diagram decreases over the length of the beam is found when non-linear geometry is used. This would contribute on having a better understanding on how the lattices would deform non-linear under pure bending.
  - A changing Poisson's ratio with non-linear geometry is observed in the numerical models. Therefore, it is advised to do research in the effect of changing deformation of the geometry based on the Poisson's ratio in the three principal directions.
- Upscaling of auxetic lattices

- Fabrication of an upscaled lattice is labour intensive for several reasons: cutting of the reinforcement bars, assembling of the rebar and connecting the welds using the robots. However, it is therefore recommended to fully automate the whole process. Where the bars are cut and directly assembled by the robots. Having this process fully automated, enables a continuous production of prefabricated steel cages without the need of labour.
- For future modelling it is recommended to include solid elements (C3D4) elements in the model. As a result, a better approximation of the failure mechanism can be obtained and plastic failure of the nodes is prevented. Besides, it is worth using rigid plates in the models to be closer to reality when testing the lattices and contact between the struts should be allocated. Finally, friction of the edge struts should be given that lead to an increase in peak load and stiffness of the lattice.

References

[1] D. Pasini A. Vigliotti. “Stiffness and strength of tridimensional periodic lattices”. In: *Comput. Methods Appl. Mech. Engrg.* 229-232 (2012), pp. 27–43.

[2] ABAQUS. *ABAQUS Analysis User’s Manual*. 2023. URL: https://classes.engineering.wustl.edu/2009/spring/mase5513/abaqus/docs/v6.6/books/usb/default.htm?startat=pt06ch23s03alm07.html (visited on 03/21/2023).

[3] S. Bronder et al. “Design Study for Multifunctional 3D Re-entrant Auxetics”. In: *Adv. Eng. Mater* (2022).

[4] T. Bock. “The future of construction automation: Technological disruption and the upcoming ubiquity of robotics”. In: *Automation in Construction* 59 (2015), pp. 13–21.

[5] R. Brighenti et al. “Nonlinear deformation behaviour of auxetic cellular materials with re-entrant lattice structure”. In: *Fatigue Fract Engng Mater Struct,* 39 (2016), pp. 599–610.

[6] S. Parascho E.P.G. Bruun S. Adriaenssens. “Structural rigidity theory applied to the scaffold-free (dis)assembly of space frames using cooperative robotics”. In: *Automation in Construction* 141 (2022).

[7] The economist. *Efficiency eludes the construction industry*. 2017. URL: https://www.economist.com/business/2017/08/19/efficiency-eludes-the-construction-industry (visited on 10/11/2023).

[8] EOS. *EOS M 290 Technical Data*. 2023. URL: https://www.eos.info/en/industrial-3d-printer/metal/eos-m-290?&temporaryAccessAnchor=14 (visited on 04/13/2023).

[9] L. Geng, W. Wu, and L. S. Daining Fang. “Damage characterizations and simulation of selective laser melting fabricated 3D re-entrant lattices based on in-situ CT testing and geometric reconstruction”. In: *International Journal of Mechanical Sciences* 157-158 (2019), pp. 231–242.

[10] M. Giftthaler et al. “Mobile Robotic Fabrication at 1:1 scale: the In situ Fabricator”. In: *Constr. Robot* (2017).

[11] A. Gross, P. Pantidis, and S. Gerasimidis. “Correlation between topology and elastic properties of imperfect truss-lattice materials”. In: *Journal of the Mechanics and Physics of Solids* 124 (2019), pp. 577–598.

[12] D. Gu. “Materials creation adds new dimensions to 3D printing”. In: *Sci. Bul.* (2016).

[13] Chan Soo Ha et al. “Chiral three-dimensional lattices with tunable Poisson’s ratio”. In: *Smart Materials and Structures* 25 (2016).

[14] W. Hao, J. Liu, and H. Kanwal. “Compressive properties of cementitious composites reinforced by 3D printed PA 6 lattice”. In: *Polymer Testing* 117 (2022).

[15] H. M. A. Kolken and A. A. Zadpoor. “Auxetic mechanical metamaterials”. In: *RSC Adv.* 7 (2017), pp. 5111–5129.

[16] H.M.A. Kolken et al. “Merging strut-based and minimal surface meta-biomaterials: Decoupling surface area from mechanical properties”. In: *Additive manufacturing* 52 (2022).

[17] U. D. Larsen, O. Signund, and S. Bouwsta. “Design and fabrication of compliant micromechanisms and structures with negative Poisson’s ratio,” in: *J. Microelectromech. Syst.* 6.2 (1997), pp. 99–106.

[18] T.C. Lim. “A 3D auxetic material based on intersecting double arrowheads”. In: *Phys. Status Solidi B* 253.7 (2016), pp. 1252–1260.

[19] L. Liu et al. “Elastic and failure response of imperfect three-dimensional metallic lattices: the role of geometric defects induced by Selective Laser Melting”. In: *J. Mech. Phys. Solids* 107 (2017), pp. 160–184.

[20] I. G. Masters and K. E. Evans. “Models for the elastic deformation of honeycombs”. In: *Composite structures* 35 (1996), pp. 403–422.

[21] Nejc Novak et al. “Response of Chiral Auxetic Composite Sandwich Panel to Fragment Simulating Projectile Impact”. In: *Phys. Status Solidi* 257 (2021).

[22] I. Ntintakis and G. E. Stavroulakis. “Infill Microstructures for Additive Manufacturing”. In: *Appl. Sci.* (2022).

[23] S. Parascho. “Cooperative Robotic Assembly Computational Design and Robotic Fabrication of Spatial Metal Structures”. In: *ETH Zurich* (2019).

[24] M.G. Rashed et al. “Metallic microlattice materials: A current state of the art on manufacturing, mechanical properties and applications”. In: *Science Direct* (2016).

[25] F. Scarpa and P. Tomlin. “On the transverse shear modulus of negative Poisson’s ratio honeycomb structures”. In: *Fatigue Fract. Eng. Mater. Struct* 23.8 (2000), pp. 717–720.

[26] B. Schagen. “Feasibility study - Additional Research Project”. In: *TU Delft Repository* (2023).

[27] F. Smith, F. Scarpa, and G. Burriesci. “Simultaneous optimization of the electromagnetic and mechanical properties of honeycomb materials”. In: *SPIE’s 9th Annual International Symposium on Smart Structures and Materials* (2002), pp. 582–591.

[28] N. G. STEPHEN. “mindlin plate theory: best shear coefficient and higher spectra validity”. In: *Journal of Sound and Vibration* 202.4 (1997), pp. 539–553.

[29] G. Tzortzinis, A.Gross, and S. Gerasimidis. “Auxetic boosting of confinement in mortar by 3D reentrant truss lattices for next generation steel reinforced concrete members”. In: *Extreme Mechanics Letters* 52 (2022).

[30] T. Vitalis. “METALLIC AUXETIC TRUSS LATTICE STRUCTURES”. In: (2022).

[31] J. Whitty, F. Nazare, and A. Alderson. “Modelling the effects of density variations on the in-plane Poisson’s ratios and Young’s Moduli of periodic conventional and re-entrant”. In: *Cell. Polym.* 21.2 (2002), pp. 69–98.

[32] L. Yang, H. West O. Harrysson, and D. Cormier. “Mechanical properties of 3D re-entrant honeycomb auxetic structures realized via additive manufacturing”. In: *Int. J. Solids Struct.* 69 (2015), pp. 475–490.

[33] L. Yang et al. “Compressive properties of Ti–6Al–4V auxetic mesh structures made by electron beam melting”. In: *Acta Mater.* 60.8 (2012), pp. 3370–3379.

[34] L. Yang et al. “Modeling of uniaxial compression in a 3D periodic re-entrant lattice structure”. In: *J. Mater. Sci.* 48 (2013), pp. 1413–1422.

[35] L. Yang et al. “Non-stochastic Ti–6Al–4V foam structures with negative Poisson’s ratio”. In: *Materials Science and Eng. A.* 558 (2012), pp. 579–585.

[36] L. Yang et al. “Shear properties of the re-entrant auxetic structure made via electron beam melting”. In: *Solid Freeform Fabrication Symposium* ().

[37] C. Y. Yap et al. “Review of selective laser melting: Materials and applications”. In: *Appl. Phys. Rev.* 2 (2015).

A

Appendix A - Unit cell designs

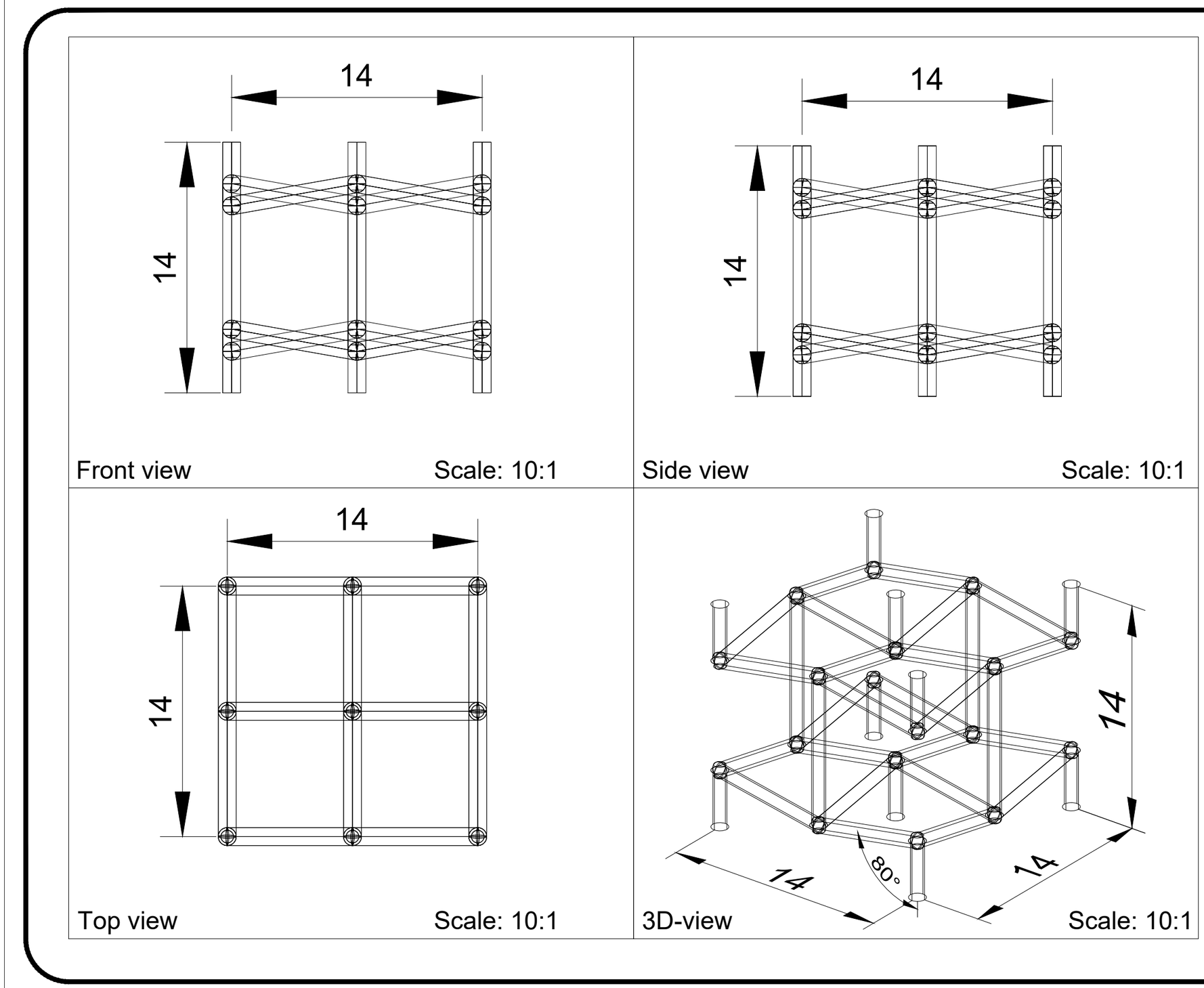

Figure A.1: 80 degrees unit cell

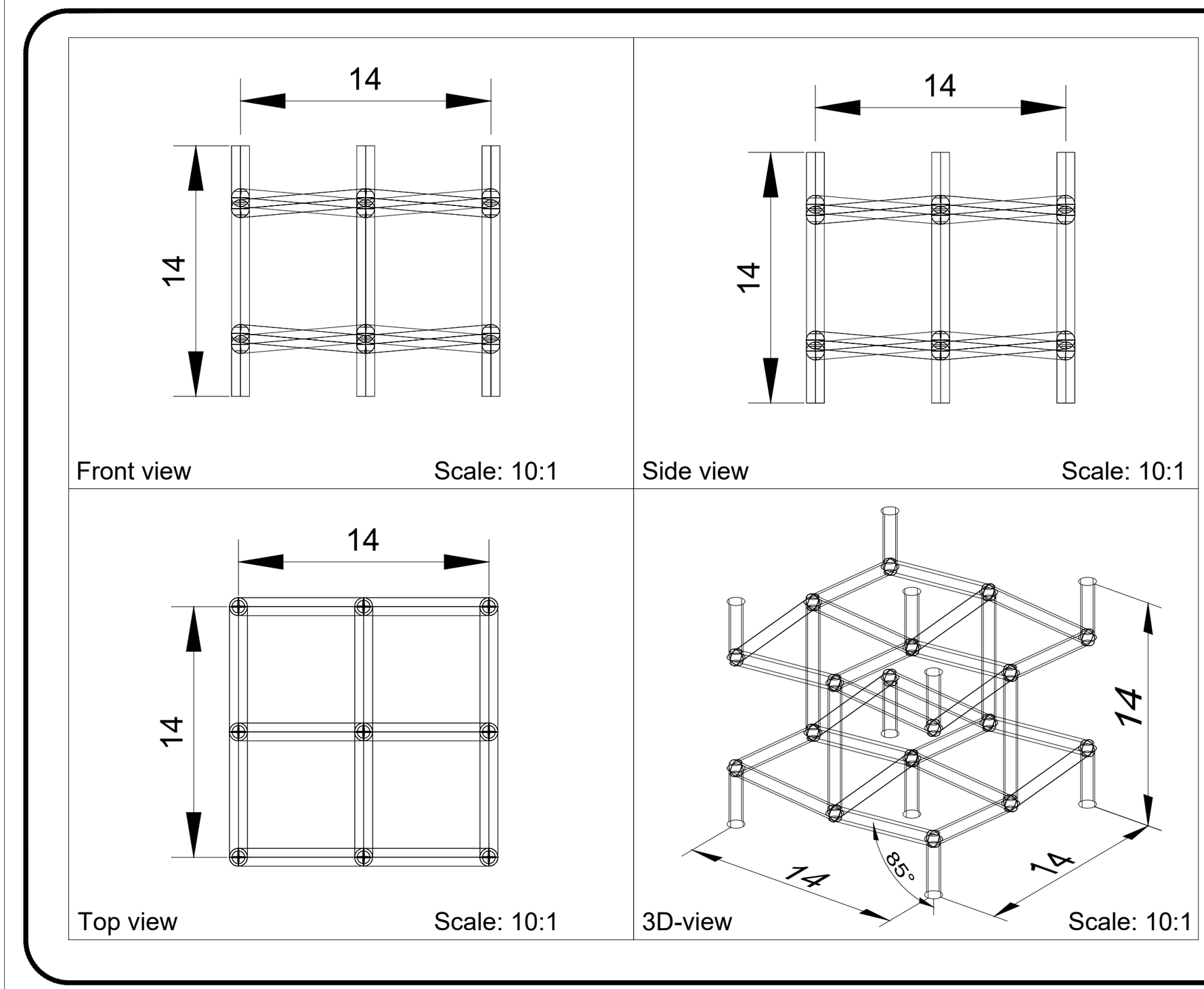

Figure A.2: 85 degrees unit cell

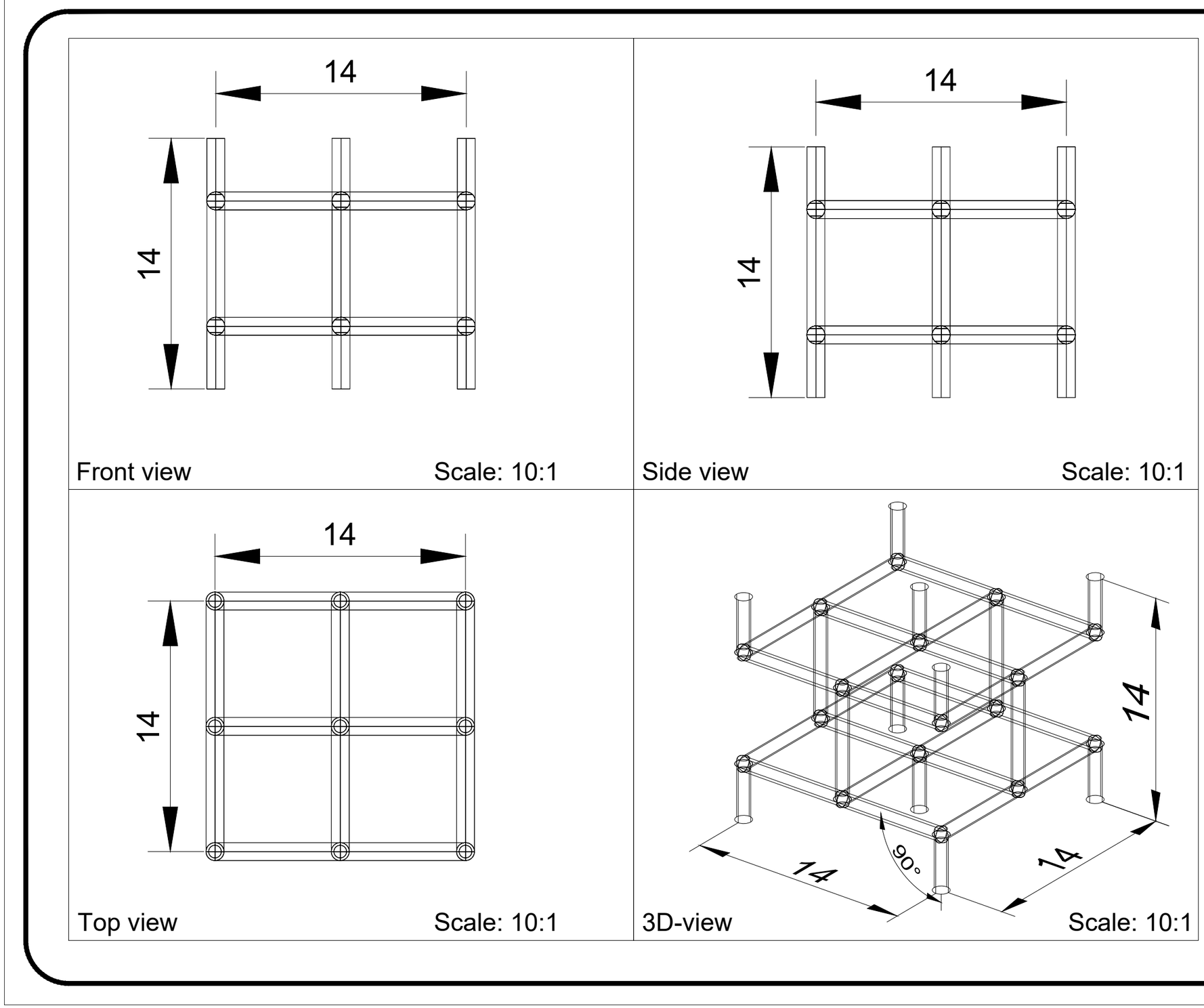

Figure A.3: 90 degrees unit cell

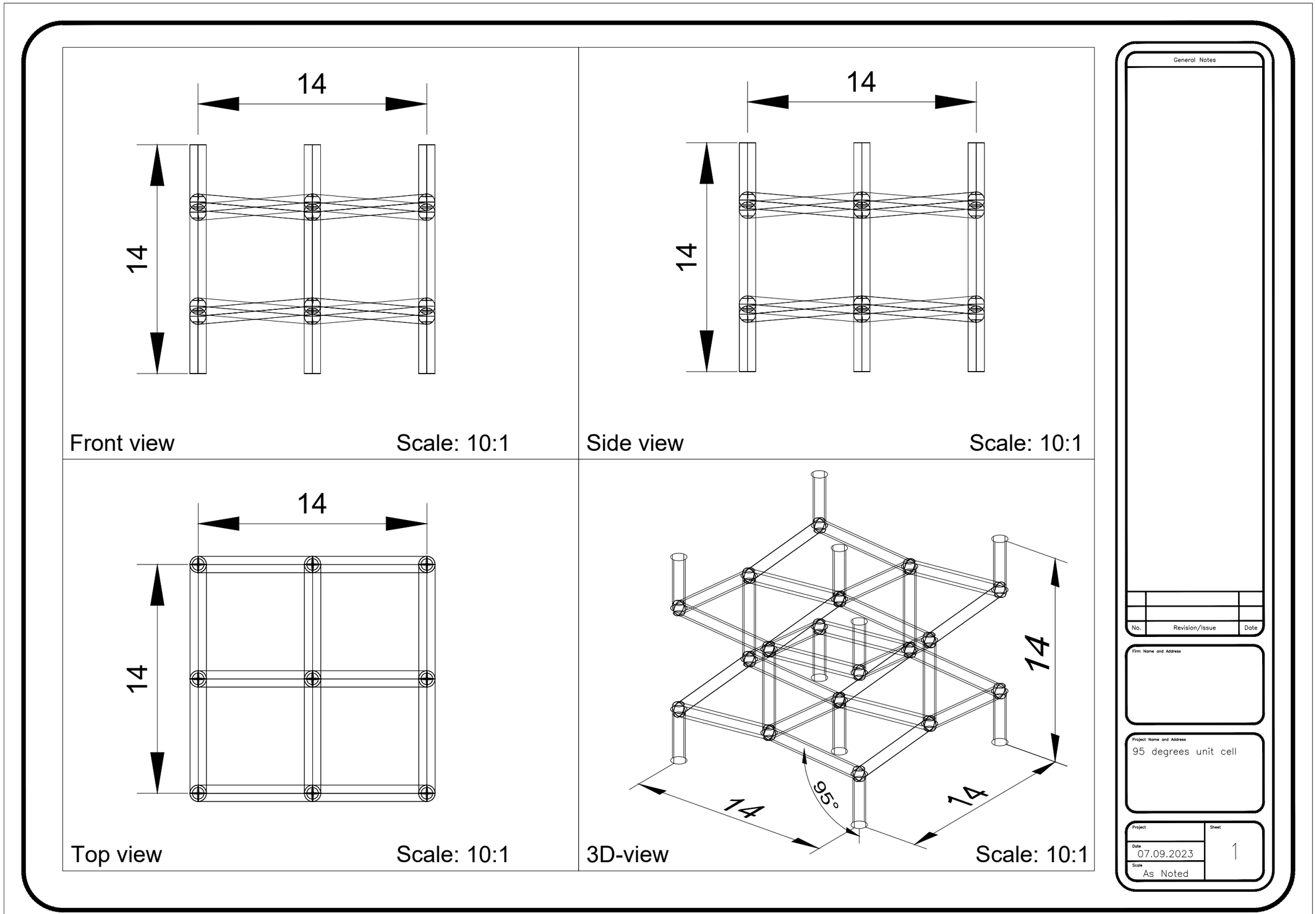

Figure A.4: 95 degrees unit cell

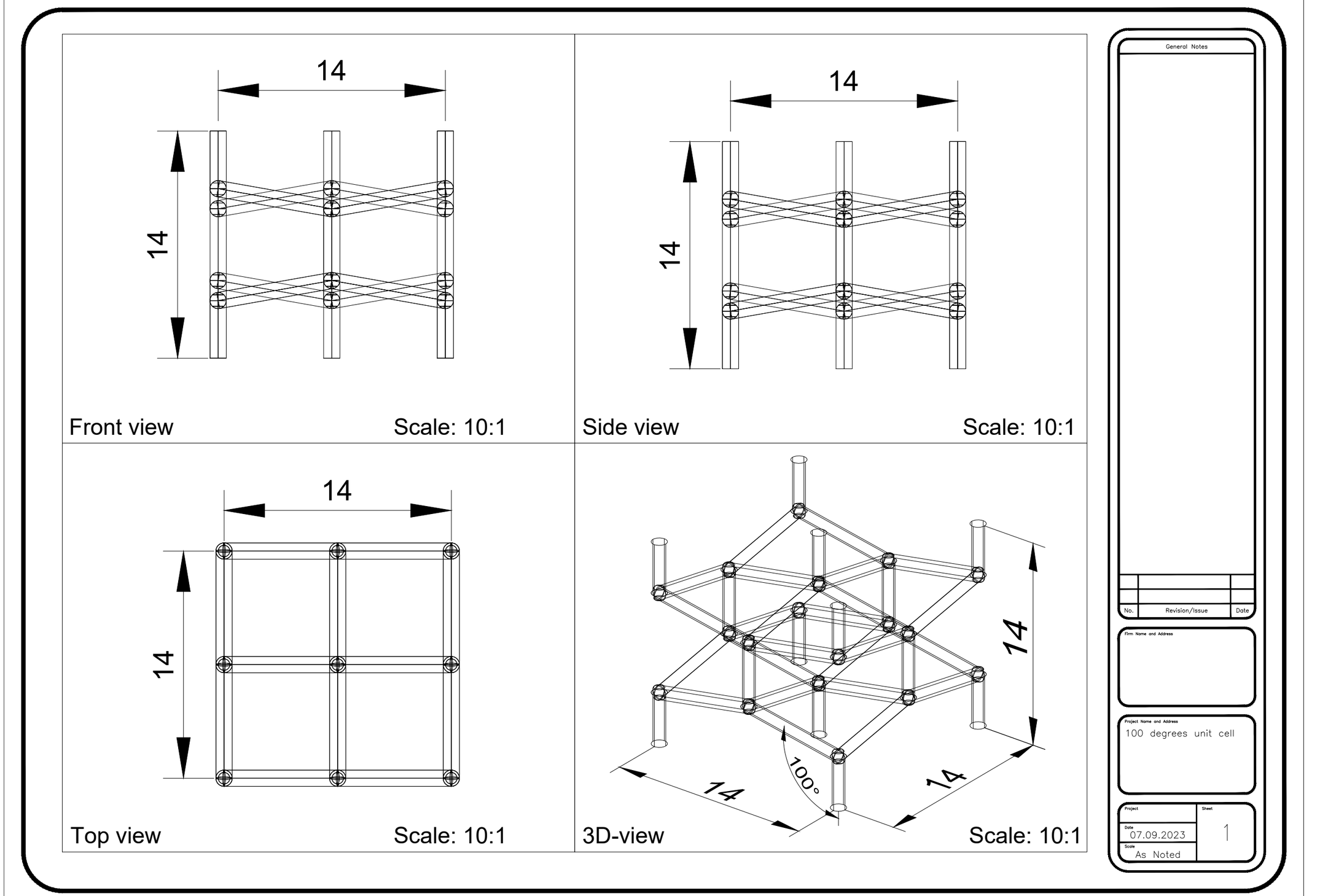

Figure A.5: 100 degrees unit cell

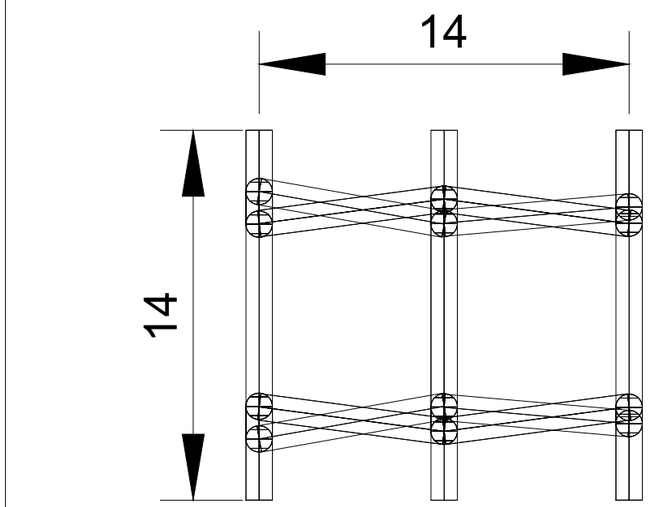

Front view Scale: 10:1

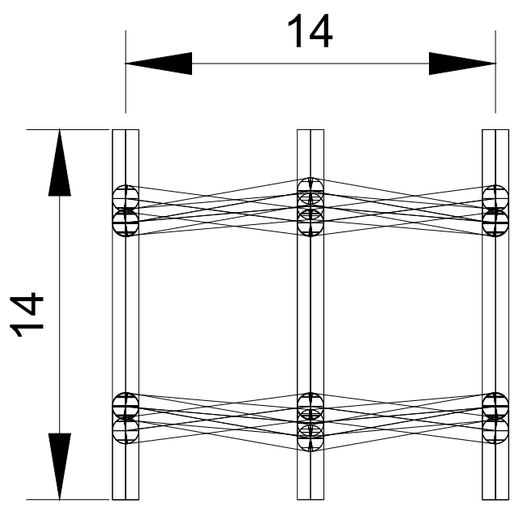

Side view Scale: 10:1

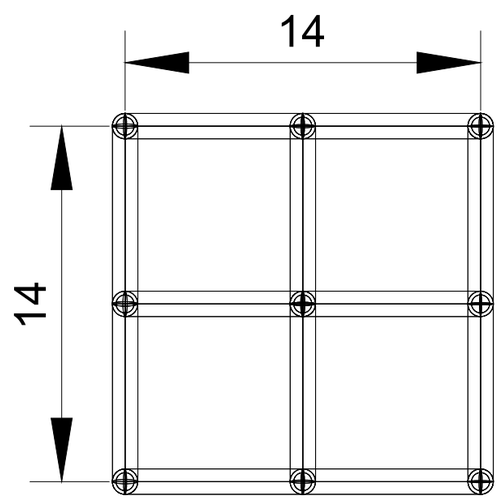

Top view Scale: 10:1

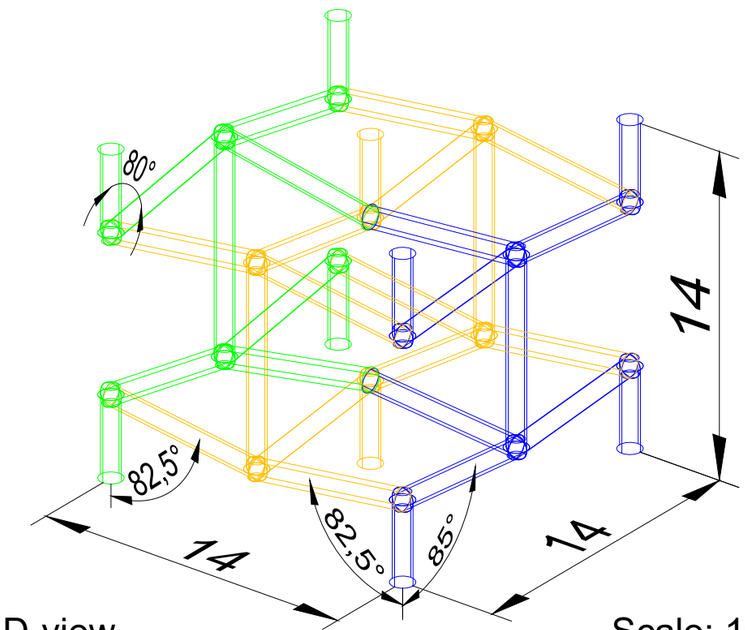

3D-view Scale: 10:1

General Notes

No.	Revision/Issue	Date

Firm Name and Address

Project Name and Address
8085 degrees unit cell

Project	Sheet
Date 06.09.2023	1
Scale As Noted	

Figure A.6: 80/85 degrees unit cell

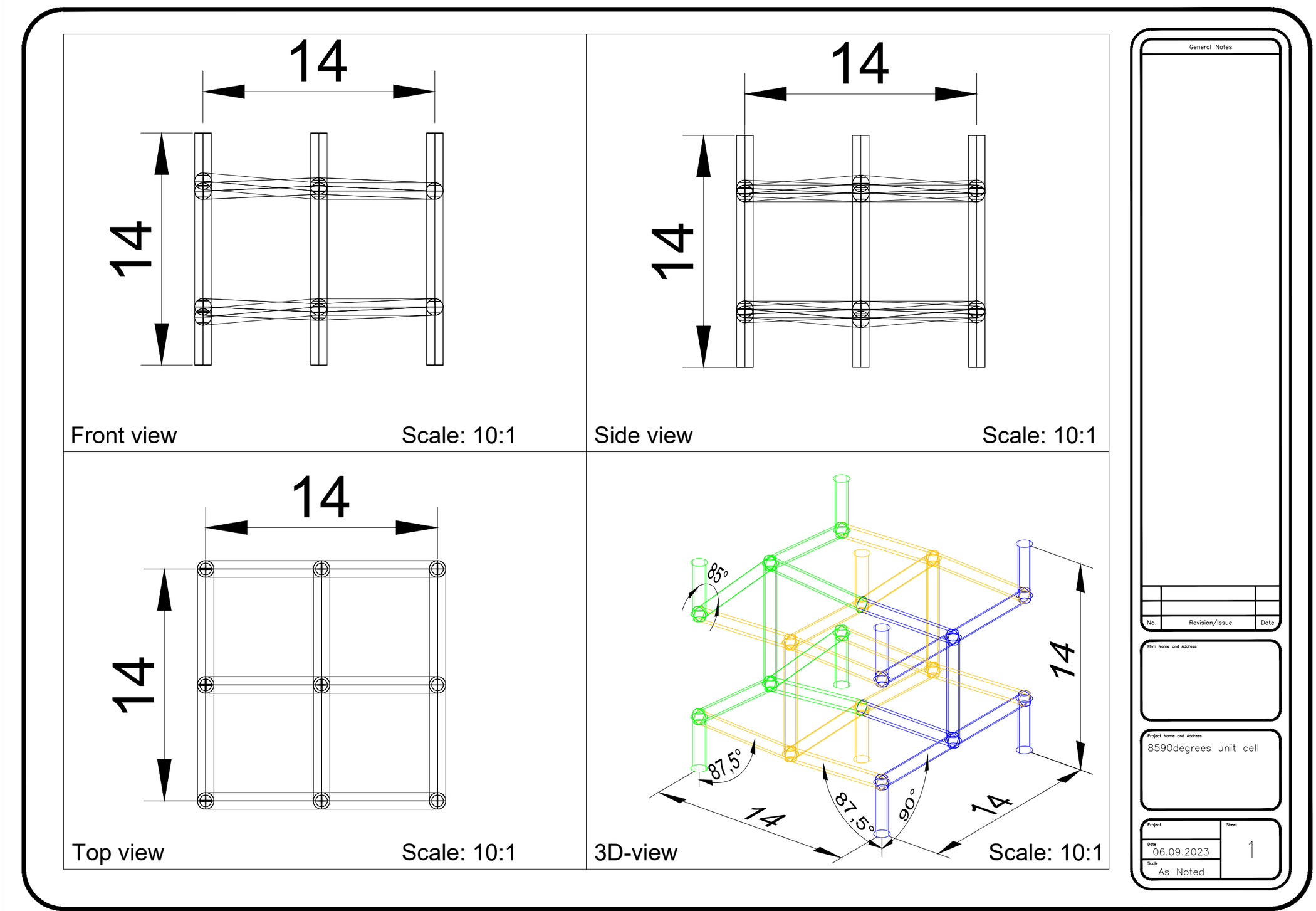

Figure A.7: 85/90 degrees unit cell

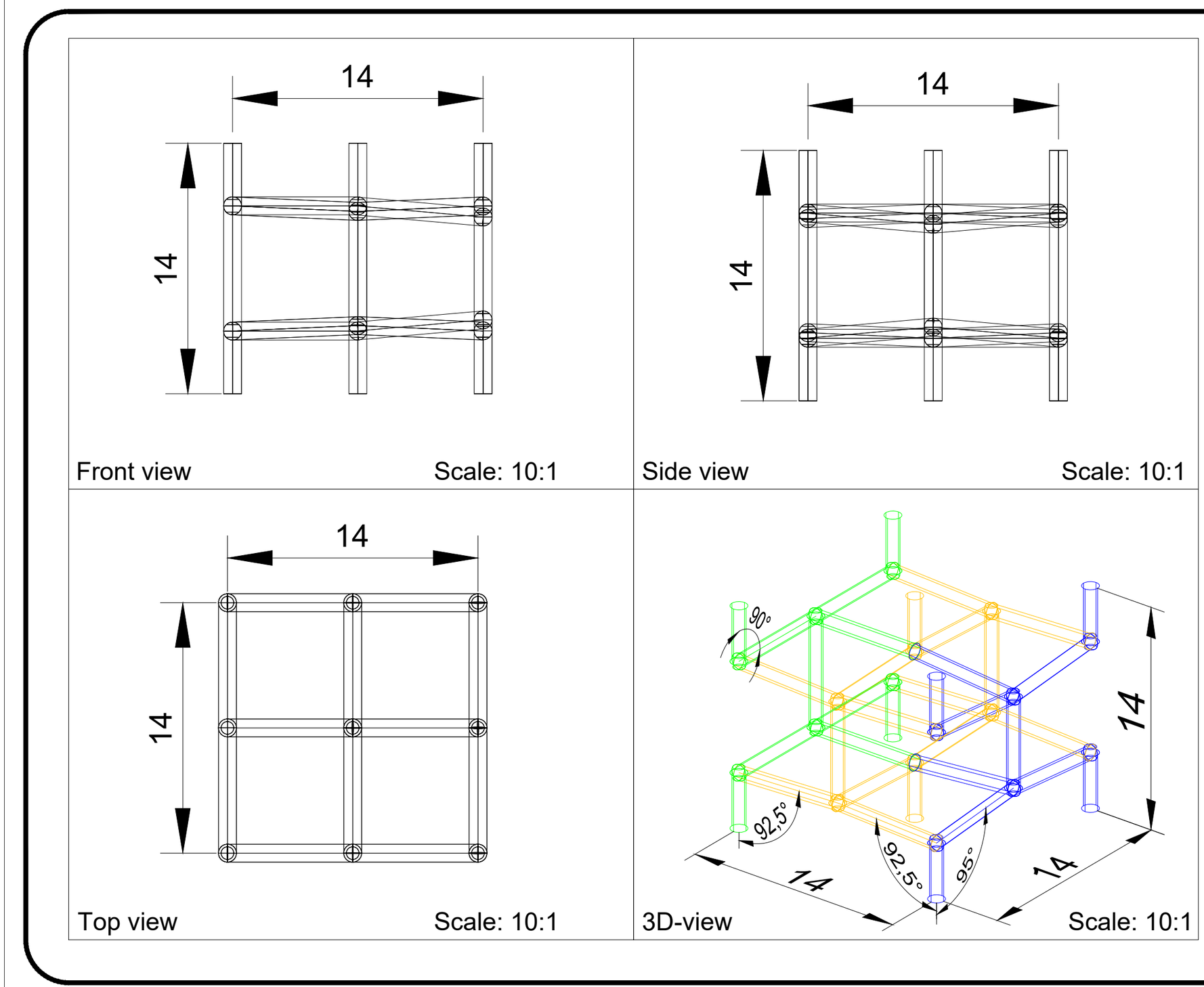

Figure A.8: 90/95 degrees unit cell

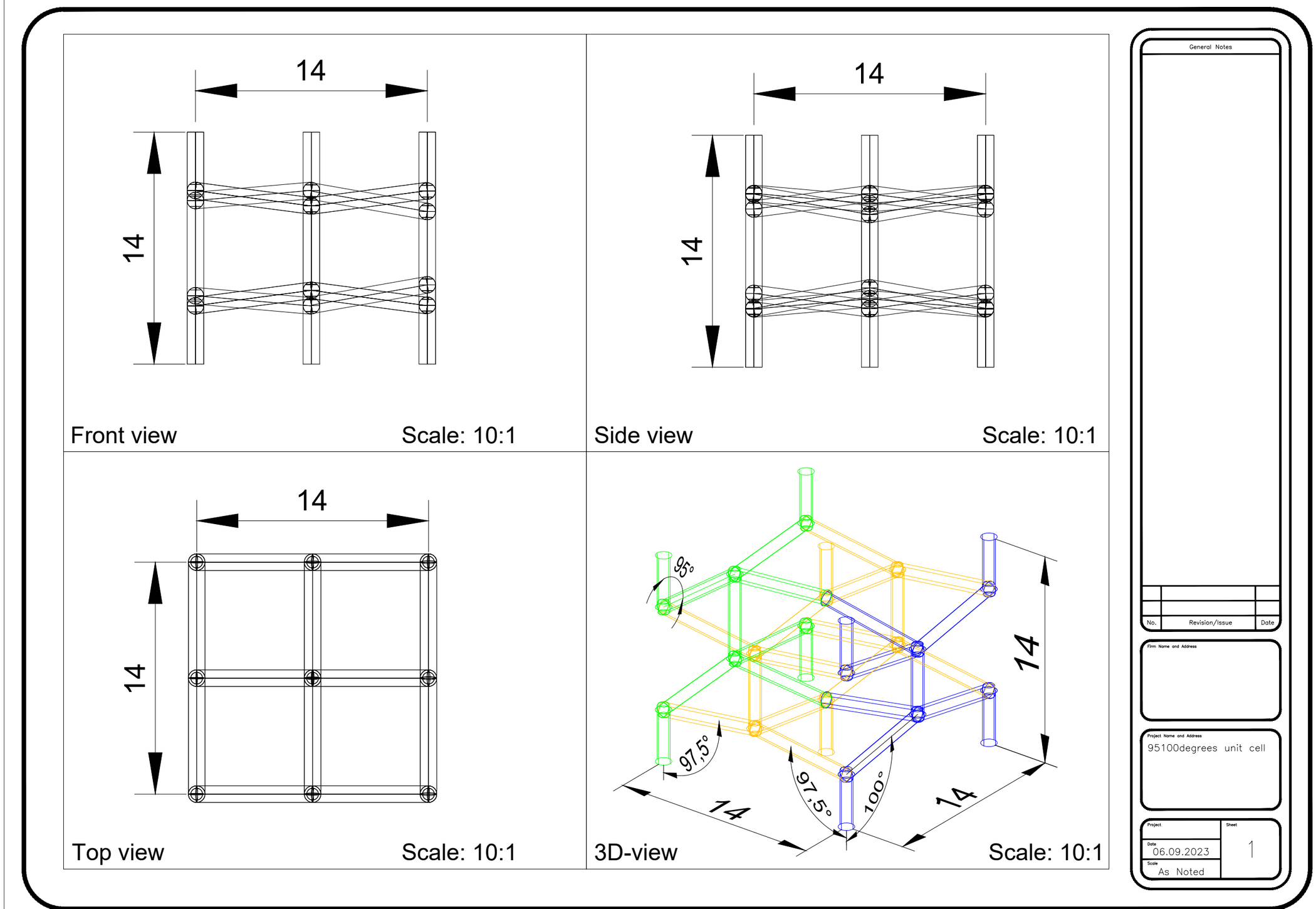

Figure A.9: 95/100 degrees unit cell

B

Appendix B - Beams

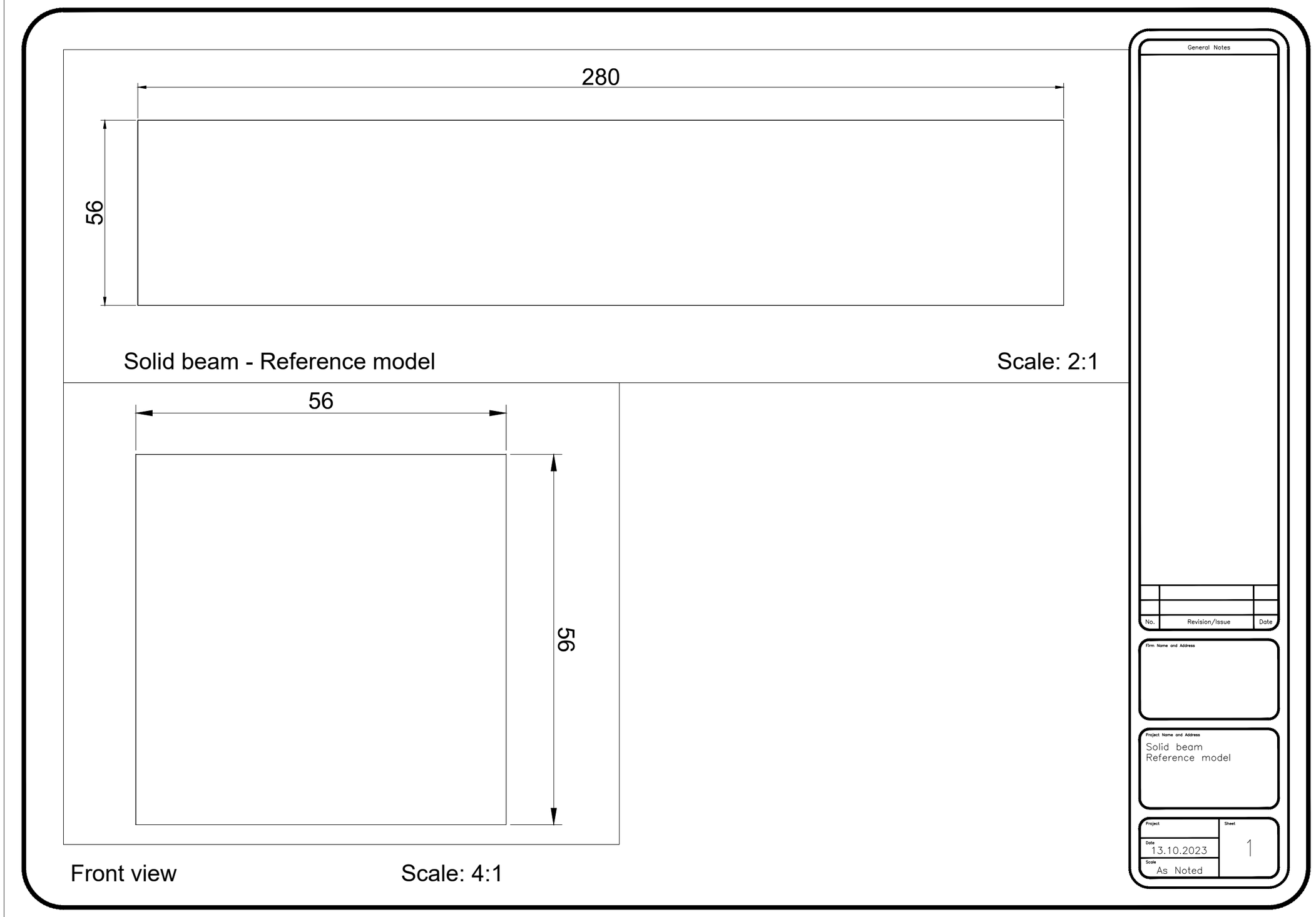

Figure B.1: Solid beam - reference model

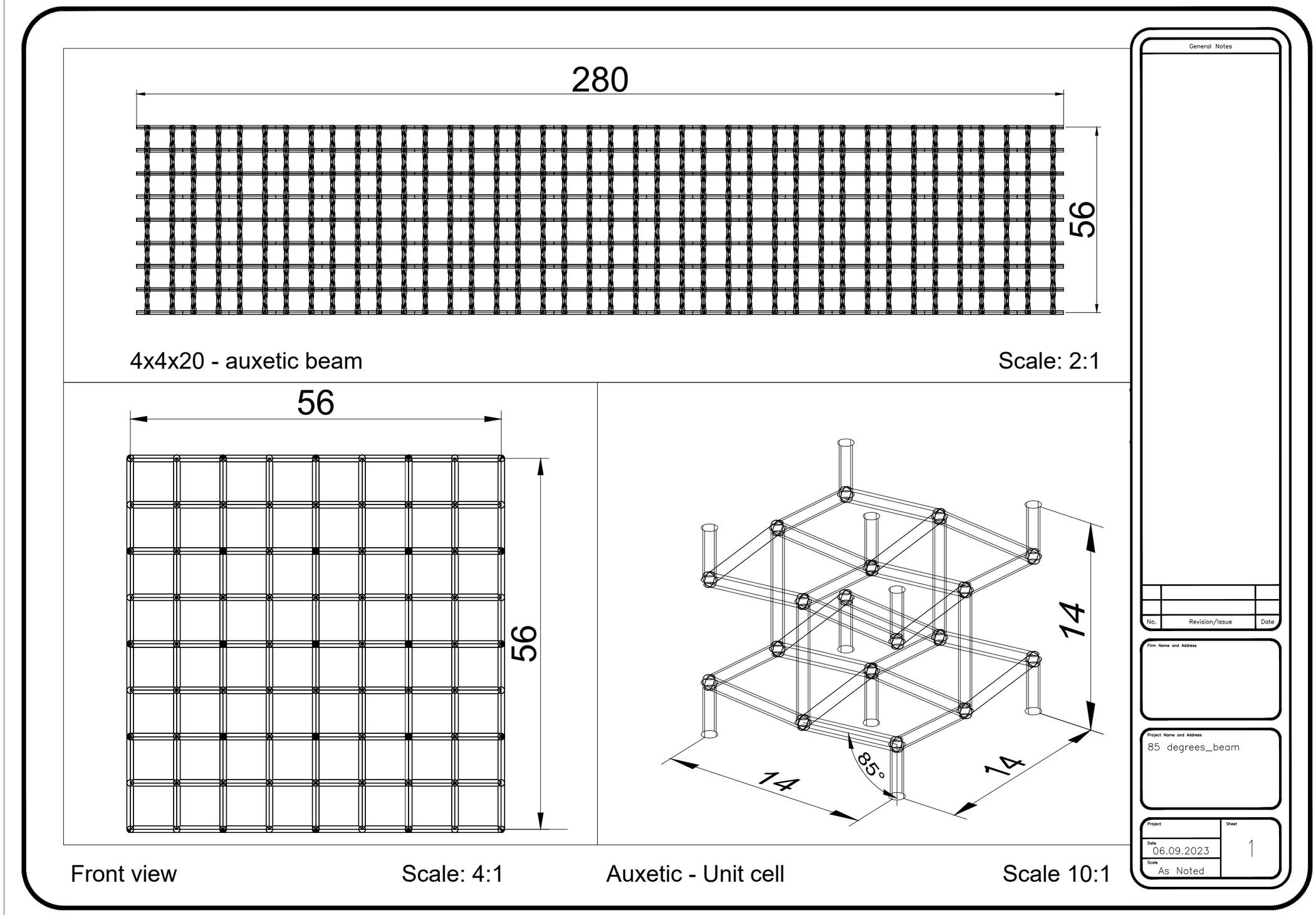

Figure B.2: Auxetic beam

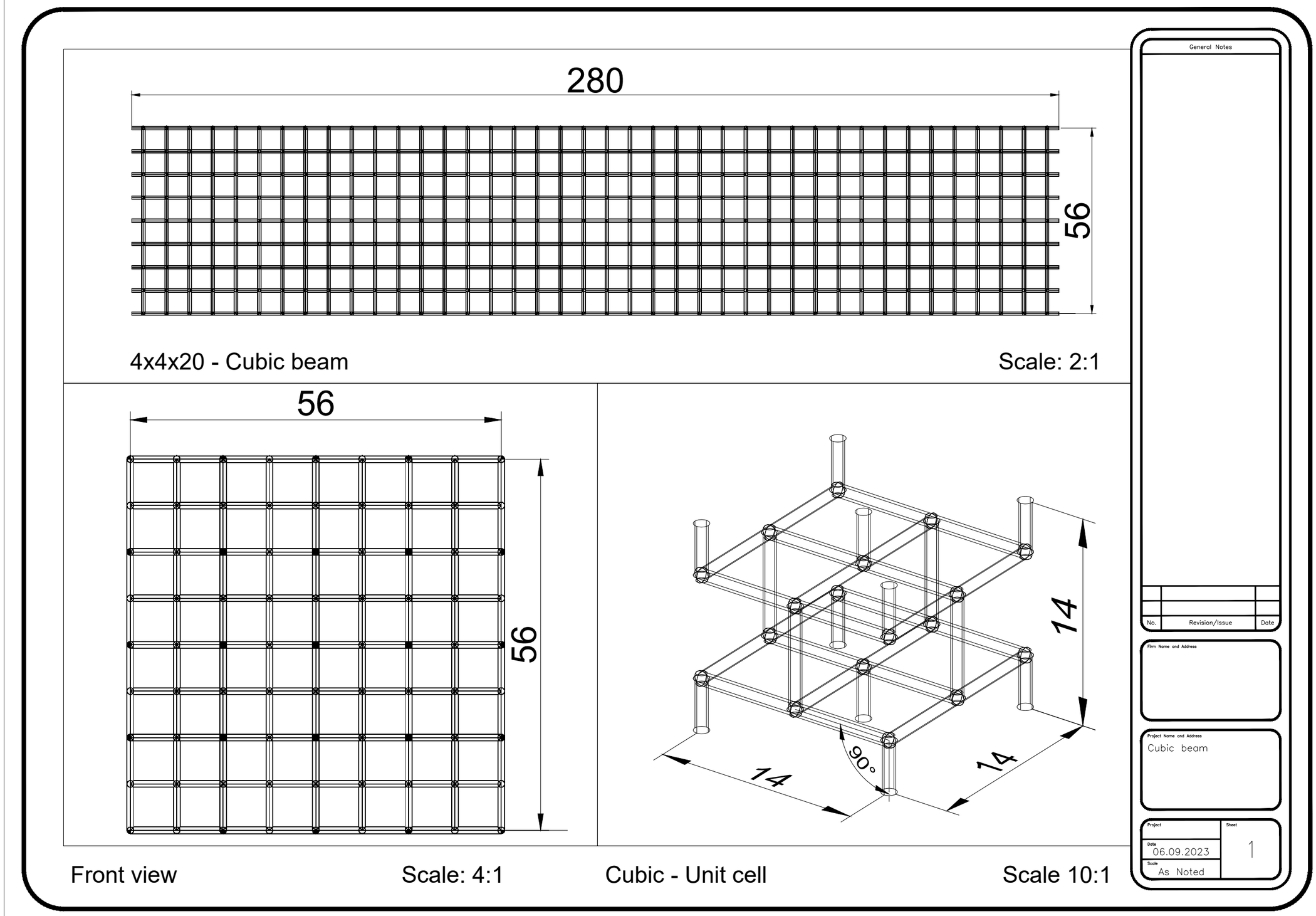

Figure B.3: Cubic beam

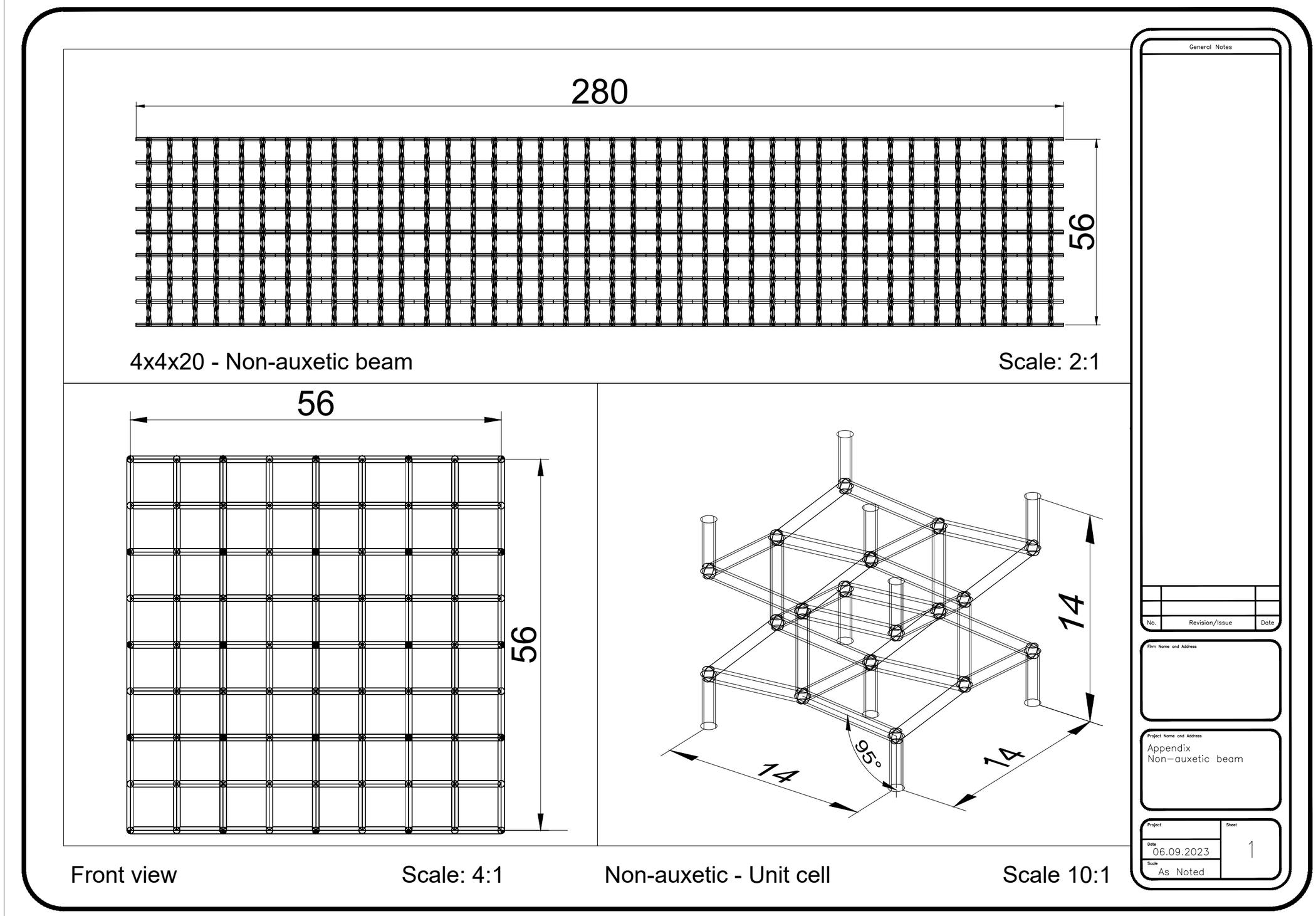

Figure B.4: Non-auxetic beam

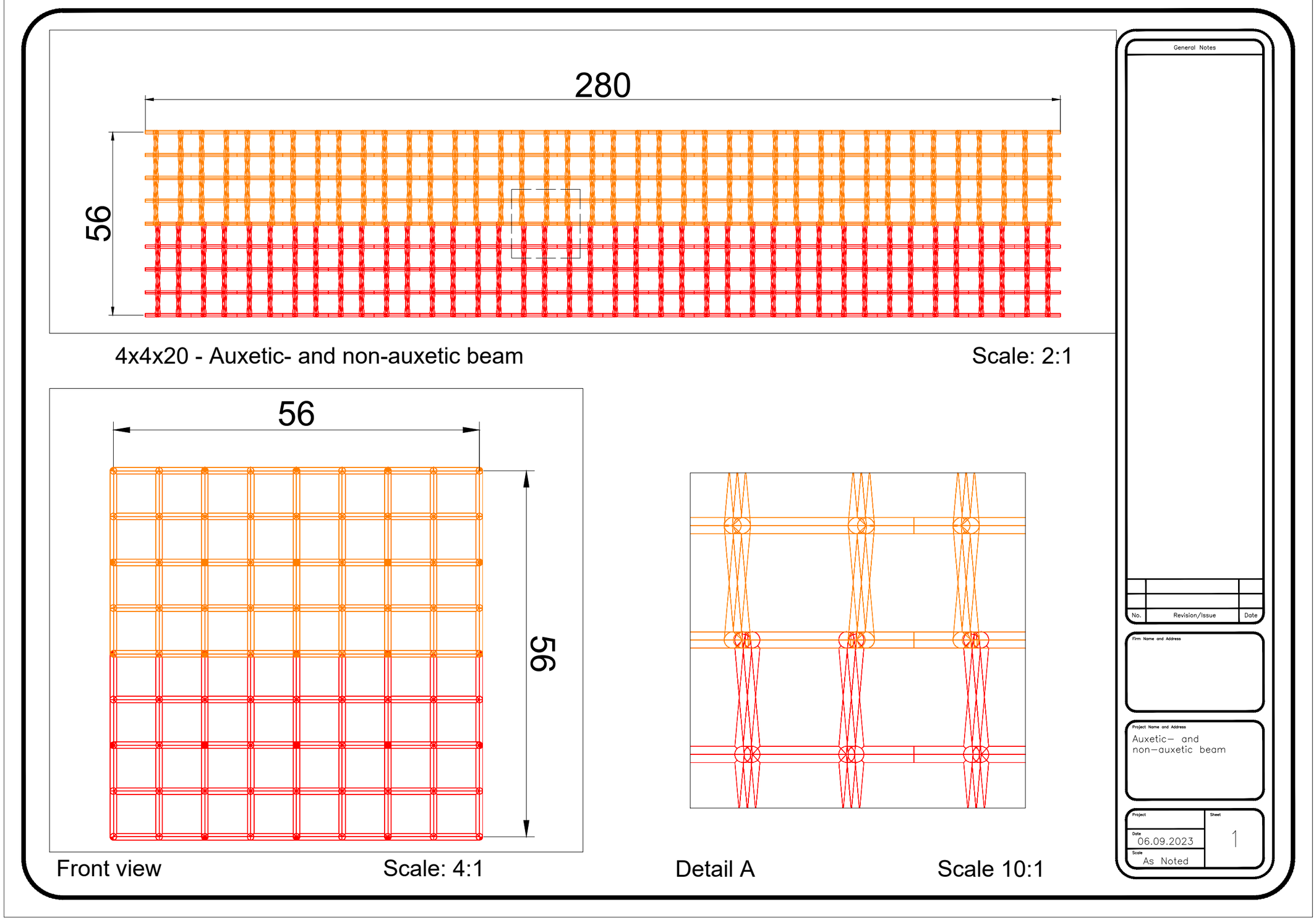

Figure B.5: Auxetic-and non-auxetic beam

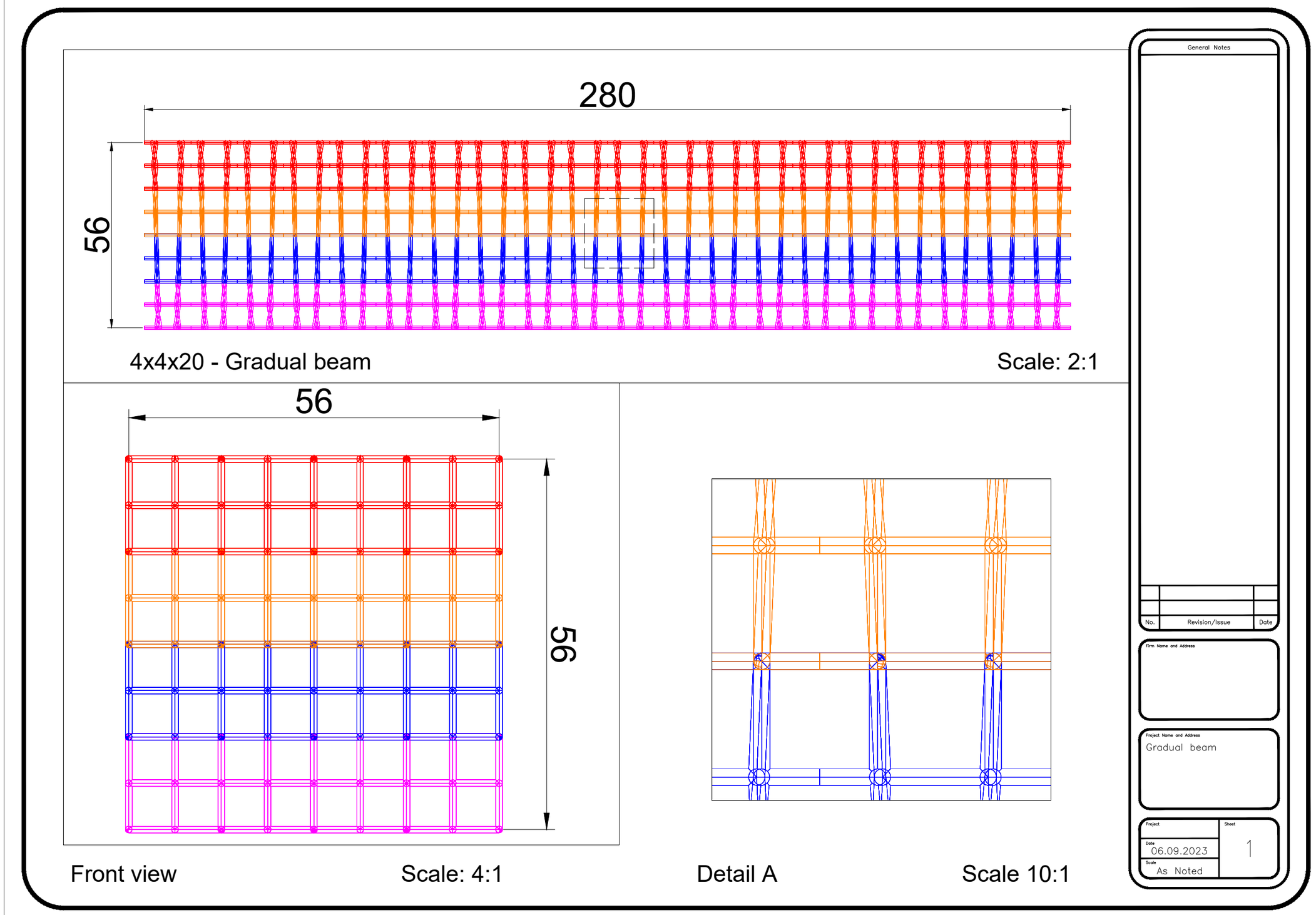

Figure B.6: Gradual beam

C

Appendix C - Tables Numerical study

Table C.1: Auxetic beam - begin unit cell - data ABAQUS

Auxetic beam - Begin unit cell		
Length	**Moment**	**Shear**
[mm]	[Nmm]	[N]
0	10250	6.64E-06
14	10250	4.77E-06
28	10250	1.24E-05
42	10250	4.77E-06
56	10250	0
70	10250	0
84	10250	7.63E-06
98	10250	1.91E-06
112	10250	6.68E-06
126	10250	1.91E-05
140	10250	5.72E-06
154	10250	7.63E-06
168	10250	7.63E-06
182	10250	5.72E-06
196	10250	1.10E-06
210	10250	9.54E-06
224	10250	4.77E-06
238	10250	0
252	10250	1.91E-06
266	10250	1.05E-05
280	10250	1.15E-05

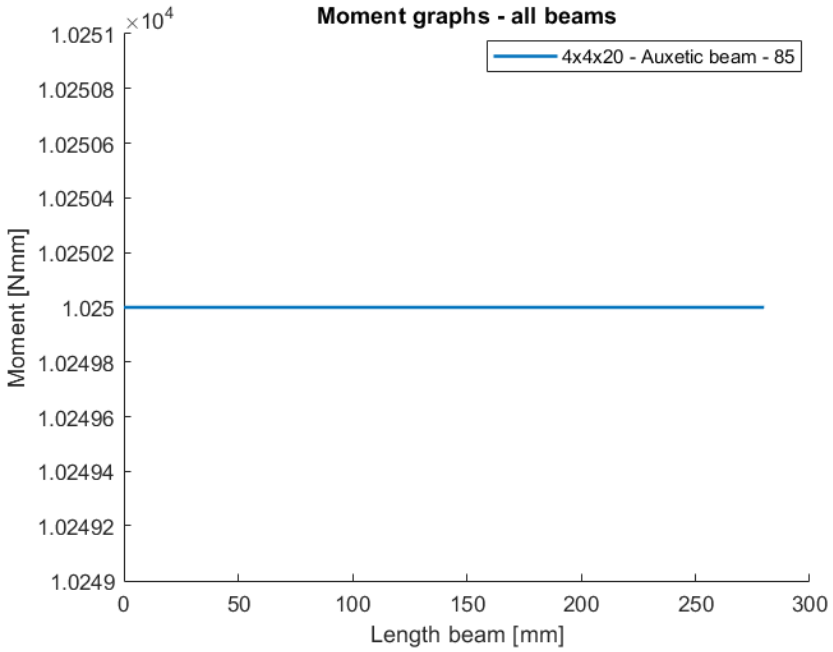

Figure C.1: Auxetic beam- Moment diagram

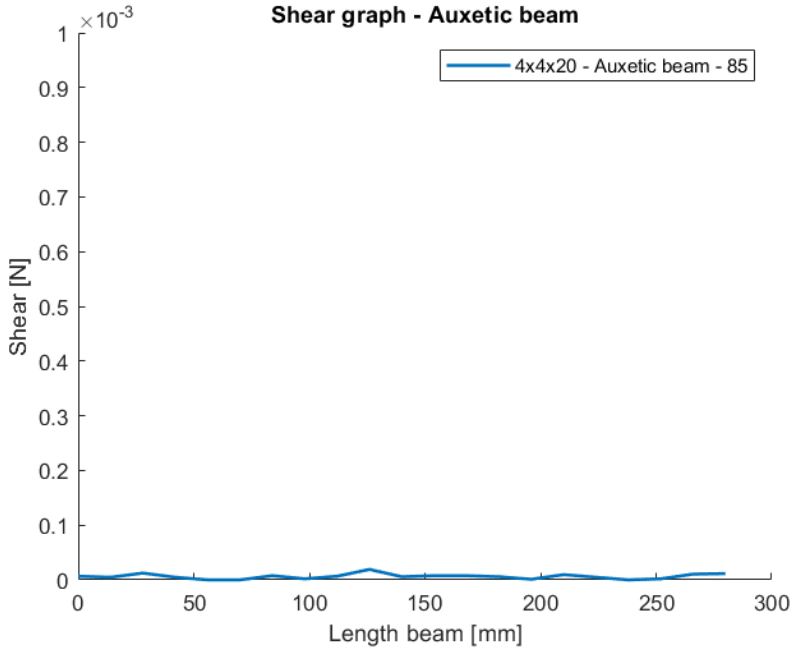

Figure C.2: Auxetic beam - Shear diagram

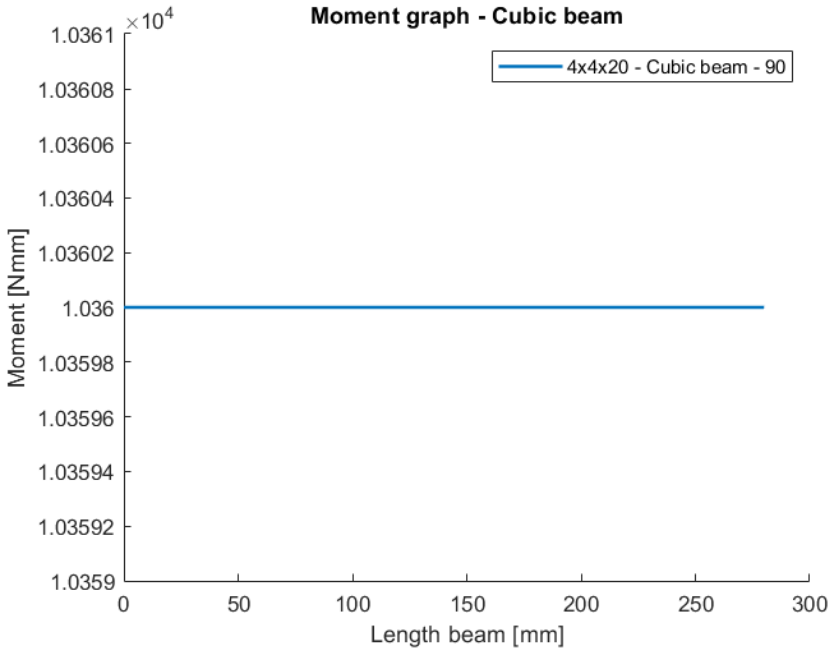

Figure C.3: Cubic beam- Moment diagram

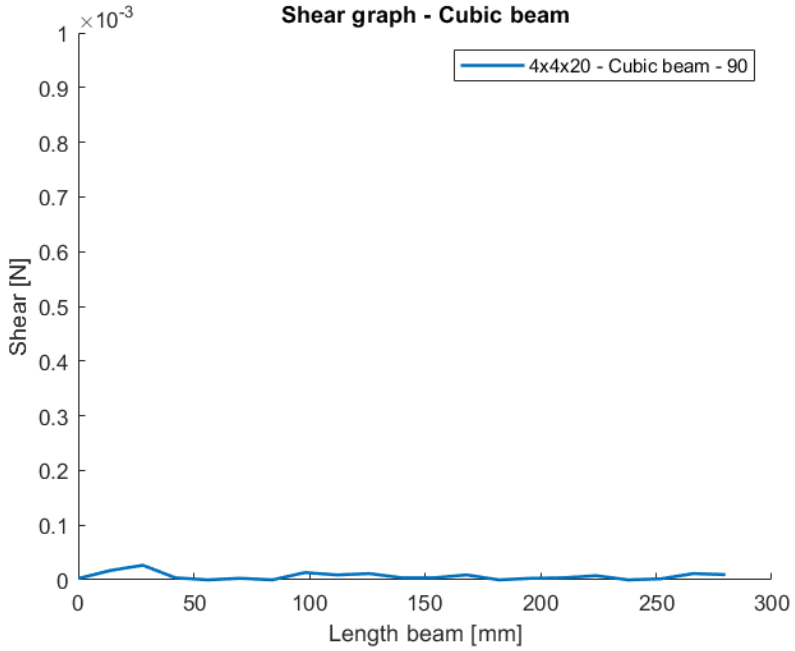

Figure C.4: Cubic beam - Shear diagram

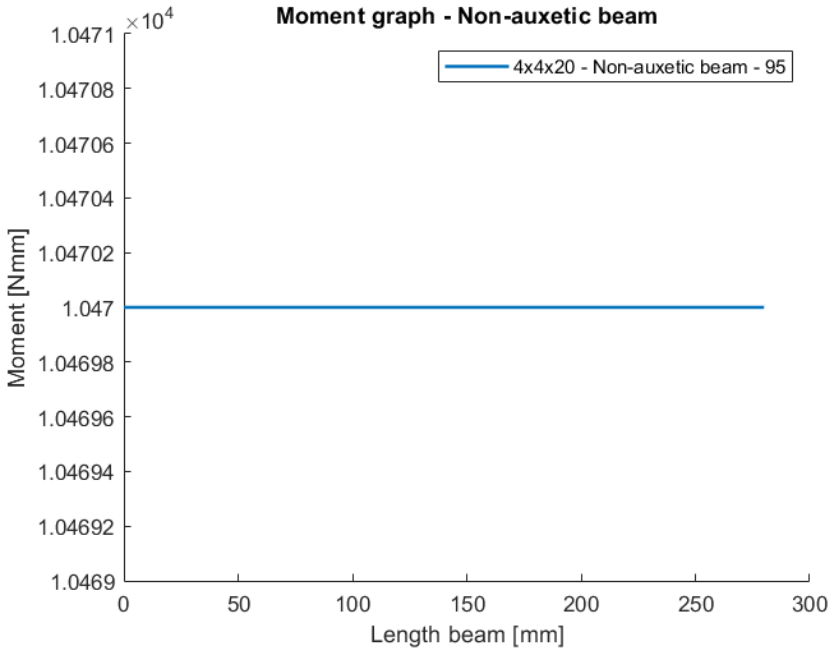

Figure C.5: Non-Auxetic beam- Moment diagram

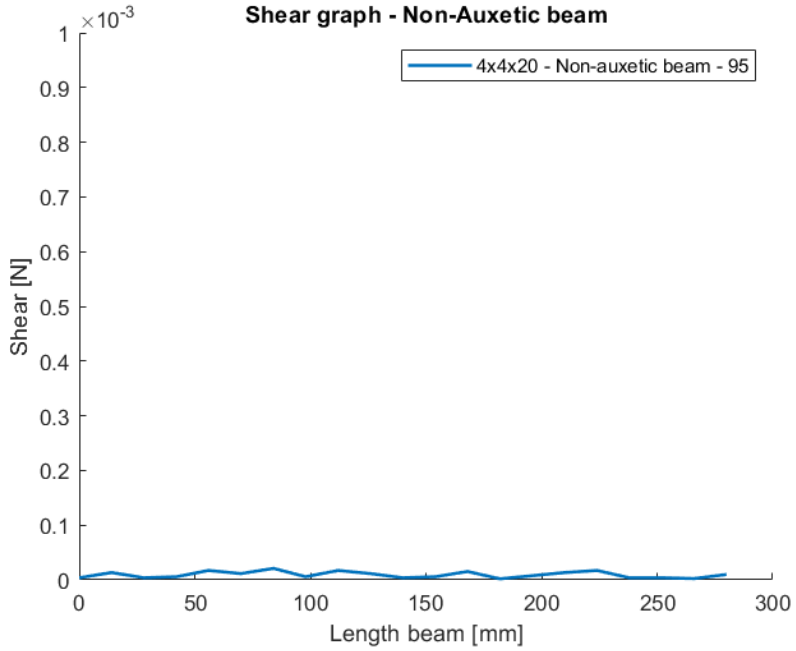

Figure C.6: Non-Auxetic beam - Shear diagram

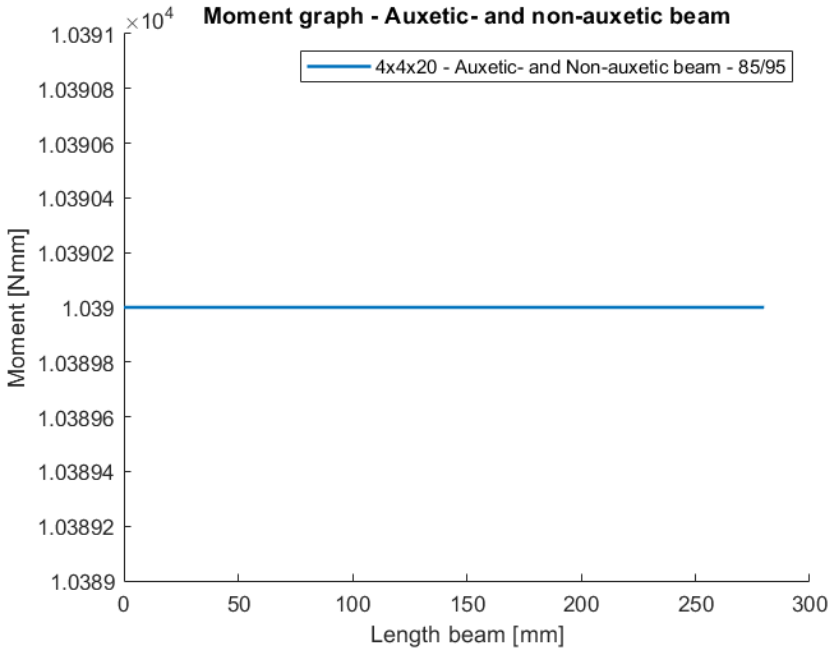

Figure C.7: Auxetic- and Non-Auxetic beam- Moment diagram

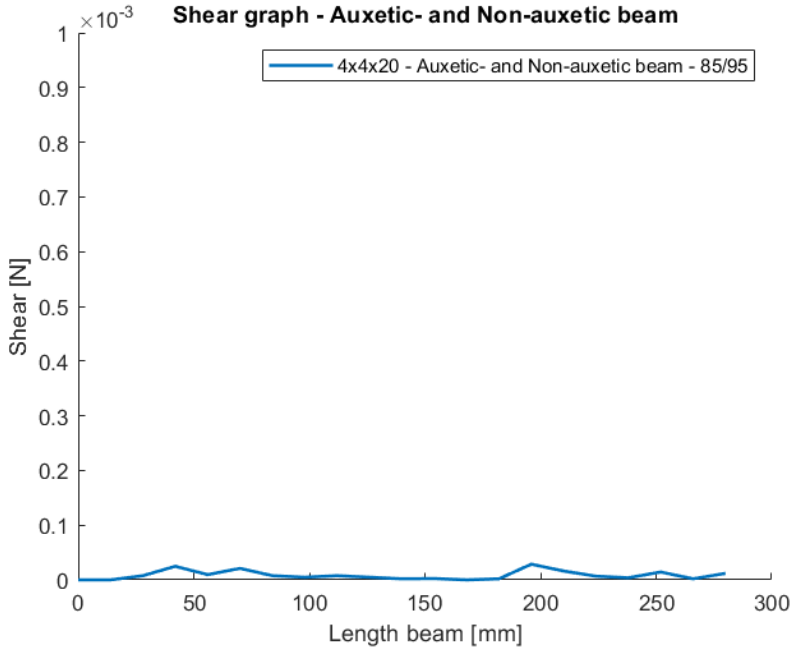

Figure C.8: Auxetic- and Non-Auxetic beam - Shear diagram

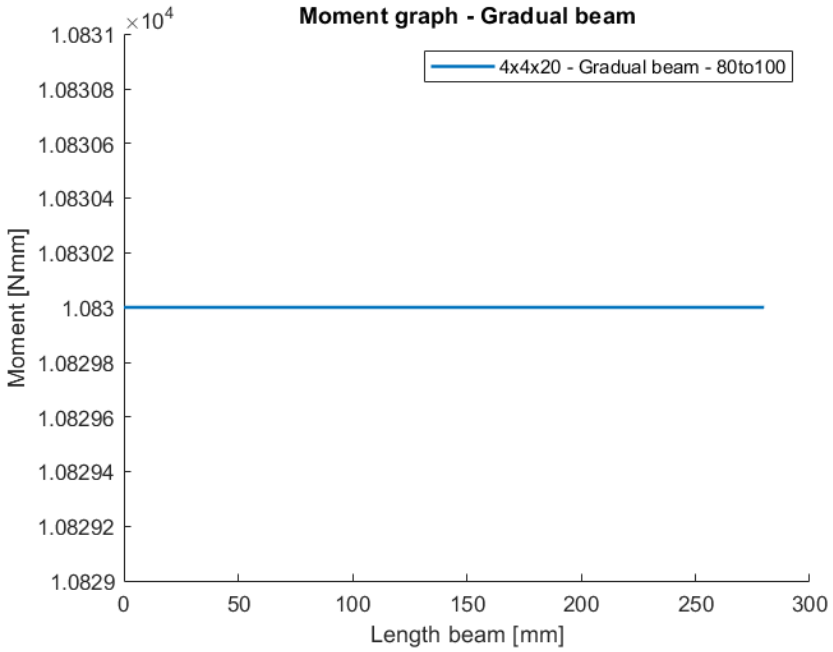

Figure C.9: Gradual beam- Moment diagram

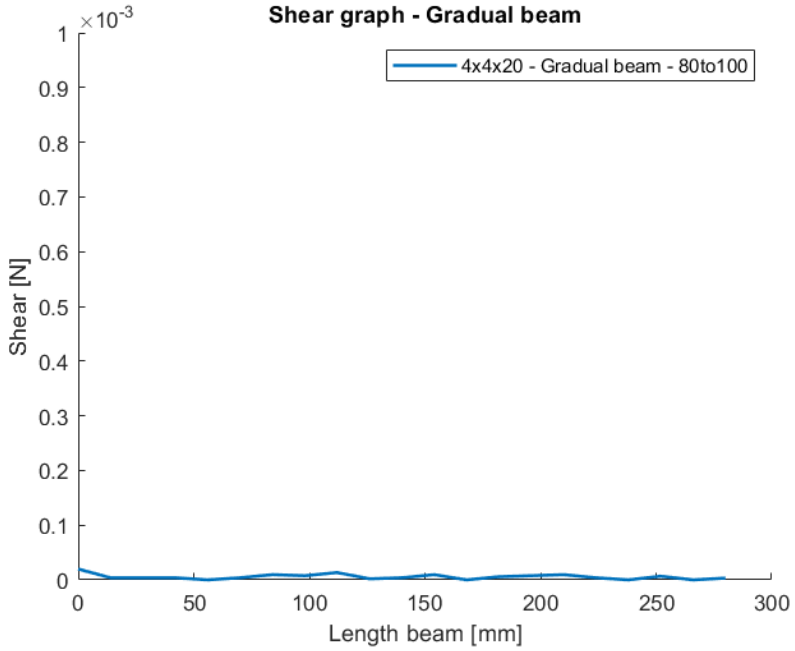

Figure C.10: Gradual beam- Shear diagram

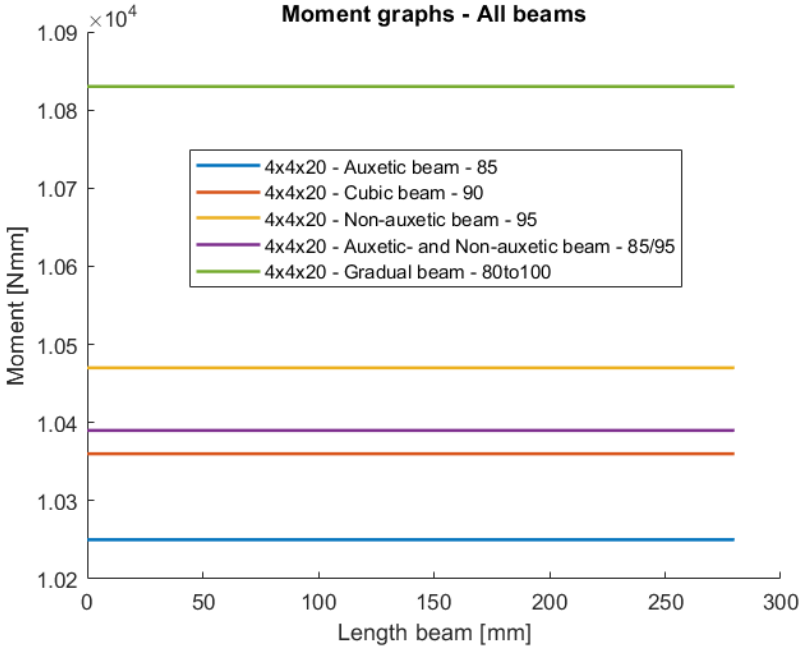

Figure C.11: Moment graphs - all beams

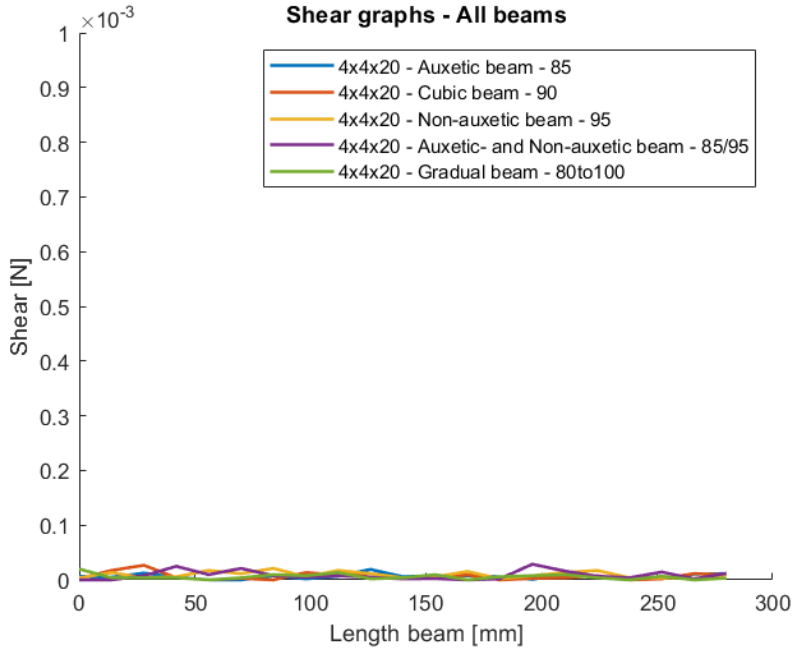

Figure C.12: Shear graphs - all beams

D

Appendix D - Effective modulus calculation Yang et al.

Yang et al. Paper - Rectangular section

Design Parameters:

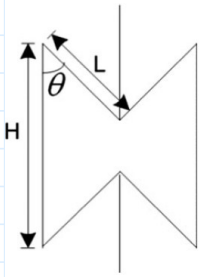

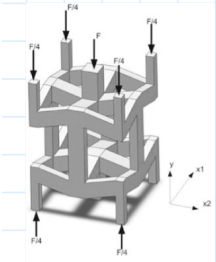

Vertical strut length	$H := 7\ mm$
Re-entrant strut length	$L := 7\ mm$
Re-entrant angle	$\theta := 90\ deg$
Thickness	$t := 1.2\ mm$
Modulus of steel	$E := 210\ GPa$
Poisson's ratio	$\nu := 0.3$
Shear modulus ABAQUS manual 6.6 - 17.2.1	$G := \frac{E}{(2\ (1+\nu))} = (8.077 \cdot 10^{10})\ Pa$
	$\sigma := 1\ \frac{N}{mm^2}$
Force component	$F := 2\ \sigma \cdot L^2 \cdot \sin(\theta)^2 = 98\ N$
Relationships force components	$P := \frac{F}{4} \cdot \sin(\theta) = 24.5\ N$
	$T := \frac{F}{4} \cos(\theta) = (1.5 \cdot 10^{-15})\ N$
	$M := \frac{(F \cdot L)}{8} \cdot \sin(\theta) = 85.75\ N \cdot mm$
	$A := t^2 = 1.44\ mm^2$

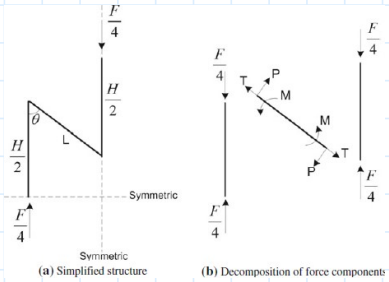

Compressive deformation of the vertical struts	$\Delta y_1 := \frac{F \cdot H}{E \cdot A} = 0.002\ mm$
The angle of deflection from Timoshenko Beam-theory	$\Theta := \frac{d\omega}{dx} + \gamma$
Geometrical factor cross-section	$\kappa := \frac{5}{6}$
Moment of inertia	$I := \frac{1}{12} \cdot t^4 = 0.173\ mm^4$
Maximum deflection angles	$\theta_1 := \frac{M \cdot L}{6 \cdot E \cdot I} + \frac{P}{\kappa \cdot G \cdot A} = 0.172\ deg$
	$\theta_2 := \frac{M \cdot L}{6 \cdot E \cdot I} + \frac{P}{\kappa \cdot G \cdot A} = 0.172\ deg$

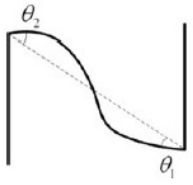

Deflection angles of the re-entrant strut

Size change

$$\Delta x := L \cdot \theta_1 \cdot \cos(\theta) = \left(1.29 \cdot 10^{-18}\right)\ mm$$

$$\Delta y_2 := L \cdot \theta_1 \cdot \sin(\theta) = 0.021\ mm$$

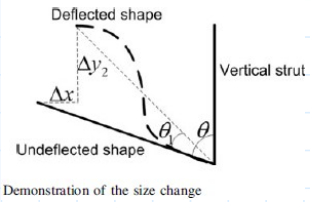

Demonstration of the size change

Strut Ratio

$$\alpha := \frac{H}{L} = 1$$

Strain y

$$\varepsilon_y := \frac{(\Delta y_1 + \Delta y_2)}{(H - L \cdot \cos(\theta))} = 0.003$$

Effective modulus of an 3D re-entrant lattice structure

$$E_y := \frac{\sigma}{\varepsilon_y} = 299.964\ MPa$$

Verification formula - Effective modulus

$$E_y := \frac{(\alpha - \cos(\theta))}{\left(\frac{\left(2 \cdot \alpha \cdot L^2 \cdot \sin(\theta)^2\right)}{E \cdot t^2} + \left(\left(\frac{L^4}{2\ E \cdot t^4} + \frac{\left(3 \cdot L^2\right)}{\left(5 \cdot G \cdot t^2\right)}\right) \cdot \left(\sin(\theta)^4\right)\right)\right)} = 299.964\ MPa$$

If Euler-Bernoulli beam theory would apply with

$$4\alpha t^2 \ll L^2 \sin^2\theta$$

$$Left := 4 \cdot \alpha \cdot t^2 = 5.76\ mm^2$$

$$Right := L^2\ \sin(\theta)^2 = 49\ mm^2$$

so Left << Right doesn't apply

$$E_y := 2 \cdot (\alpha - \cos(\theta)) \cdot \left(\frac{t}{L \cdot \sin(\theta)}\right)^4 \cdot E = 362.729\ MPa$$

Yang et al. Paper - Circular section

Design Parameters:

Vertical strut length $H := 7\ mm$

Re-entrant strut length $L := 7\ mm$

Re-entrant angle $\theta := 90\ deg$

radius $r := 0.6\ mm$

Diameter $D := 1.2\ mm$

Modulus of steel $E := 210\ GPa$

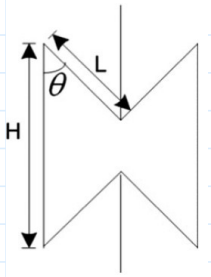

Poisson's ratio $\nu := 0.3$

Shear modulus
ABAQUS manual 6.6 - 17.2.1

$$G := \frac{E}{(2\ (1+\nu))} = (8.077 \cdot 10^4)\ MPa$$

$$\sigma := 1\ \frac{N}{mm^2}$$

Force component $F := 2\ \sigma \cdot L^2 \cdot \sin(\theta)^2 = 98\ N$

Relationships force components

$$P := \frac{F}{4} \cdot \sin(\theta) = 24.5\ N$$

$$T := \frac{F}{4} \cos(\theta) = (1.5 \cdot 10^{-15})\ N$$

$$M := \frac{(F \cdot L)}{8} \cdot \sin(\theta) = 85.75\ N \cdot mm$$

$$A := \pi \cdot r^2 = 1.131\ mm^2$$

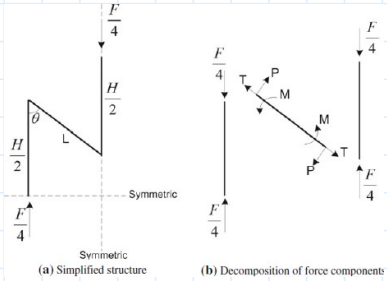

Compressive deformation of the vertical struts

$$\Delta y_1 := \frac{F \cdot H}{E \cdot A} = 0.003\ mm$$

The angle of deflection from Timoshenko Beam-theory

$$\Theta := \frac{d\omega}{dx} + \gamma$$

Geometrical factor cross-section

$$\kappa := \frac{5}{6}$$

Moment of inertia

$$I := \frac{(\pi \cdot D^4)}{64} = 0.102\ mm^4$$

Maximum deflection angles

$$\theta_1 := \frac{M \cdot L}{6 \cdot E \cdot I} + \frac{P}{\kappa \cdot G \cdot A} = 0.287 \ deg$$

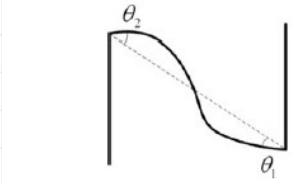

Deflection angles of the re-entrant strut

$$\theta_2 := \frac{M \cdot L}{6 \cdot E \cdot I} + \frac{P}{\kappa \cdot G \cdot A} = 0.287 \ deg$$

Size change

$$\Delta x := L \cdot \theta_1 \cdot \cos(\theta) = (2.144 \cdot 10^{-18}) \ mm$$

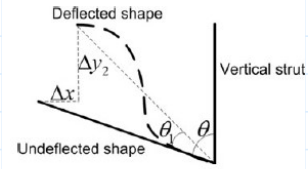

Demonstration of the size change

$$\Delta y_2 := L \cdot \theta_1 \cdot \sin(\theta) = 0.035 \ mm$$

Strut Ratio

$$\alpha := \frac{H}{L} = 1$$

Strain y

$$\varepsilon_y := \frac{(\Delta y_1 + \Delta y_2)}{(H - L \cdot \cos(\theta))} = 0.005$$

Effective modulus of an 3D re-entrant lattice structure

$$E_y := \frac{\sigma}{\varepsilon_y} = 184.683 \ MPa$$

$$E_y := \frac{(\alpha - \cos(\theta))}{\left(\frac{\left(2 \cdot \alpha \cdot L^2 \cdot \sin(\theta)^2\right)}{E \cdot A} + \left(\left(\frac{(8 \cdot L^4)}{(3 \ E \cdot \pi \cdot D^4)} + \frac{(3 \cdot L^2)}{(5 \cdot G \cdot A)}\right) \cdot \left(\sin(\theta)^4\right)\right)\right)} = 184.683 \ MPa$$

E

Appendix E - Upscaled bow-tie architecture

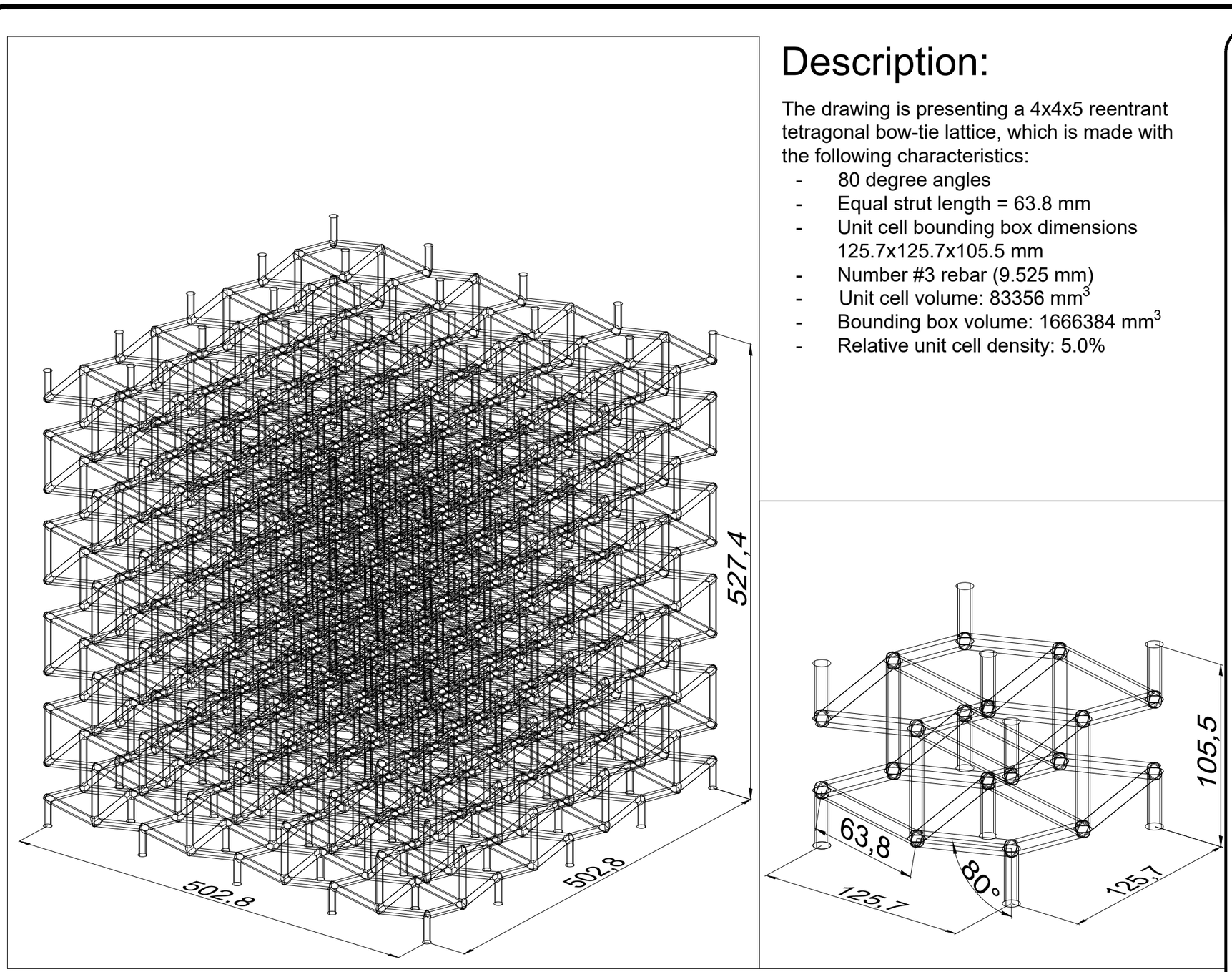

Description:

The drawing is presenting a 4x4x5 reentrant tetragonal bow-tie lattice, which is made with the following characteristics:

- 80 degree angles
- Equal strut length = 63.8 mm
- Unit cell bounding box dimensions 125.7x125.7x105.5 mm
- Number #3 rebar (9.525 mm)
- Unit cell volume: 83356 mm^3
- Bounding box volume: 1666384 mm^3
- Relative unit cell density: 5.0%

General Notes

No.	Revision/Issue	Date

Firm Name and Address

Project Name and Address
Tetragonal bow-tie lattice
Number #3 diameter
Units: mm

Project	Sheet
UMass	1
Date: 12.04.2023	
Scale: As Noted	

Tetragonal_Bowtie_Design_80 Scale: 1:2 [mm] Unit cell Scale 1:1 [mm]

Figure E.1: 80 Degrees upscaled bow-tie lattice